Parameter extraction and analysis of cardiorespiratory sound for sleep and heart state monitoring

September 2018

Fang Yu

Graduate School of Science and Engineering
Yamaguchi University

Abstract

Healthcare has drawn wide public concern in modern society. Sleep spending one third of the life is indispensable to maintain healthy functions and improve the quality of life. Monitoring and analyzing overnight breathing sound signal and heart sound signal will be connected with the early detection of lifestyle diseases and the prevention of severe cardiovascular diseases. More and more people are suffered from sleep-related disorders, not only in the elderly but also in young adults. The sleep-related disorders will affect the sleep quality seriously. In particular, apnea syndrome will increase the risk of cardiovascular disease complications like heart failure. They will threaten people's health and life. Therefore, monitor and analyze breathing sound and heart sound during night sleep play an important role on healthcare at home.

In clinic, polysomnography (PSG) is the golden standard to evaluate the sleep states. Apnea-hypopnea index (AHI) is used to diagnose obstructive sleep apnea (OSA) which is a typical sleep-related disorder. At present AHI only can be provided by PSG detection. However, PSG should be tested in hospital because of the complex and professional operation. It is not suitable for daily monitoring at home.

This research focuses on the ventilation of oxygen and carbon dioxide by sleep respiration and monitoring of the sleep states with the breathing sound signal. The breathing data is acquired portably by a smart phone and a wireless earphone. The waveform segmentation method of breathing cycle and phase is proposed with high accuracy. Based on the segmented breathing cycles, the identification algorithm of apnea and hypopnea is developed by the time duration of each cycle to detect AHI. Moreover the identification method of normal and abnormal breathing is proposed based on the Mel frequency spectrum analysis which is used widely in speech recognition. Finally, the proposed analysis methods are applied for heart sound analysis. The usefulness of the proposed methods is verified by abnormal heart sound analysis.

This thesis is composed of six chapters.

In chapter 1, the aim and significance, the current studying situation, research key points, nodus and studying methods of sleep state and heart state monitoring have been described. The outline of this thesis is introduced as well.

There are regular breathing, irregular breathing, snore, apnea during the whole night sleep. To guarantee the veracity of the sleep breathing signal analysis, the complex sleep breathing waveforms should be segmented correctly at the beginning. Since the overnight breathing sound data is quite large, a fast and effective segmentation method is the basis of this research. In chapter 2, the waveform segmentation method based on the moment waveform extraction is proposed. The time characteristic waveform (TCW) and characteristic moment waveform (CMW) are extracted regarding the breathing signal as the periodic signal. Then the breathing cycles and inspiration/expiration can be segmented successfully based on the local extremums of CMW and TCW. A set of testers including young students and a patient suffered from OSA is used to validate the efficiency of the proposed method. The average successful rate of breathing cycle segmentation can reach to 98.4% compared with the results of manually counting.

The chapter 3 introduces the identification of apnea and hypopnea based on the segmentation algorithm proposed in chapter 2. Then the detection method of AHI which can diagnose the severity of OSA is proposed. Apnea is defined by breathing pause lasting more than 10 seconds explicitly. But the hypopnea has not clear definition, estimated by ventilation reducing less than 50% or breathing cycle lasting more than 6 seconds. In this chapter, AHI can be detected by computing the times of apnea and hypopnea events from the segmented waveforms. And the threshold values used to identify hypopnea is examined by comparing with the monitoring results of blood oxygen saturation. Although the number of test cases is small, the detected AHI value is close to the diagnostic result of PSG. The proposed AHI detection can be said to be useful.

In chapter 4, Mel frequency spectrum is introduced from speech signal processing to detect the snore and other abnormal breathing states. Mel frequency spectrum converts the linear frequency spectrum to Mel frequency simulating the acoustic character of human ear. It has high resolution in low frequency part and rough resolution in the high frequency part. For each frame in time domain, the Mel scale label is extracted to represent the maximum value of energy in Mel frequency domain. Then the present times of each Mel scale label are computed to display the frequency energy distribution. The normal breathing component, abnormal breathing component and snoring component can be identified by the fixed Mel scale label set. The whole night monitoring results of sleep breathing sound signal are applied to validate the efficiency of the proposed algorithm. In addition, the ratio of normal breathing and abnormal breathing is proposed as a new index to evaluate sleep quality.

In chapter 5, the proposed breathing waveform segmentation method and Mel

frequency spectrum analysis method are applied to identify normal and abnormal heart sound. Heart sound signal is recorded by a portable acquisition system including stethoscope, auscultation cloth and a smart phone or an IC-recorder. The segmentation method proposed in chapter 2 is applied to segment the cardiac cycles and systole/diastole with adjusted parameters. The efficiency of the segmentation algorithm described in chapter 2 is confirmed again by 99% successful rate for normal heart sound data and 95% for abnormal cases. Then Mel-scale spectrum is calculated for the systolic and diastolic murmurs intervals to identify the abnormal heart sound from a data set including normal case and congenital heart disease case. Mel frequency spectrum analysis method introduced in chapter 4 can be used for heart sound analysis compared with the clinical diagnostic results. The application will be expanded to overnight heart state monitoring for early detection of heart failure and other heart diseases in the future.

The conclusion is drawn and the future work is discussed in chapter 6.

論文概要

健康管理は、現代社会において幅広い関心を集めている。睡眠は、健康な機能を維持するために不可欠であり、生活の質を向上させるための基本的な役割を果たす。終夜の呼吸音や心音をモニタリング・分析することで、生活習慣病の早期発見や心血管疾患の重症化の予防につながる。高齢者だけでなく若年成人にも、睡眠関連障害が増えている。睡眠関連障害は睡眠の質に影響し、特に、無呼吸症候群は心不全など循環器系疾患合併症の発生リスクを増大させ、人々の健康と生命を脅かす。したがって、夜間睡眠時の呼吸音と心音をモニタリングし、分析する技術を確立することは、在宅医療・看護に重要な役割を果たすことになる。

睡眠状態を評価するには、睡眠ポリグラフ（PSG）システムがゴールドスタンダードとして使用されている。典型的な睡眠関連障害である閉塞性睡眠時無呼吸（OSA）を診断するために、無呼吸・低呼吸指数（AHI ）が用いられる。現在 AHI は、PSG による検査しか提供されない。しかし、PSG 検査は煩雑で高度な専門性を要するため、自宅で手軽のモニタリングには適していない。

本研究では、呼吸による酸素と二酸化炭素の換気状態に着目し、睡眠時の寝息呼吸音を無線マイクロフォンで計測し、呼吸の吸気相と呼気相による呼吸の周期を高精度に抽出するための波形分割方法を提案すると共に、分割した波形に基づく呼吸の周期情報から無呼吸並びに低呼吸を検出するアルゴリズムを開発し、呼吸音データから AHI を求めることを試みる。さらに、音声解析技術によく用いられるメル周波数解析法を展開し、正常呼吸並びに異常呼吸の判別方法を提案する。最後に本研究で提案した周期波形の分割方法とメル周波数解析方法を心音解析に応用することを試み、異常心音分析への有用性を検証する。

本論文は、6 章から構成されている。

第 1 章では、睡眠研究及び心音研究に関する研究背景と目的、現状を説明する。また、本論文の概要について述べる。

第 2 章では、睡眠時の寝息呼吸音に、リズムの正しいものや不規則なもの、いびき、無呼吸などがある。寝息呼吸音を正しく分析するため、様々な寝息呼吸波形を精度よく分割することが重要である。また、一晩の呼吸音データがかなり大きいことから、高速かつ効率な呼吸波形分割アルゴリズムを開発することは本研究の基礎となる。本章では、呼吸波形を周期波形と見なした場合の寝息呼吸音を時間特徴波形（TCW）と特性モーメント波形（CMW）として抽出し、CMW と TCW の局所的な極値に基づき、吸気相と呼気相による呼吸の周期を分割する方法を提案する。正常例と閉塞性睡眠時無呼吸症候群（OSA）症例の終夜寝息呼吸音データに対して、提案された波形分割方法を適用し検証を行った。自動検出した結果を手作業で求めた結果と比較したところ、呼吸周期の平均抽出率が 98.4%であり、本分割方法の有効性が確認された。

第 3 章では、第2章で提案した呼吸波形分割アルゴリズムを用い、睡眠時無呼吸と低呼吸の推定を行う。寝息呼吸音の分割波形から睡眠時無呼吸症候群の重症度を診断する AHI を推定する方法を開発する。睡眠時無呼吸は 10 秒以上呼吸停止と明確に定義されているが、低呼吸は、換気が 50%以下または呼吸周期が 6 秒以上という定義があるものの、曖昧さが残っている。本章では、分割した呼吸周期波形から睡眠時無呼吸・低呼吸の停止時間と回数を算出し、さらに、血中酸素濃度の計測結果と照らし合わせて低呼吸を推定するための閾値を精査し、AHI を推定するアルゴリズムを提案した。症例数がまだ少ないが、本提案方法で求めた AHI の推定結果が PSG の診断結果と近い値となっており、本 AHI 推定方法が有用であると言える。

第 4 章では、いびきや不規則な異常な呼吸を検出するため、音声解析技術によく用いられるメル周波数スペクトル解析法を導入する。メル周波数スペクトラムは、低周波数の部分を解像度高めに、高周波数の部分を粗めにすることで、線形周波数スペクトルを人間の聴覚特性に合うようにメル周波数に変換するものである。具体的には、まず各時間フレームに対し、メル周波数域におけるエネルギーの最大値をメルスケールラベルとして求める。次に、メルスケールラベルの度数分布を求め、正常な呼吸成分、異常な呼吸成分及びいびきの呼吸成分を、メルスケールラベルの度数分布として表し、正常呼吸、異常呼吸ならびにいびきの判別を試みた。終夜睡眠時寝息呼吸音の解析に本アルゴリズムを適用し、その有効性を確認した。さらに、睡眠時の正常呼吸と異常呼吸の割合を睡眠の質に関する新しい評価指数として提案した。

第 5 章では、呼吸データの波形分割方法とメル周波数スペクトル解析法を心音の解析に応用し、正常心音と異常心音の判別を試みる。心音信号は、電子聴診器と、スマートフォンまたは IC レコーダを用いて採集する。第 2 章で提案した呼吸音波形分割法を心音の周期特性に合わせて計算パラメータを調整し、I 音と II 音を含む心音周期と、心臓収縮期および拡張期を分割することを試みた。正常心音が 99%、異常心音が 95%と高い分割率を得ることと、第 2 章で述べた呼吸音周期分割アルゴリズムの有効性が改めて確認された。さらに、心臓収縮期および拡張期の各区間におけるメル周波数スペクトラムを求め、正常と先天性心疾患を含む心音データに適用した結果より、第 4 章で提示したメル周波数分析法が異常心音の判別にも有用であることが分かった。今後終夜の心音をモニタリングし、異常心音を解析することで、心不全や心疾患の早期発見に期待したい。

第 6 章では、この研究の結論と今後の展望について述べる。

Contents

Chapter 1

Introduction

1.1 Background

Healthcare related issues become the hot spots of society around the world. Sleep is indispensable to support human's health as it spends one third of the life. It is one of the most important factors for human's health condition is sleep. Poor sleep quality will affect peoples' daily life seriously. There are some diseases related with the poor sleep quality and threatens peoples' lives, such as insomnia, insomnia depression and sleep related breathing disorders. Specially, the sleep related breathing disorders are easy to make people feel tired, which will affect the normal life [1], yields adverse cardiovascular outcomes, even lead to death [2].

Obstructive sleep apnea (OSA) and central sleep apnea (CSA) are the typical sleep related breathing disorders. CSA is caused by the brain's area controlling breathing functioned incorrectly. The upper airway is open. As shown in Fig.1.1, the airway is blocked while breathing for OSA case. The soft palate is long and flabby, the tongue is bigger and not very toned. They lead to the obstruction of the airway and generate the OSA. The ventilation will be changed by the obstruction of airway. There are snoring, breathing pause and other labored breathing recognized by the sleeping person and the person around.

OSA will lead to the complications of chronic disease, such as hypertension, coronary heart disease and other cardiovascular diseases. More than a half of OSA patients have complications which lead to a worse healthy condition [3].

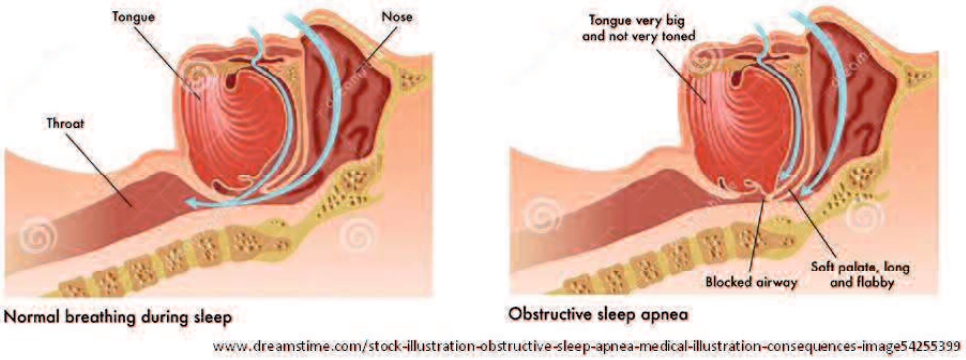

Figure 1.1 Obstructive sleep apnea

OSA will also increase the risk of several diseases, such as diabetes, cerebral stroke and Alzheimer's disease [4]. Moreover, OSA will lead to the increasing occurrence of traffic accidents because of the fatigue driving due to the drowsiness and inattention caused by OSA [5]. And the probability of occurrence for OSA patients is 2 7 times of normal people, increasing with the severity of OSA [6].

OSA will occur for different age groups and the morbidity is increasing in recent twenty years [7]. More than 20% of adults are suffered from OSA with different level. OSA morbidity of male is higher than that of female. Over 6% of Children, mainly 2-5 years old, have OSA which will affect their growth greatly [8].

But there is poor awareness of OSA for general population. Less than 25% of OSA sufferers know that they suffer from OSA [52]. According to some investigations, more than a half of respondents think OSA will not affect their life and is not necessary to take treatment. After recognized the harmfulness of OSA, only 21.95% of respondents have taken the test and treatment. The expensive cost takes about 40% of reasons for respondents to refuse the test and treatment [10].

In clinic, the polysomnography (PSG) is the golden standard for detecting the sleep state. PSG can acquire a series of monitoring indices with lots of sensors. It's the only way to provide the Apnea Hypopnea Index (AHI) exactly to diagnose OSA. But PSG is not only expensive-cost but also complicated for common patients [11]. Moreover, because the operation of PSG is uncomfortable for the testers while sleeping, the results of PSG will be influenced by low-quantity sleep. It is not suitable for daily monitoring at home to prevent the OSA and follow the process after accepting the treatment. Hence a smart monitoring of OSA for home healthcare is required.

The smart wearable is a new trend of the smart monitoring system [12–14]. The main function of the smart wearable system is to acquire the human vital signs portably in real-time. There are wearable Electrocardiograph (ECG), electroencephalograph (EEG), blood pressure, pulse, respiration, sleep, motion monitoring and so on [15–18] for healthcare monitoring. They can satisfy the basic conditions of better monitoring of real-time, long-term, dynamic physiological and pathological processes. The monitoring based on smart wearable could be expedient for the management of chronic illnesses. And it can provide convenience for special populations, such as the aged, pregnant women and children [19, 20].

Obstruction will lead to the decreasing ventilation while inspiration and expiration. The changes of ventilation can be reflected by breathing sound signal, such as snoring, apnea, hypopnea and so on. AHI is defined by the number of apnea and hypopnea events appearing in one hour during whole night sleep. An apnea lasting more than 10 seconds will lead to lower oxygen supply to the brain [21]. Usually, the ventilation of hypopnea will reduce to less than 50% of ventilation while normal breathing or cause the value of oxygen levels declining by more than 4%. They are very important to detect AHI value for OSA monitoring.

Various respiratory signals have been recorded by the smart wearable for sleep breathing state monitoring, including the tracheal signals from throat [22] and suprasternal notch [23], the breathing sound signals from the nose and mouth [24, 25] like shown in Fig.1.2. The mask would affect the normal sleep and the breathing sound data mixed noise during the breathing pause at 1.5 minutes.

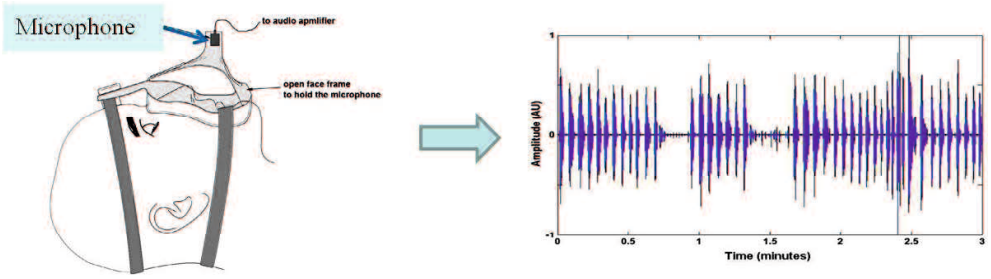

Figure 1.2 Acquisition system shown in reference [25].

In previous study, researcher worked hard on breathing frequency and feature extraction of different breathing states. Researchers extracted respiratory rate(RR) as the key indicator for monitoring sleep apnea [26], using Hilbert transform [27], wavelet transform [22], genetic algorithm [23], the short-time Fourier transform, Shannon entropy and autocorrelation [24]. The selection of the threshold value for envelope extraction will change accompanied with the speed of breathing for

different individuals. So the adaption of the threshold values (the time scale parameters) will affect the accuracy of sleep RR detection.

Researches also focused on the snoring detection [28–31] to evaluate the level of OSA, respiratory phase analysis [32, 33] for apnea detection and other parameter extraction of breathing sound signal [25, 34].

Based on the results of previous studies and my experiments, it is found that breathing sound segmentation and breathing state identification are two problems in sleep breathing state monitoring. One problem is how to reduce the computational complexity of the analysis algorithms for the long-time data, that is the real time capability. Another one is how to guarantee the accuracy of the detection results. Most of researches always focused on a short period of the breathing signal and the accuracy of the analysis results is not sufficient for the healthcare. In my study, a sleep monitoring system by breathing sound signal for OSA detection at home will be proposed.

My study keeps the ventilation of oxygen and carbon dioxide while sleep in mind. Considering the conditions of the sleep breathing state monitoring, a smart wearable for acquisition of breathing sound signal from the nose and mouth is applied in our study shown in chapter 2. A wireless microphone can record the breathing sound signal by being fixed near the nose with a cosmetic tape. Then the data can be transferred to a smartphone for storage via bluetooth. This wearable is hardly affected by the sleep position which can make tester sleep well. Finally the data will be transmitted to a computer and analyzed by software for detect OSA. The analysis system will be introduced in chapter 2 to 4.

Abnormal ventilation while sleep breathing will cause the less support of blood oxygen which will improve the high risk of cardiovascular diseases, such as heart infarction, cerebral infarction, stroke and so on. So the heart monitoring while sleep is necessary and helpful to prevent the heart diseases and evaluate heart function state for daily healthcare.

In clinical, the common means of heart monitoring are ECG, color ultrasonic cardiogram and auscultation [35–37]. ECG is a popular method to check up on the wrong with cardiorespiratory function over decades. The ECG can observe the heart function by heart rate and show the situation about ventricle and atria to detect arrhythmia, ventricular atrial hypertrophy and so on. The accuracy of ECG detection usually depends on the larger number of electrode slice. Although ECG can be embedded in the smart wearables monitoring system, its examine result is not comprehensive on the structural integrity and function of heart valves

compared with phonocardiogram [36]. Color ultrasonic cardiogram uses the ultrasonic echo to show the details of the defect of heart and the blood flow distribution can be displayed directly and noninvasively. But the accuracy of the huge instrument relates with the development of machine and is rely on the operation of the doctors [37].

Auscultation is the traditional means to diagnosis heart disease. Doctors determine the heart disease by hearing the heart murmurs of heart signal by stethoscope [38]. The accuracy of auscultation is lower which is easy to be affected by the surrounding noise and the posture of the subjects. Most important of all, it needs lots of practices and experiences, even for doctors [39]. Considering the need of daily monitoring and healthcare at home, the auscultation by heart sound signal become a common useful way in the early stage.

Researchers have processed heart sound signal from the denoising [40], heart feature extraction [41–43] and classification by machine learning [44,45]. Parameters is also vital for heart state monitoring by reflecting the condition of heart function, abnormality of heart structure and so on.

Compared with breathing sound signal, heart sound signal has similar features in time domain. The two basic physiological signals are quasi-periodic signals. A cardiac cycle is made up of systole and diastole. One breathing cycle can be divided into inspiration and expiration. So the proposed methods for breathing sound analysis can be applied to analyze heart sound signal to monitor the abnormal heart states.

The sleep breathing sound signal and heart sound signal are the subjects for healthcare in my research. The study will be helpful to monitor the breathing state and heart state during sleep. And the sleep monitoring system will be supplemented and improved in the further for healthcare at home.

1.2 Overview

The research on ”Parameter extraction and analysis of cardiorespiratory sound for sleep and heart state monitoring” is divided into 6 chapters in this dissertation.

Chapter 1 introduces the background and overview of this research.

Chapter 2 describes the sleep breathing waveform segmentation method. The proposed method is based on the moment waveform. The time characteristic waveform (TCW) is extracted firstly. Then the characteristic moment waveform (CMW) is transformed from the TCW. Moreover, the enhance processing method of amplitude contrast diminution is proposed to improve the segmentation accuracy. The breathing cycle is segmented by the local maximum value of CMW and TCW. Respiratory phases of each breathing cycle are also segmented robustly for further research.

Chapter 3 introduces the breathing state identification in time domain. Based on the sleep breathing waveform segmentation, the abnormal breathing states are defined and identified. The apnea and hypopnea can be identified by the time duration of breathing cycle. Then the AHI has been detected based on the identification results. The pause time of apnea can be detected as a useful index to monitor OSA severity. The efficiency of the sleep breathing state identification has been validated compared with the monitoring results of blood oxygen level. All night sleep data for OSA case and two young testers are used to detect AHI value for daily monitoring.

Chapter 4 introduces the identification of sleep breathing states in frequency domain. Mel frequency spectrum analysis method is applied to find the relationship of frequency energy distribution and different sleep breathing states. The Mel scale label is extracted and to identify the normal/abnormal breathing and snoring states by the present times. The proportion of normal/abnormal sleep states during the whole sleep is proposed as an important index to reflect the condition of ventilation. It will be meaningful to analyze OSA and evaluate the sleep state.

Chapter 5 introduces the heart state monitoring. The proposed segmentation method in chapter 2 and Mel frequency spectrum analysis method in chapter 4 are applied to detect the abnormal heart states. The proposed segmentation method is effective to segment the cardiac cycles and extract the intervals of heart murmurs. Mel frequency spectrum analysis is useful to identify the heart murmurs of a congenital heart disease.

Conclusion and future work have been drawn in Chapter 6.

Chapter 2

Sleep breathing sound waveform segmentation

2.1 Acquisition system of the sleep breathing sound signal

With the development of the smart wearable, more researchers have interests in sleep breathing state analysis by acoustic signals.The acoustic signals mainly come from two aspects, breathing sound signal of nose and mouth, tracheal signals from throat and the suprasternal notch.

In our study, the sleep breathing sound signal is collected by a portable and wearable acquisition device from nose and mouth. It includes a smart phone with android system and a wireless microphone for high sleep quality. The purpose of our research is to develop a cheap and easy use sleeping monitoring system for home use, so that the commercial wireless headset (such as PTM 165) will be one better choice for our research. Compared with the acquisition positions inferred, the microphone is fixed near the nose by a kind of makeup tape to acquire a stable breath signal during whole night sleeping. The environment of date acquisition is shown in Fig.2.1. The original sample frequency is 44.1 kHz.

The test system for OSA detection is shown in Fig.2.2. The sleep breathing data recored by the wireless headset is transmitted to a smart phone by bluetooth and saved. Then the data is transmitted to a computer by USB or WIFI. The data

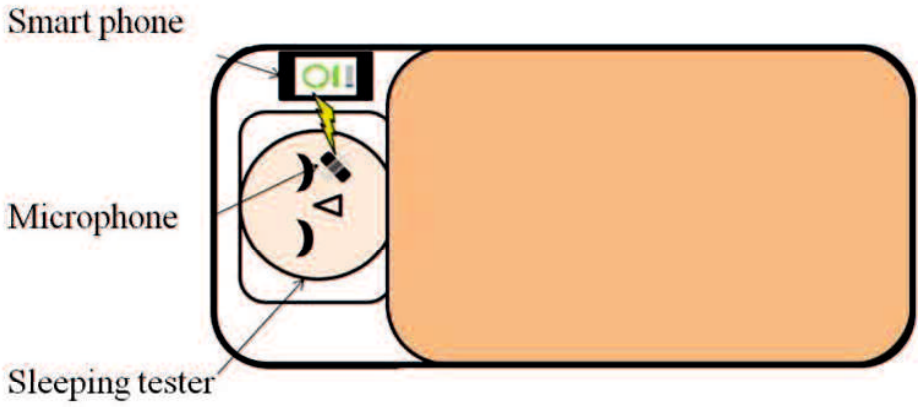

Figure 2.1 Sleep respiratory signal acquisition system

will be analyzed by software. Here the sample frequency is 11025Hz by down-sampling.

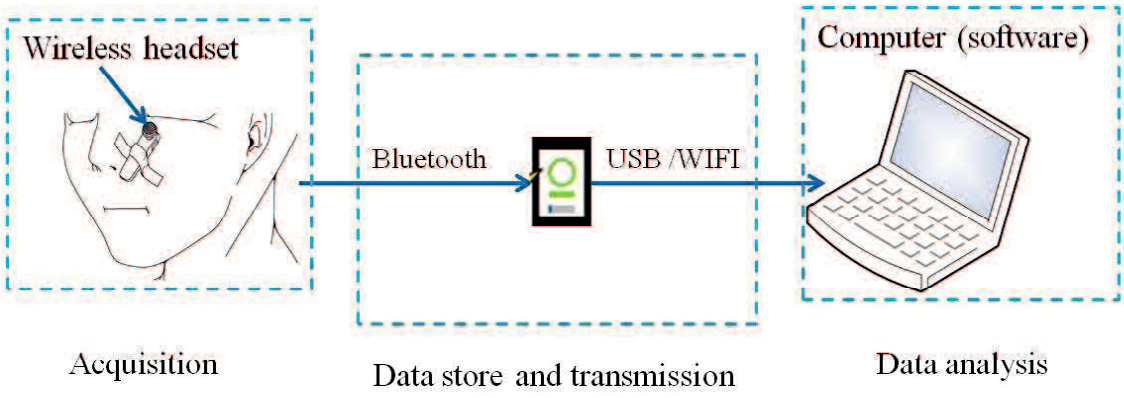

Figure 2.2 Test system for OSA detection

The real sleep breathing sound signal recorded by our system is shown in Fig.2.3. (a) is one-night sleep breathing sound data. It lasts about 5 hours and the intensity of breathing changes greatly. (b) is a part of stable normal breathing sound data from the fifth hour and (c) is a part of complex breathing sound data from the third hour. There are some obvious breathing pauses shown in (c), they are related with the obstruction of airway. So we can detect the abnormal breathing state for OSA by recorded breathing sound signal.

Five young students (Twenties) and a OSA patient (Fifties) are selected as testers. Utilizing the acquisition system of sleeping breathing sound signal, about 374-minute length data is recorded and the breathing cycles are counted manually

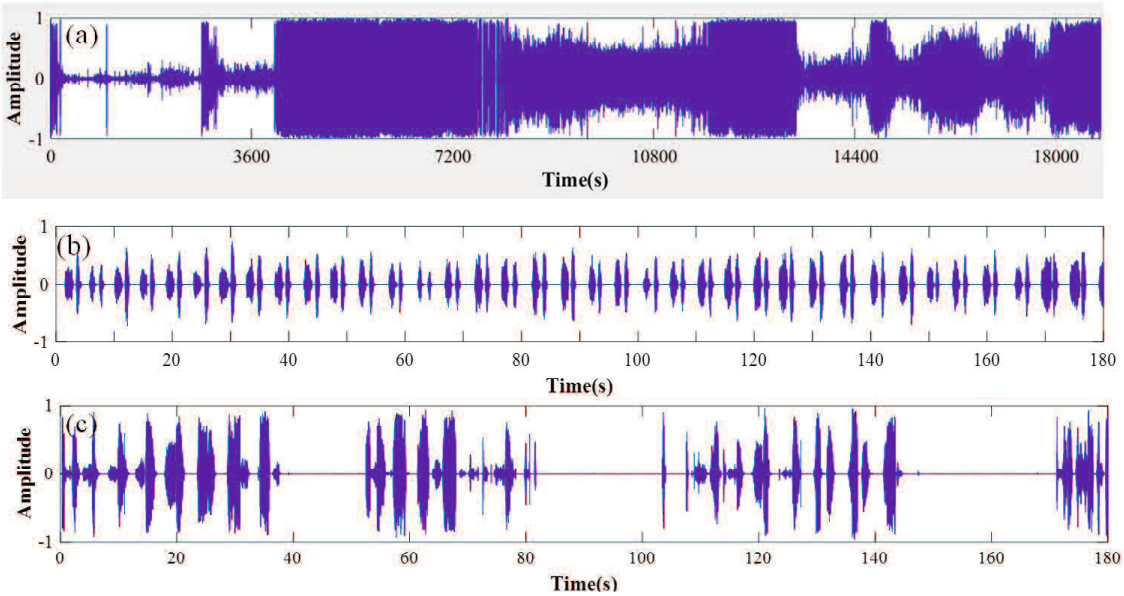

Figure 2.3 The sleep breathing sound data recorded by the test system

with the guidance of the pro-doctor for the reference. The information of the experimental data is listed in Table 1 and the OSA case is No.6.

Table 2.1 Experimental data.

Case No.	1	2	3	4	5	6	Total
Test Time (min)	57	62	85	50	60	60	374
Test Cycle Number	890	891	1177	702	678	663	5001

2.2 Sleep breathing sound signal and its segmentation

In my study, we want to detect AHI value for OSA monitor by identify the events of apnea and hypopnea. So the segmentation of breathing cycle is the basic of further analysis. It can not only provide the monitoring parameters, including sleep respiratory rate and breathing phases, but also be useful for analyzing breathing intensity, breathing vibration in details.

For breathing cycle segmentation, the envelop extraction with a threshold is a common measure. Hilbert transform and Shannon entropy are usually used for

waveform extraction [22, 46, 47]. According to the features of the biomedical signals, single degree of freedom model(SDOF) [47], homomorphic filter [48] and other means are also applied for extracting waveform.

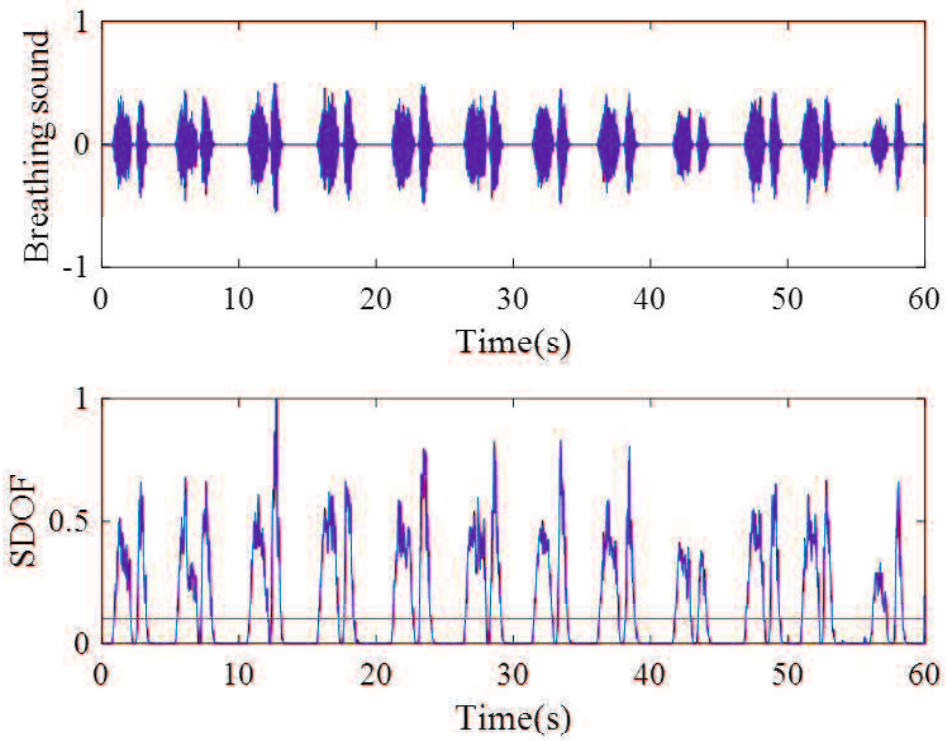

Figure 2.4 Breathing sound signal segmentation via envelop extraction and threshold value (case 1)

There are three parts of sleep breathing sound signal selected from one tester. The SDOF model envelop is extracted as an example to segment the breathing sound signal with a threshold value. In the case shown in Fig.2.4, the intensity of inspiration and expiration are similar of each breathing cycle. The threshold value of Shannon envelope is set as 0.05 and for SDOF model envelope is 0.1. With the help of threshold value, 13 breathing cycles can be segmented successfully.

As shown in Fig.2.5, the intensity of inspiration is much stronger than that of expiration, the threshold value should be adjusted to 0.2. The red cycle represents a breathing cycle with an abnormal inspiration which leads the segmented mistake by two kinds of envelope extraction.

For the case 3, the intensity and period of each breathing cycle around hypopnea are unstable shown in Fig.2.6. Hence the threshold value can not be selected easily and the breathing cycles can not be segmented successfully.

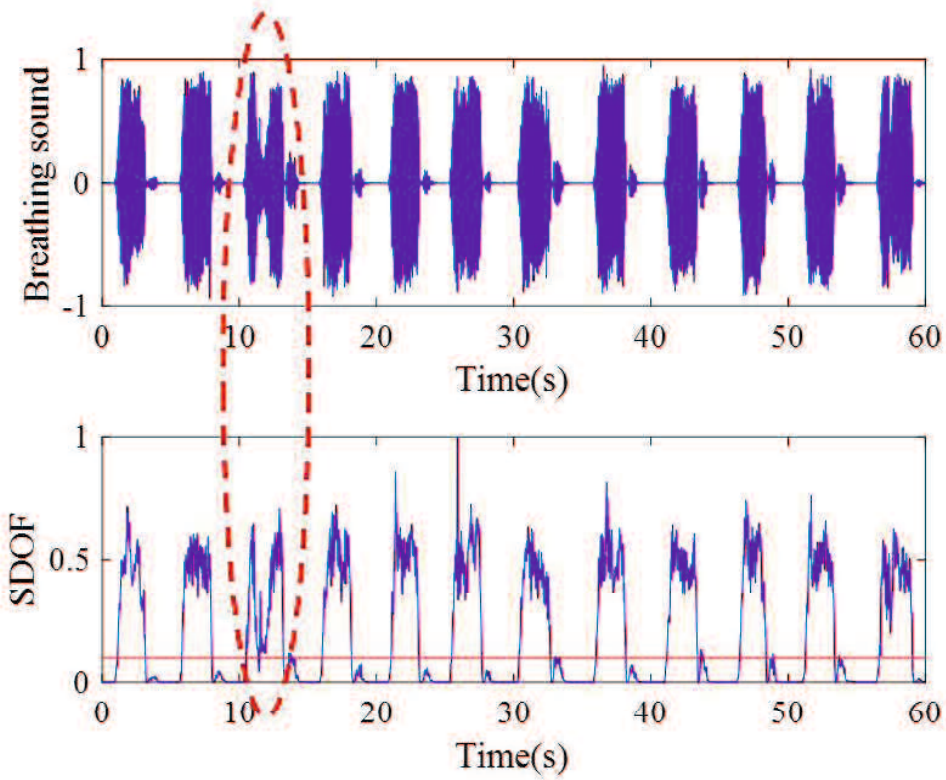

Figure 2.5 Breathing sound signal segmentation via envelop extraction and threshold value (case 2)

As shown in above cases, there are lager vibration of breathing intensity and respiratory rate during whole night sleep breathing monitoring. It is very difficult to segment the breathing cycles correctly only based on common envelop extraction with a suitable threshold value. To accomplish sleep state monitoring, a sleep breathing segmentation method with high accuracy and adaptation is necessary. The computation speed should also be considered for such a long-time monitoring.

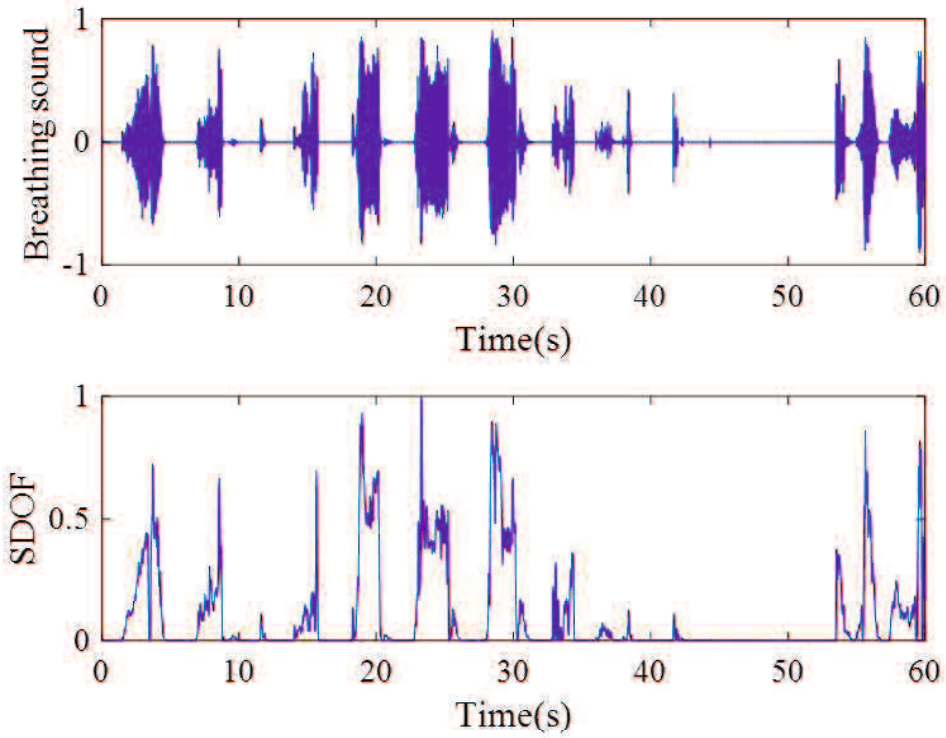

Figure 2.6 Breathing sound signal segmentation via envelop extraction and threshold value (case 3)

2.3 Sleep breathing cycle segmentation via moment waveform algorithm

2.3.1 Theory of the moment waveform algorithm

Waveform extraction is always applied at the beginning of the signal processing in time domain. The waveform should keep the useful information of sleep breathing sound signal as much as possible and make the impaction of noise as less as possible. In this thesis, time characteristic waveform (TCW) is extracted first with multi-scale adjustment. And then the characteristic moment waveform (CMW) is proposed for sleep breathing sound segmentation based on TCW.

The precondition is assuming the noise part of the sleep breathing sound signal as a signal with zero-mean and unit variance. Suppose the sleep breathing sound signal is $r(t)$, the random noise signal is $n(t)$, and the real output signal is $y(t) = r(t) + n(t)$. TCW of sleep breathing sound signal, denoted by $c(t, \delta)$, defined as the

variance of the output $y(t)$ can be gotten by

$$c(t,\delta) = \int_{t-\delta}^{t+\delta} (y(t) - \bar{y}(t))^2 d\tau = \int_{t-\delta}^{t+\delta} y(\tau)^2 d\tau - 2\delta\bar{y}(t)^2 \tag{2.1}$$

$$\bar{y}(t) = \frac{1}{2\delta} \int_{t-\delta}^{t+\delta} y(\tau) d\tau. \tag{2.2}$$

Then the CMW is calculated by the thought of image shape identification in image processing with another time scale l, which is represented by $I(t,\delta,l)$. It is calculated according to Eq.2.3.

$$I(t,\delta,l) = \int_{t-l}^{t+l} (\tau - t)^2 c(\tau,\delta) d\tau, \tag{2.3}$$

And the normalization presentation is presented as

$$n(t,\delta,l) = \frac{\int_{t-l}^{t+l} (\tau - t)^2 c(\tau,\delta) d\tau}{\int_{t-\delta}^{t+\delta} c(\tau,\delta) d\tau} \tag{2.4}$$

where δ and l are neighborhood of time t, which is called width time scale.

2.3.2 Advantage of the moment waveform algorithm

It is easy to find that the calculated amount will increase with larger time scale δ and l. The integral waveforms are applied to compute the TCW and CMW. The calculations of TCW and CMW are independent with the time scale parameters. And the calculated amount is small by fast algorithm, just using additions and multiplications [49].

For a discrete signal with length N, the computations of TCW and CMW only need $8N$ and $15N$ additions and multiplications respectively. The proposed moment waveform method had been compared with the wavelet method which is the one of the most popular method in signal segmentation. According to the experimental results, the computational complexity of discrete wavelet transform is

206 N, and that of the proposed method is $23N$. And the segmentation success rate of the discrete wavelet transform method is 72% to 93% and that of the proposed method is 100% [49]. And the operation time for analyzing one-hour sleep breathing sound data via MATLAB software is less than 24 seconds. It has great potential in developing real time health monitoring system.

According to our experimental statistic, a normal sleep breathing cycle is about 3 to 5 seconds and the time inspiration/expiration phase duration with a range of (0.3, 1) seconds. So the scale l is usually set to (1.5, 3), about half of sleep breathing cycle. The time scale δ is set as 0.1, about $1/10$ of the phase duration.

2.3.3 Sleep breathing cycle segmentation method based on TCW and CMW

After choosing the suitable time scales, TCW and CMW are extracted according to Eqs.2.1 to 2.4 and the sleep RR index can be detected as following steps.

Step 1. Calculate the local minimum point sequence of CMW;

Step 2. Calculate the local minimum point sequence of TCW by a computation window with central point as the local minimum point of CMW shown in the middle plants of Fig.2.7;

Step 3. Find local maximum point sequence of CMW;

Step 4. Adjust the cycle segment points of CMW by the help of the local minimum point sequence of TCW. The segment points shown in the bottom of Fig.2.7;

Step 5. Combine the breathing pause mistaken as a separated cycle by a threshold value. If the average amplitude of the cycle is smaller than the average amplitude of one-hour data, it will be combined with the shorter adjacent cycle.

Step 6. Compute the time duration of each breathing cycle by cycle segmented points. Respiratory rate value can be acquired by counting the number of the cycle segment point per minute as well .

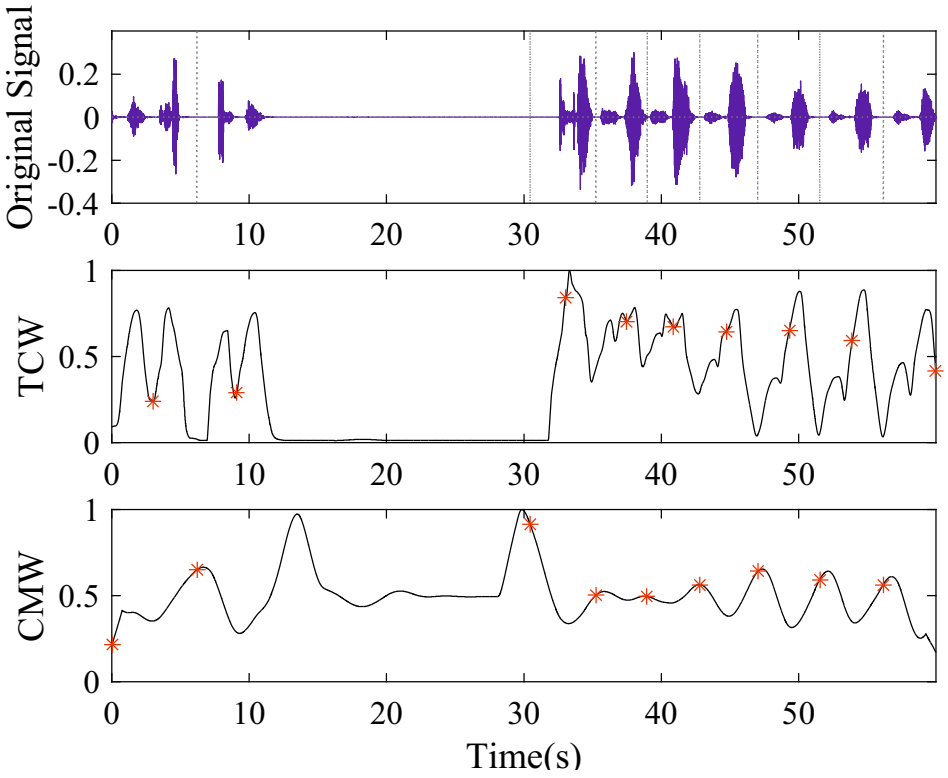

Figure 2.7 Results of breath cycle segmentation of an apnea case

An apnea case are taken for examples to show the efficiency of the cycle segmentation. The breathing cycles are segmented correctly based on the TCW and CMW displayed by the gray dashed line as shown from Fig.2.7. The CMW shows the breathing period clearly which is essential to segment the cycles accurately. The proposed method shows outstanding stability and accuracy for the complex breathing sound signal analysis.

The segmentation results of case 1 to 3 are shown in Fig.2.8 to 2.10. Whatever for the normal stable breathing or the abnormal breathing, the breathing cycles can be segmented correctly.

The accuracy of the segmentation is represented by successful rate defined by Eq.2.5.

$$\text{Successful rate}(\%) = \frac{N_{Detection}}{N_{Reference}} \tag{2.5}$$

where $N_{Detection}$ is the correctly segmented number by proposed method, $N_{Reference}$ is the number counted manually as the reference value.

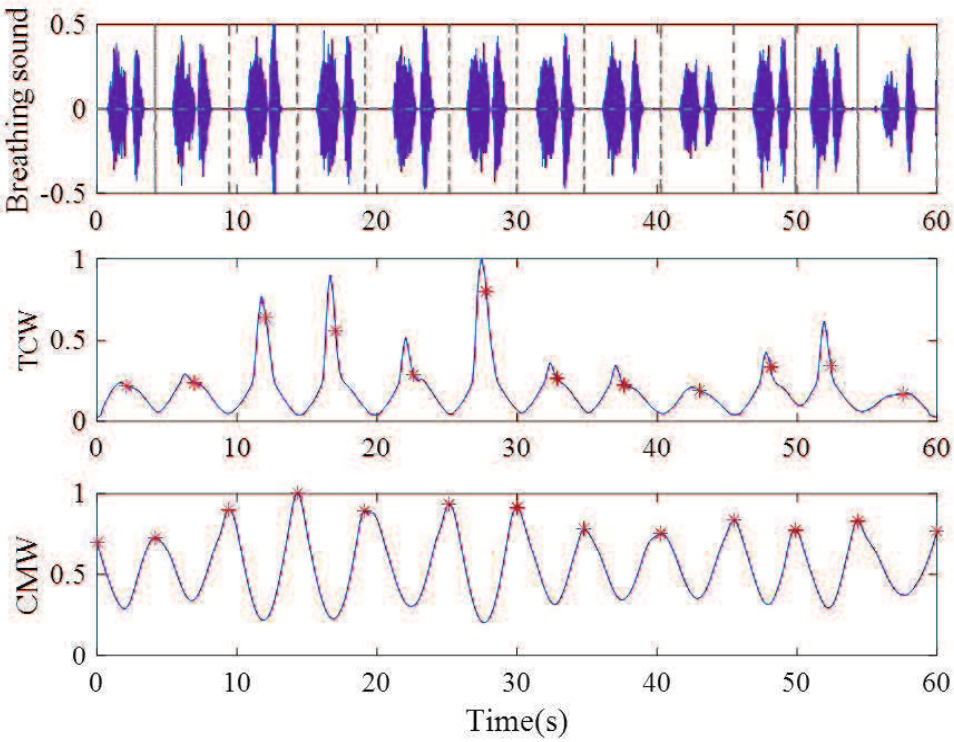

Figure 2.8 Results of breath cycle segmentation of case 1

Table 2.2 Segmentation results of respiratory cycle segmentation

Case No.	Correctly segmented Cycle Number	Successful Rate (%)
1	849	95.39
2	851	95.51
3	1156	98.22
4	683	97.29
5	667	98.38
6	617	93.06
Total	4823	96.44

For the Table2.2, the accuracy of the proposed segmentation method can reach to 98%. It shows the efficiency compared with common measures.

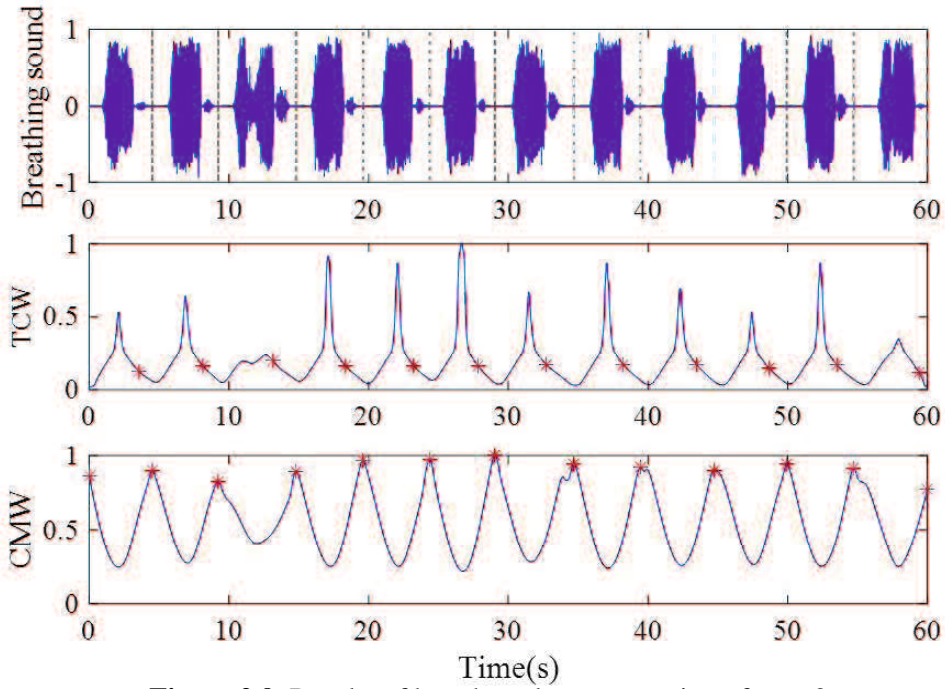

Figure 2.9 Results of breath cycle segmentation of case 2

2.3.4 Preprocessing for amplitude contrast diminution

In fact, the intensity of sleep breathing sound signal will change greatly and impact the efficiency of the proposed sleep breathing waveform segmentation. The weak breathing sound will be covered by the heavy breathing and surrounding noise as shown in Fig2.11. Therefore, the amplitude contrast of different breathing cycle should be decreased at first. The enhanced preprocessing method is first introduced in detail as follows.

The entropy of the original signal $H(t)$ is defined by

$$H(t) = E[y(t)] = -\xi y(t) \cdot \ln y(t) \tag{2.6}$$

$$\begin{cases} \xi = -1 \ (y(t)>0) \\ \xi = 0 \ (y(t) = 0) \\ \xi = 1 \ (y(t)<0) \end{cases} \tag{2.7}$$

Then decrease the volume and intensity difference by cutting off the strong intensity part, the output signal is

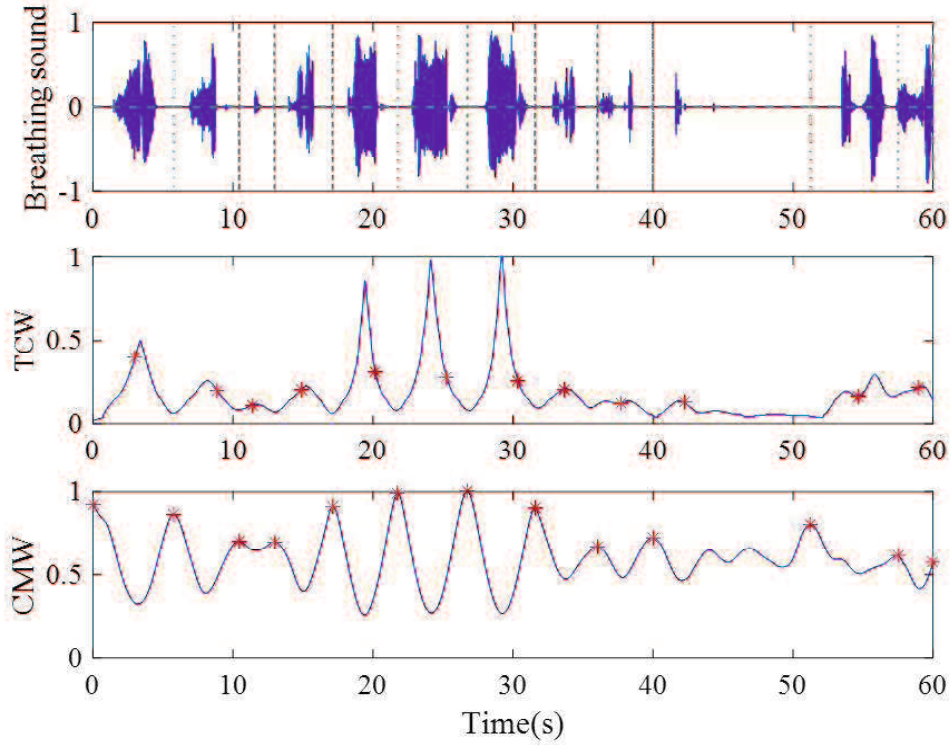

Figure 2.10 Results of breath cycle segmentation of case 3

$$\begin{cases} H_{cut}(t) = a \cdot H(t) \pm b \cdot av \ (|H(t)|>av) \\ H_{cut}(t) = c \cdot H(t) \ (|H(t)|<av) \end{cases} \tag{2.8}$$

where av is the mean value of the $H(t)$, a and b are weaken factors and c is the enhancement factor. According to the experimental results by try and error, a is selected as 0.4, b is 0.6 when $H(t)$ is positive, and -0.6 when $H(t)$ is negative, c is set as 1.5 to enhance the amplitude of weak breathing cycle. The final preprocessed signal is given by

$$y_{enhance}(t) = H_{cut}(t) \cdot (1 - l) + l \cdot H_{cut}(t)^{20}, \tag{2.9}$$

where l set as 0.85 experimentally is the limiting amplitude factor.

A section of sleeping breathing sound signal with large intensity variation is shown in Fig.2.12(a). Compared with the cycles in the both end, the amplitude of three breathing cycles in the middle is too small to be detected. And after a series

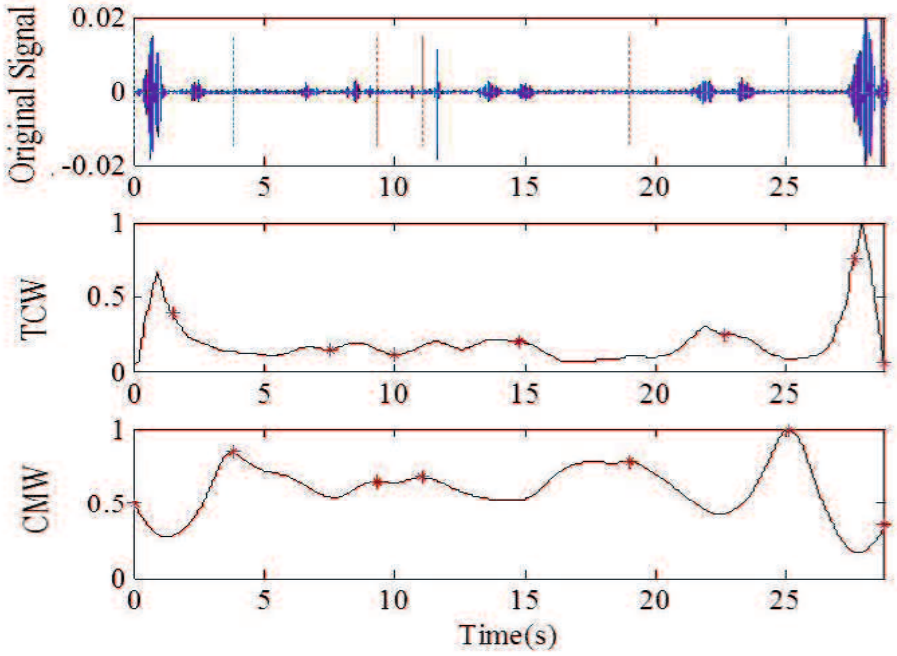

Figure 2.11 Sleep breathing sound signal waveforms with changing intensity and noise

of processing shown in Fig.2.12(b, c), it is clear found that the amplitude contrast of each breathing cycle has been shrunk as shown in Fig.2.12(d). It will improve the accuracy of breathing cycle segmentation.

Through the enhanced processing, the intensity difference between strong and weak breathing sound signals becomes smaller. The cycle segmentation results after the enhanced processing are displayed in Fig.2.13. As shown in Fig.2.11, the noise from mouth movement affects the cycle segmentation, i.e. a wrong cycle is segmented between the second and third breathing cycles. After enhanced processing. As shown in Fig.2.13, the moment waveform become smoother and has more obvious periodicity. The four breathing cycles are segmented correctly.

Through a series of processing introduced above, the intensity difference between strong and weak respiratory signals becomes small and its efficiency is validated. The results of breathing cycle segmentation before and after applying the enhanced preprocessing method are summarized in Table 2.2.

Without preprocessing, the scale parameter l are selected as 2, 2.5, 3,seconds for test cases. While applying the enhanced preprocessing method, the scale parameters (δ, l) is set as (0.1, 2.5) for all cases.

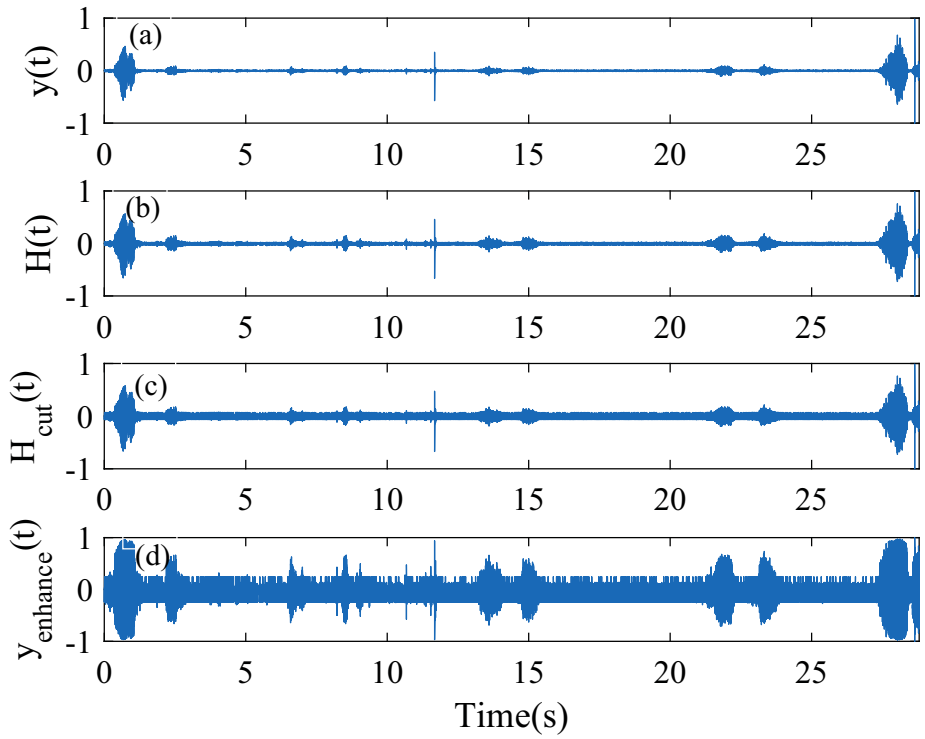

Figure 2.12 Sleep breathing sound signal waveforms, original signal waveform (a) and the procedure of the preprocessing (b) to (d).

Table 2.3 Respiratory cycle segmentation with the enhanced preprocessing method

	Without preprocessing		**With preprocessing**	
Case No.	Cycle Number	Successful Rate (%)	Cycle Number	Successful Rate (%)
1	849	95.39	872	97.98
2	851	95.51	865	97.08
3	1156	98.22	1172	99.58
4	683	97.29	694	98.86
5	667	98.38	672	99.12
6	617	93.06	646	97.44
Total	4823	96.44	4921	98.40

From Table 2.3, it can be found that the method without preprocessing can detect the breathing cycle with at least 93.06% of successful rate. And the average successful rate is improved to 98.40% by the same predicted time scale parameters for different cases when applying the enhanced preprocessing method. Especially, the successful rate of OSA case can reach to 97.44%, which satisfies

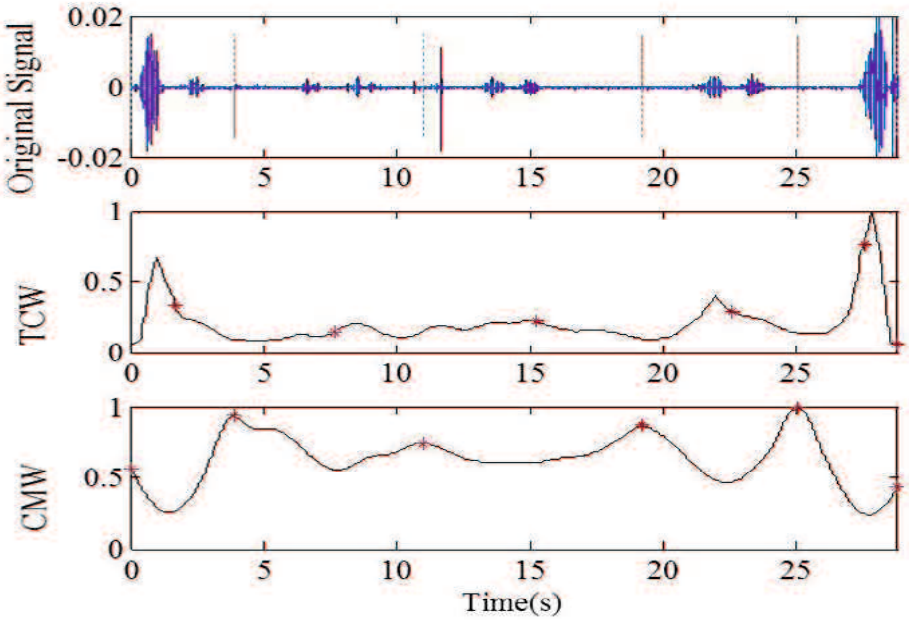

Figure 2.13 The cycle segmentation results after the enhanced processing

the experimental requirement of sleep breathing sound segmentation in this stage. Therefore, the use of the proposed enhanced preprocessing method shows more adaptability and veracity.

2.4 Inspiration and expiration segmentation

Monitoring the sleep breathing involves the detection of respiratory phases. A breathing cycle is constructed by four phases: inhalation, inspiratory pause, exhalation and expiratory pause [50]. The breathing cycle is defined here as starting with the onset of inspiration at the moment when air inflow starts. When the airflow stops, the inspiratory phase ends. Then the inspiratory pause begins and lasts until air begins to flow out from the lungs. Next, the expiratory phase starts. The expiratory phase is followed by the expiratory pause, which lasts until the end of the breathing cycle [51]. Researchers have done the analysis of respiratory sounds in the time or frequency domain or time-frequency domain to detect the breath phases. Fast Fourier Transform (FFT)-based summation method was proposed and sufficient evidence regarding the use of spectral changes for de-

tecting breath phases is provided [52]. The averaged normalized power spectral density was used to develop a fuzzy model for the detection of breath phases with accuracy of 98% [53]. An adaptive Neuro-Fuzzy inference model based on normalized average power spectral density was proposed with small root mean square error [54].

In our study, the procedure of inspiration and expiration segmentation based on moment waveform is shown as following steps.

Step 1. Processing of amplitude contrast diminution.

Step 2. Extraction of TCW and CMW.

Step 3. Calculate the local minimum point sequence of TCW as the segmented points from inspiration to expiration, the position saved as the $C_{Middle}(i)$. i is the number of the segmented points of the inspiration and expiration phases .

Step 4. Calculate the local maximum point sequence of CMW as the segmented points from expiration to inspiration,the position saved as the $C_{Boundary}(j)$. j is the number of points of the cycle boundary.

Finally, segmentation of inspiration and expiration are shown in Fig.2.14. The time durations of inspiration and expiration are represented in Fig.2.14.

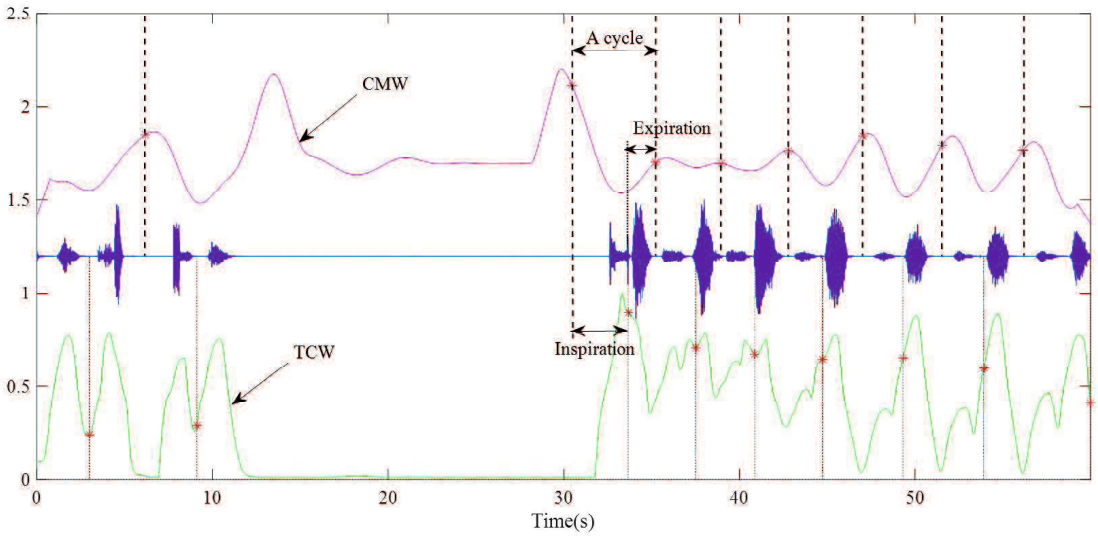

Figure 2.14 Inspiration and expiration segmentation

Segmentation results of case 1 to 3 are shown in Figs.2.15,2.16 and 2.17. Al-

though there are some deviation, most of breathing cycles can be separated into inspiration and expiration.

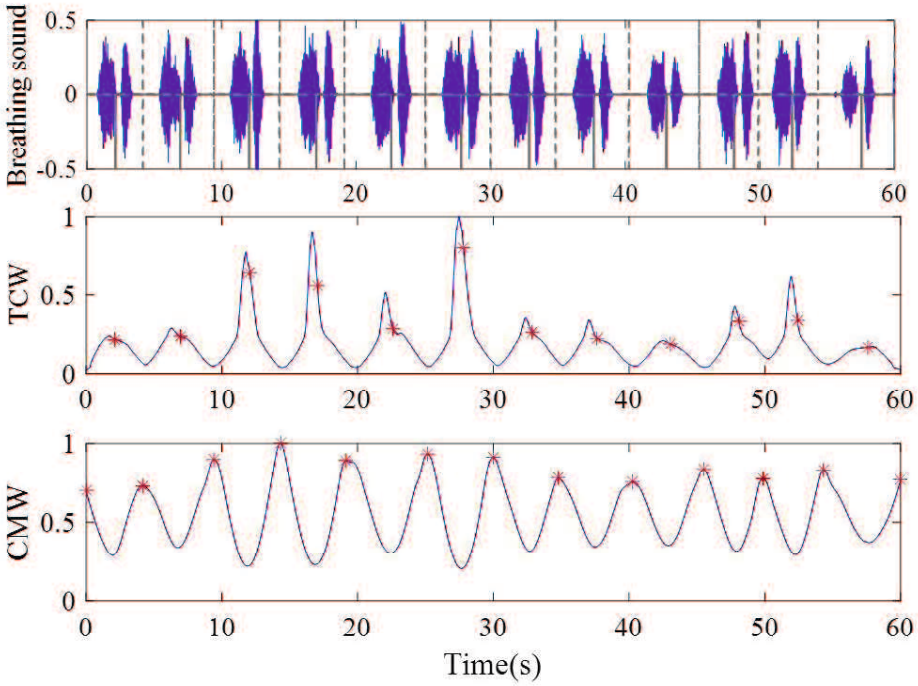

Figure 2.15 Inspiration and expiration segmentation for case 1

The sleep breathing sound data from six cases are applied to segment the inspiration and expiration by the proposed method. The results are shown in Table 2.4.

Table 2.4 Detection results of respiratory phases segmentation

Case No.	Total Breathing Cycle Number	Successful segmented inspiration and expiration Number	Successful Rate (%)
1	890	860	96.63
2	891	855	95.96
3	1177	1160	98.56
4	702	685	97.58
5	678	663	97.79
6	663	641	96.68

As the results listed in Table 2.4, the successful rate of the proposed detection method can reach to 98.56%. For OSA case, 96.68% of breathing cycles can be segmented into inspiration and expiration correctly. The proposed method can

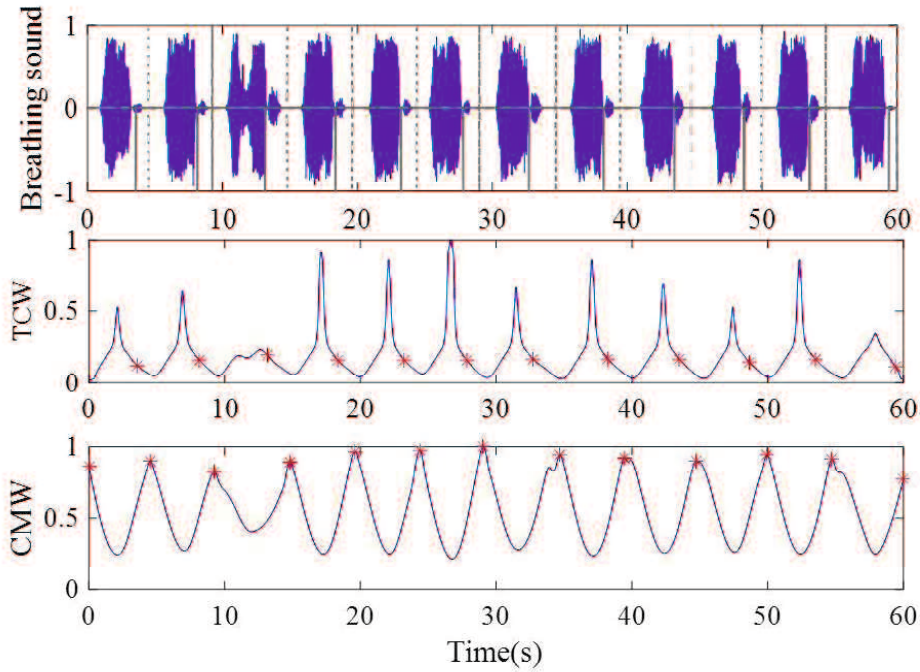

Figure 2.16 Inspiration and expiration segmentation for case 2

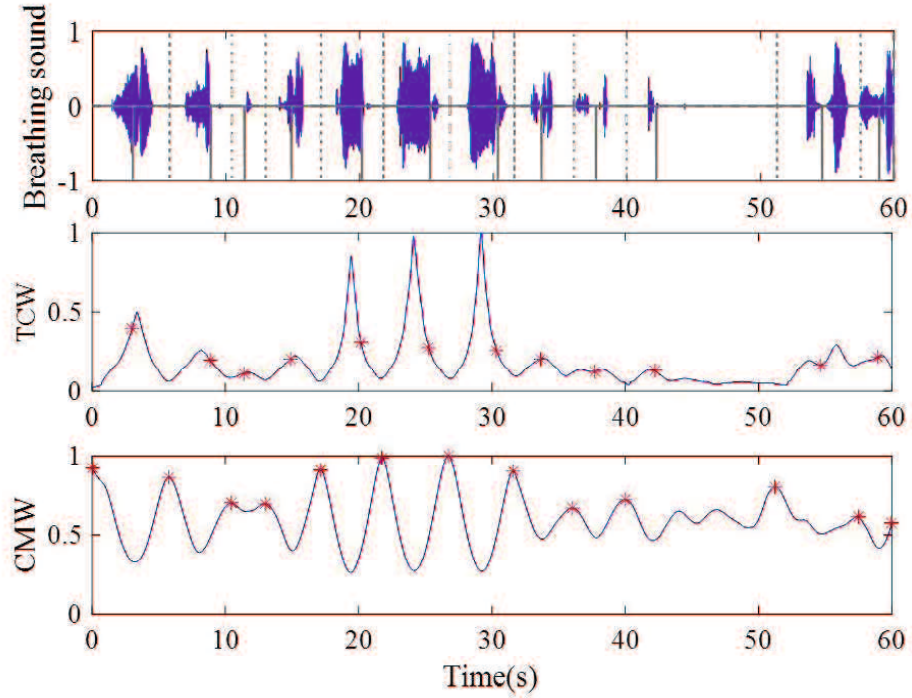

Figure 2.17 Inspiration and expiration segmentation for case 3

been validated to be effective for detection of respiratory phases, and it is the base of the continuous study.

2.5 Conclusion

Breathing cycle segmentation is the base of the further analysis for sleep state monitoring. In considering of the complexity of the breathing states during one night, a breathing waveform segmentation method is proposed in this chapter. Firstly,the enhanced preprocessing is applied to reduce the amplitude contrast diminution. Then the waveforms of TCW and CMW are extracted. With finding the local extreme points, the breathing cycle and inspiration/expiration can be segmented successfully. Moreover, the time duration of segmented breathing cycles can be acquired for continuous study.

The proposed sleep breathing waveform segmentation method has high accuracy, the average successful rate is 98.4% for breathing cycle segmentation and 96.68% for inspiration and expiration segmentation. At the same time, the parameter selection of the proposed method has high adaption for different testers as well as one tester in different monitoring time. It is a very useful automatic segmentation. And the high computation speed of the proposed method is helpful for whole night monitoring.

Chapter 3

Breathing state identification in time-domain and AHI detection

3.1 Sleep breathing state monitoring with breathing cycles

Sleep breathing sound signal is generated by the movement of air through the respiratory system, nose and mouth. It is always affected by tester's healthy condition, mental state, sleeping environment and so on. Breathing-related sleep disorders are characterized by abnormalities of respiratory pattern or the quantity of ventilation during sleep [53]. It is considered as chronic illnesses which needs long-term treatment and management. Obstructive sleep apnea (OSA) is a kind of major breathing-related sleep disorders. OSA is described by full or partial occlusion of the upper airway during sleep which can produce decreased oxyhemoglobin desaturations and sleep fragmentation [51, 54].

The Apnea-Hypopnea Index (AHI) is described by the number of apnea and hypopnea events per hour to assess OSA severity. It is an key indicator for OSA monitoring. An apnea is commonly defined by a minimum of 10s interval pause of breath. The hypopnea is overly shallow breathing or an abnormally low respiratory rate, lower than 9 times/min [55]. Usually, the ventilation of hypopnea will reduce to less than 50%of ventilation while normal breathing or cause the value of oxygen levels declining by more than 4%. The value of AHI can eluate the severity of OSA. AHI of 5-15 indicates mild, 15-30 indicates moderate and over

30 indicates severe OSA [56].

In our previous study shown in Fig.3.1, the breathing cycle time can be detected by the first peak of the frequency spectrum of 10-second breathing sound signal. It is useful for the stable sleep breathing state.

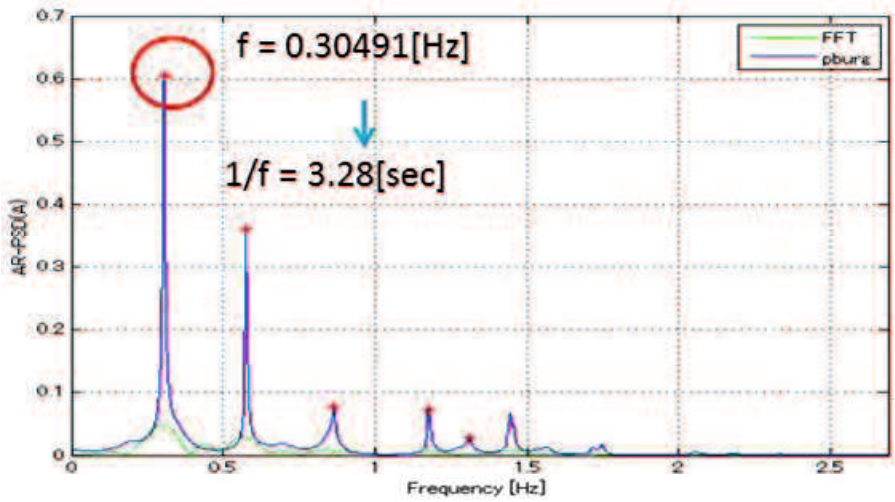

Figure 3.1 sleep breathing state monitoring

Whatever apnea and hypopnea, the blood oxygen level will decline by decreasing ventilation. Here the monitoring result of blood oxygen level is displayed and compared with the monitoring results of breathing cycles. The blood oxygen level (SpO2) is tested by a tabletop Pulse Oximeter shown in Fig.3.2.

Here one hour monitoring is shown by breathing cycle time and oxygen saturation(SpO2). In Fig.3.3. (a) is the breathing cycle time calculated by frequency spectrum. (b) is the results based on sleep breathing waveform segmentation introduced in chapter 2. The data of SpO2 is shown in the plot(c). According to the report of SpO2, the median value is 94%. Hence, the data lower than 90% mean abnormal breathing ventilation.

It is easy to find that the sleep breathing waveform segmentation can get the exacter time duration of each breathing cycle from Fig.3.3. From 300s to 900s, there are several apnea and hypopnea based on the results shown in Fig.3.3(b). The SpO2 data also display the abnormal state. Fig.3.3(b) can not show the apnea and hypopnea part clearly. From 2700s, the breathing state become stable, (a) and (b) show the similar monitoring results.

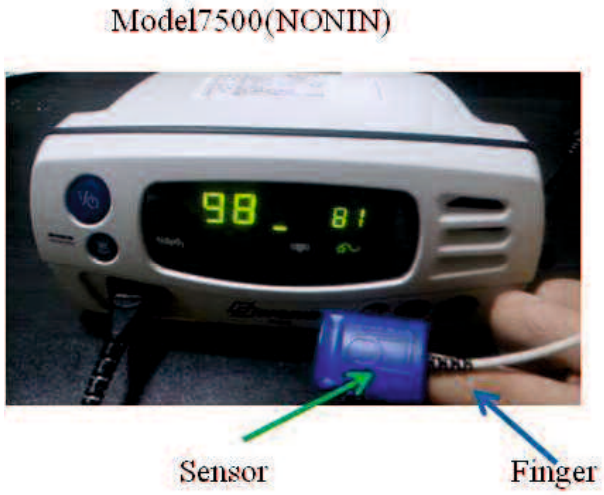

Figure 3.2 Blood oxygen level tested by a tabletop Pulse Oximeter

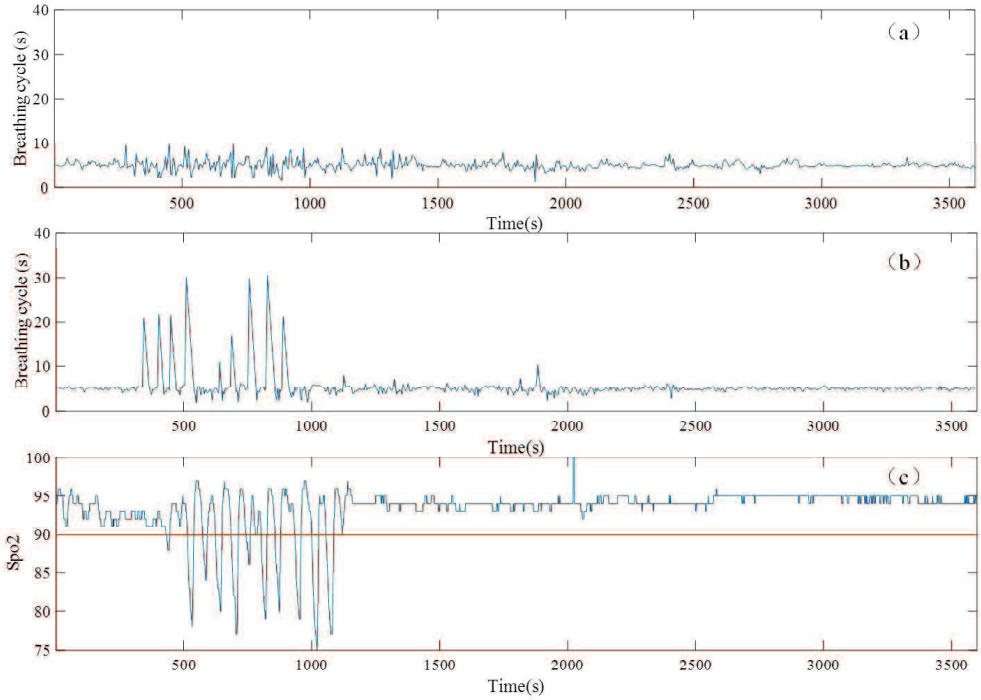

Figure 3.3 sleep breathing state monitoring

The efficiency of the proposed segmentation method is validated again by above case. Based on the segmentation results, the abnormal breathing state will be described in detail.

3.2 Definition of normal and abnormal breathing patterns

Abnormal breathing section can be reflected by changing respiratory rate, respiratory phase, respiratory intensity and so on. According to the definition of apnea and hypopnea in clinic, the normal and abnormal breathing patterns are defined in this section. Based on the segmentation results of chapter 2, the breathing patterns are described by the time durations of breathing cycles and expiration.

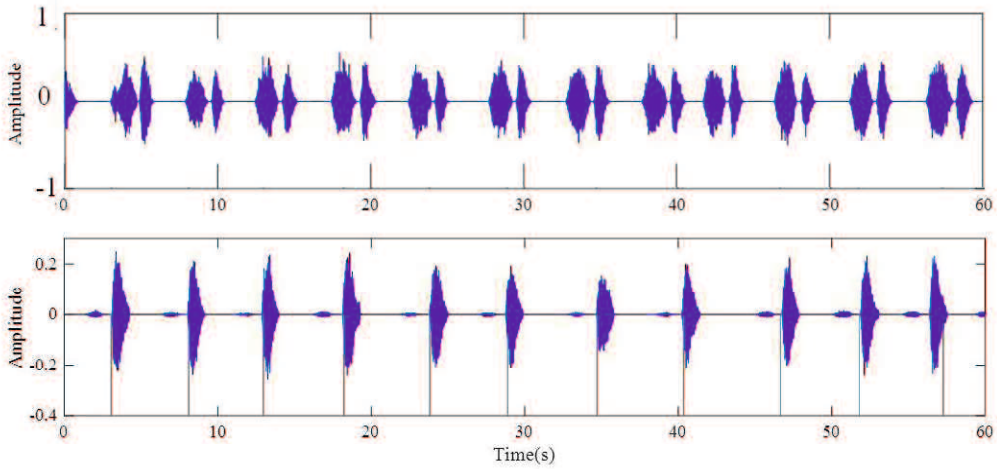

Figure 3.4 Examples of normal breathing pattern.(Pattern No.1)

Two examples of pattern No.1 is shown in Fig.3.4. The signal in the fist plot has similar intensity for both inspiration and expiration. The expiration of the signal in the second plot has much stronger intensity compared with inspiration. Although there is the intensity difference between the inspiration and expiration, the breathing period of two examples is stable. Moreover, the amplitudes of each cycle is similar.

The breathing signal with stable respiratory rate, respiratory intensity and clear respiratory phase belongs to pattern No.1, i.e. the normal breathing pattern.

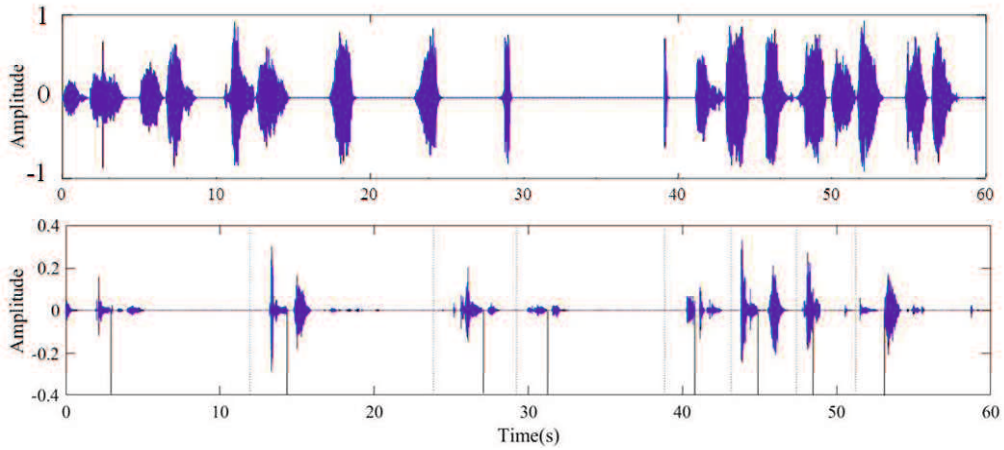

Figure 3.5 An example of hypopnea pattern.(Pattern No.2)

Fig.3.5 shows the pattern 2, hypopnea pattern. In the first plot, there is a obvious hypopnea cycle with breathing pause near 10 seconds. As shown in the bottom plot, there are eight breathing cycles which belongs to abnormal breathing while the respiratory rate is lower than 9 times/s according to the reference. The respiratory rate and intensity changes greatly. Based on the inspiration and expiration segmentation results, the abnormal expiratory pauses can be found. The expirtatory pause of some breathing cycles lasts much longer than the stable breathing (pattern No.1).

A stable normal breathing cycles will last about 5s for the normal breathing pattern shown in Fig.3.4.

Commonly, the inspiration and expiration last 1 $\sim$ 1.5s, the inspiration pause lasts about 0.2s. If the stable breathing cycle last about 5s, the expiration pause will last about 36 $\sim$ 56% of one cycle time. The expiratory pause of pattern No.2 can reach to about 8s which is more than two times of expiratory pause while breathing normally. Hence the pattern No.2 can be defined by the expiratory pause which is more than two times of normal expiratory pause and less than 10 seconds, that is hypopnea. The hypopnea could be estimated by the threshold of more than 1.2 times of the normal breathing cycle.

In addition, respiratory rate less than 9 times/min means hypopnea, so the average time duration of hypopnea event will be 6.66 seconds.

Pattern 3 is apnea pattern as shown in Fig.3.6. Apnea pattern is defined by more than 10-second breathing pause. So the apnea will last 10 seconds plus the

time duration of a stable breathing cycle at least.

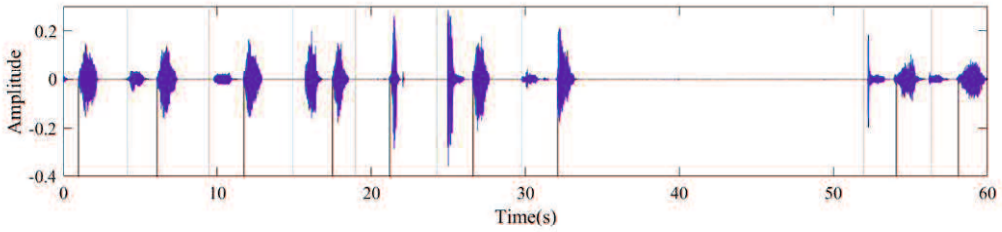

Figure 3.6 An example of apnea pattern.(Pattern No.3)

3.3 AHI detection for sleep state monitoring

3.3.1 Apnea detection based on breathing cycle segmentation

The time duration of breathing cycle can be calculated by the breathing cycle segmentation method. The changing trend of breathing cycles during one night for the OSA case is shown in the bottom plot of Fig3.7. The x axis is the monitoring time, about 5 hours. The y axis is the time duration of each segmented breathing cycle. The time duration values of each segmented breathing cycle is denoted by $dd(i)$.

In the top, the waveform of original breathing data is displayed. Y-axis is the amplitude of breathing. It shows the huge vibration of intensity during the whole night.

It can be found that the normal and stable breathing cycle last about 5 seconds. The longest apnea is more than 30 seconds. As refereed above, threshold value of apnea identification is set as dd_{stable} + 10. In this case, the threshold value is used as 15s to monitor the apnea. Eight apnea cycles have been identified in the third hour denoted by as A_i .

The changing trend of sleep respiratory rate counted by segmented cycles per minute is shown in Fig.3.8. The RR_{stabel} is 12 times/min by observing. While the RR is less than 10 times/min, that means there is a breathing pause lasting more than 10s. Based on the the threshold value, 7 abnormal values are detected. Respiratory rate represents the average value in one minute. Because the exact

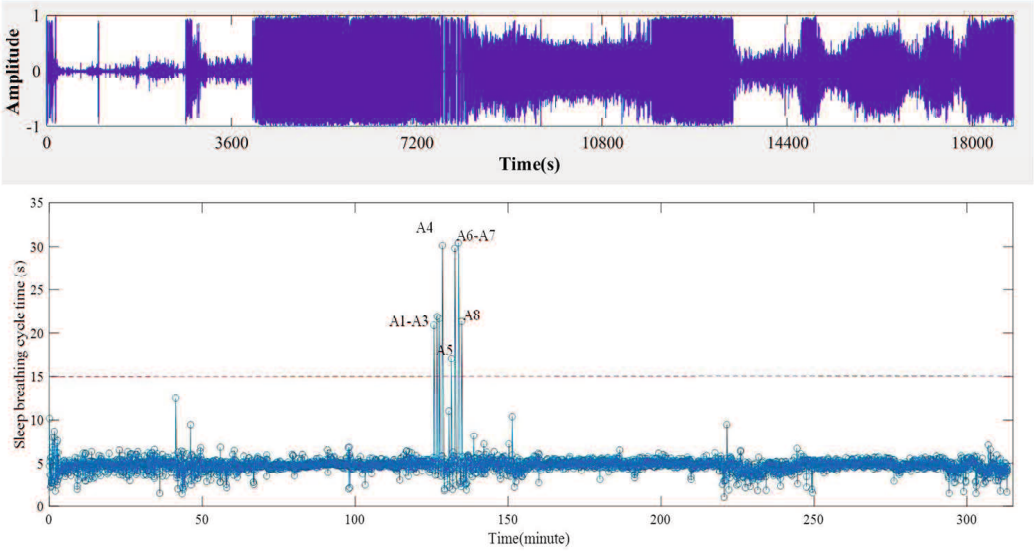

Figure 3.7 Time duration values of each segmented breath cycle during whole night

breathing cycle duration is required for AHI detection, using respiratory rate can not detect all of the apnea cycles.

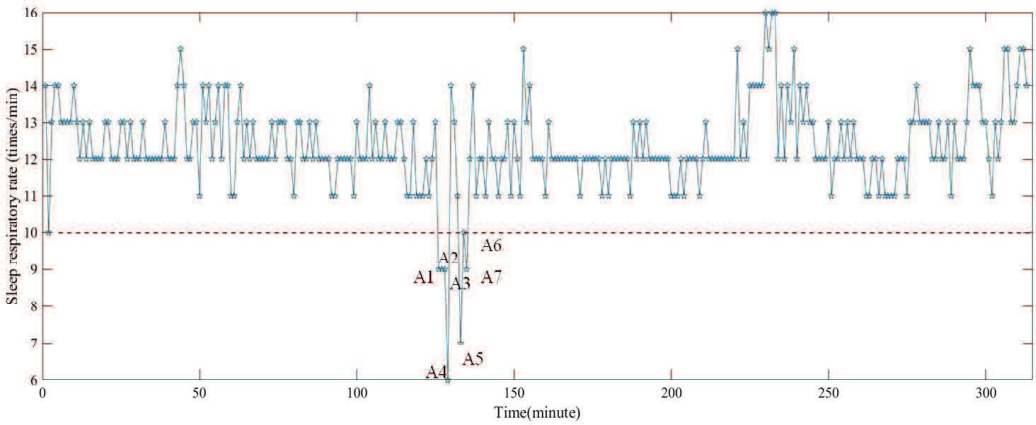

Figure 3.8 Monitoring of Sleep respiratory rate during whole night

Here the monitoring result of SpO2 is displayed in the first plot of Fig.3.9. It is used to compare with the monitoring results of our proposed identification method shown in the second plot. According to the report of SpO2 detection, the median value of SpO2 during whole night monitoring is 94 %. So the threshold value reflecting abnormal breathing is set as 90%, reducing more than 4% of the normal state.

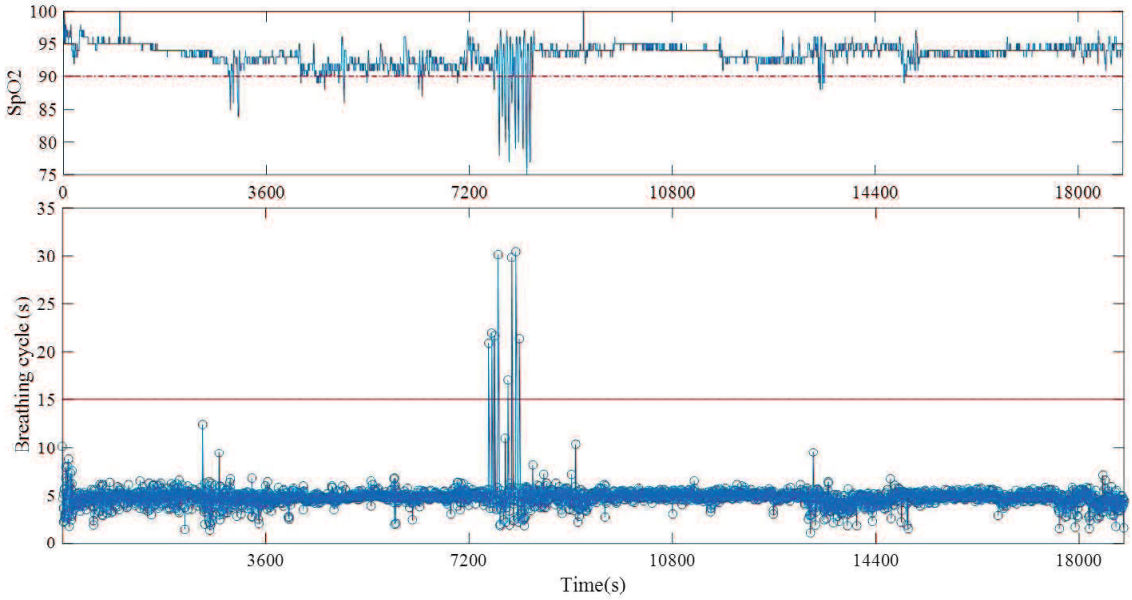

Figure 3.9 AHI detection compared with the SpO2 monitoring

Fig.3.10 displays the details of the comparison while the SpO2 changes greatly and drops down to less than 90%. From 7500 to 8200s, there are eight apnea events detected as shown in Fig.3.10. The value of SpO2 decreases in the same time. The SpO2 decreases to less than 80% of normal state showing the severe oxygen deficiency. The monitoring result of the proposed method is accord with the results of SpO2.

From 2500 to 3000 seconds, there are lots of larger values detected by the proposed method. The value of SpO2 decreases less than 85% around 3100s.

Around 13300s and 14700s, there are lots of larger values detected by the proposed method and the values of SpO2 are below the threshold value in the same time.

The obstruction of airway generates apnea and hypopnea events, leading to the less support of oxygen. The phenomenon can be reflected by the decreased value of SpO2. The efficiency of the proposed identification of apnea has been validated. It has potential to identify the hypopnea events by the time duration of breathing cycles.

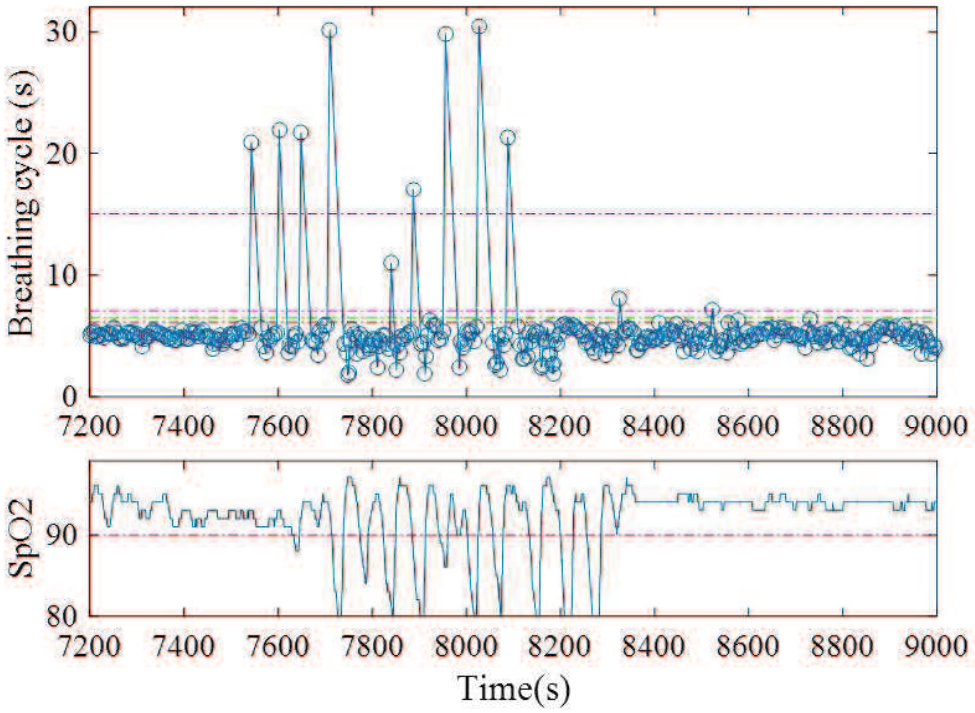

Figure 3.10 Details of AHI detection compared with the SpO2 monitoring

3.3.2 Hypopnea detection based on breathing cycle time

As the definition of hypopnea, the time duration of hypopnea cycle will last more than 1.2 times of stable breathing cycle time. For the OSA case, three threshold values are set as 6s, 6.5s and 7s respectively.

The hypopnea detection results during the whole night are shown from Fig.3.11. Thv is the threshold value. The beginning and ending of the sleep belonging to the wakefulness state would not be necessary to analyze.

Fig.3.12 displays parts of hypopnea events identified by Thv=7s. The expiration pause of hypopnea can reach to about 9 seconds. They are the typical hypopnea events.

According to the detection results while threshold value set as 6s, some detected parts are shown from Figs.3.13 and 3.14. Although there is not obvious long expiration pause compared with typical hypopnea, the detected parts shows unstable periodicity and changing breathing intensity. Moreover the noise caused

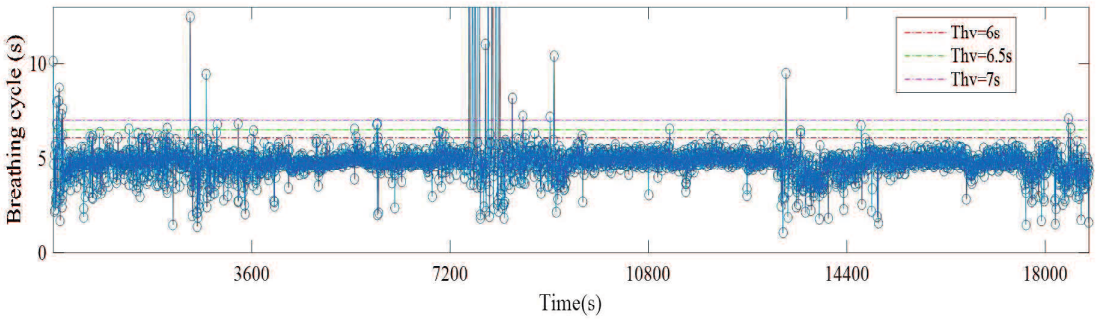

Figure 3.11 Hypopnea detection of OSA case during the first night

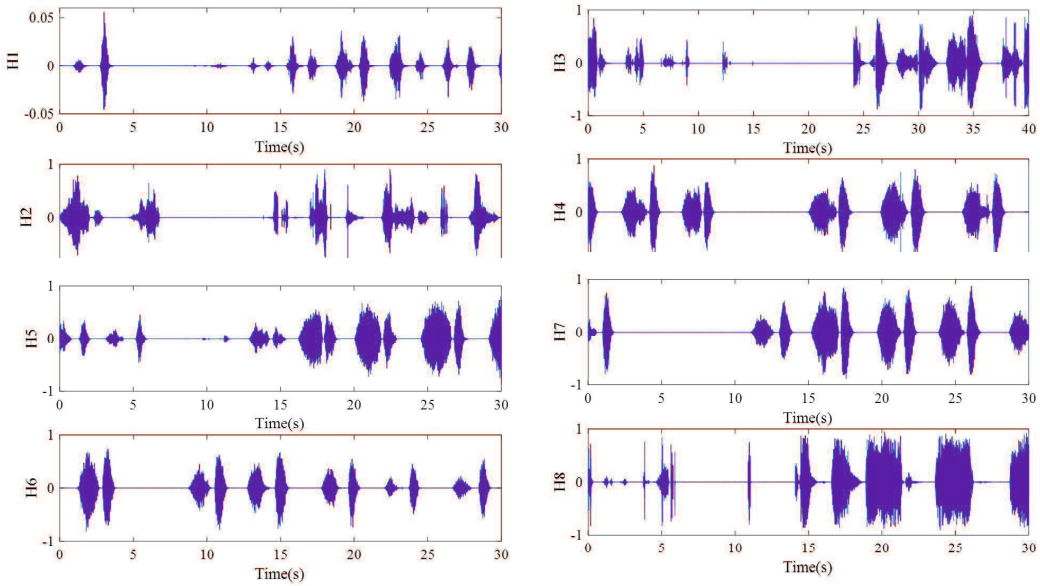

Figure 3.12 Hypopnea events detected by Thv=7s

by mouth movement can be found which affects the breathing frequency. The breathing cycles with length near the boundary of the hypopnea definition should be payed much more attention. It will be very important for OSA analysis.

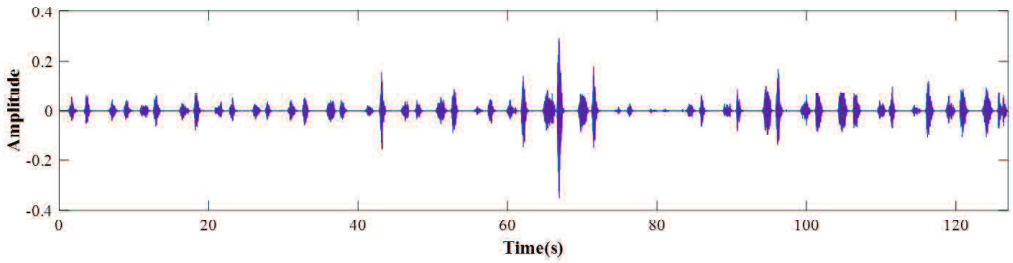

Figure 3.13 Hypopnea events detected by Thv=6s

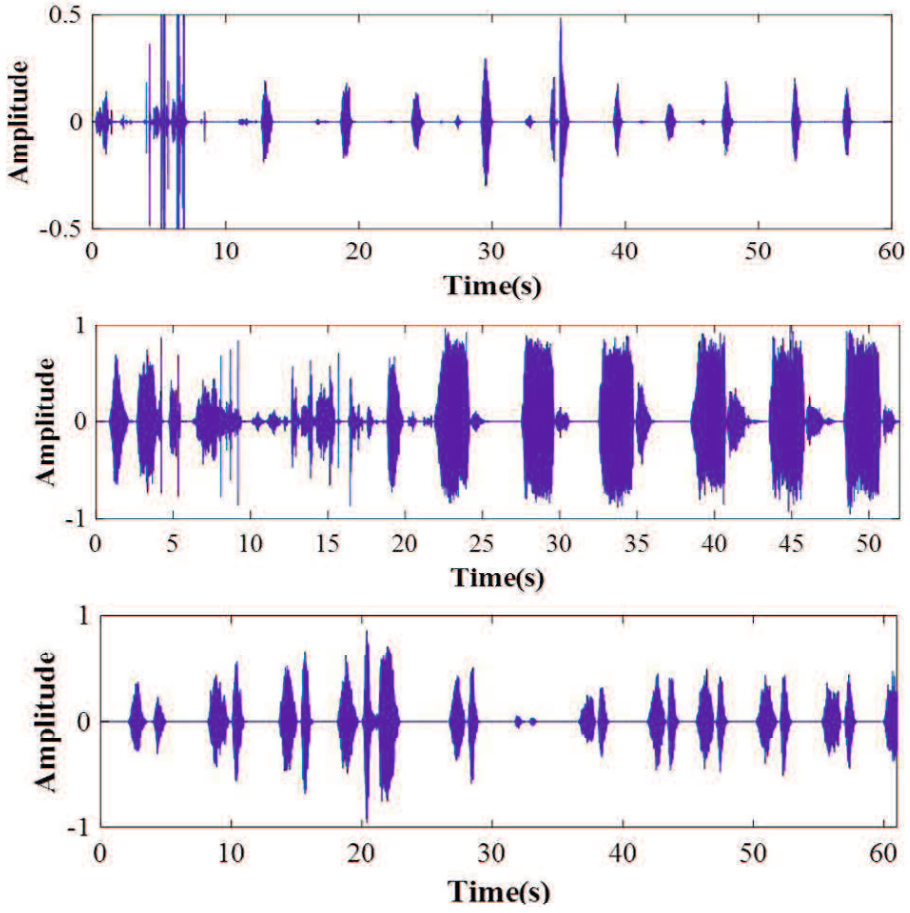

Figure 3.14 Hypopnea events detected by Thv=6s

The detection results by different threshold value can be found in Table3.1.

AHI is the number of apnea and hypopnea in one hour. In that night, the AHI is 13.6 times/hour while Thv=6s, 6.6 times/hour while Thv=6.5s, 4.4 times/hour while Thv=7s.

Table 3.1 AHI detection result of OSA case for one night monitoring

Hour No.	Apnea	Hypopnea (Thv=6s)	Hypopnea (Thv=6.5s)	Hypopnea (Thv=7s)	AHI (Thv=6s)	AHI (Thv=6.5s)	AHI (Thv=7s)
1	0	28	14	8	28	14	8
2	0	13	3	0	13	3	0
3	8	11	5	5	19	13	13
4	0	6	2	1	6	2	1
5	0	2	1	0	2	1	0
Total	8	60	25	14	68	33	22

Checking up the detected cycles, we can find that the typical hypopnea cycles can be identified correctly while Thv=7s. When Thv=6s, the critical states can be detected and should be discussed deeply in the future.

3.3.3 Time duration extraction of breathing pause for apnea

As the results shown in Fig.3.15, since each segmented part contains a breathing signal, the breathing pause can be located by the maximum of the local extremum points in the apnea cycle marked by the blue circle in the CMW. The details are shown in following steps.

Step 1. Detect the apnea cycle.

Step 2. Find the maximum point in the interval of CMW for the apnea cycle, denoted by S_{pause}.

Step 3. Calculate the time duration between the S_{pause} and the boundary points of this apnea cycle, written as T_{left} and T_{right}.

Step 4. Compare the values of T_{left} and T_{right}. The longer one is the breathing pause time of the apnea.

As introduced in above steps, the time duration of breathing pause for each apnea can be computed by the segment points of apnea shown in the figure. In a simple way, the apnea pause time can be calculated by $dd(i) - dd_{stable}$.

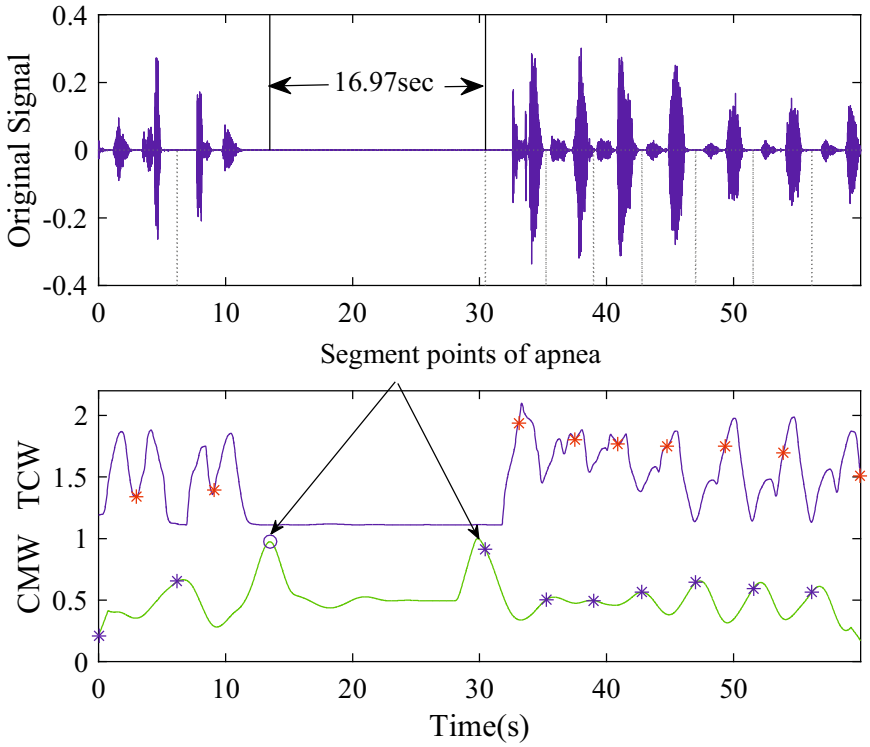

Figure 3.15 Extraction of time duration index for apnea

Figs.3.16,3.17 show the pause time calculation results at apnea event points $A1$ to $A8$ of Fig.3.7. The pause time durations of $A1$ to $A8$ are 15.33s, 13.2s, 16.8s, 24.32s, 12.1s, 22.67s, 22.7s and 17.8s respectively.

Long breathing pause lasting will lead to less oxygen support to heart and brain. It will cause increasing risk of heart infarction, cerebral infarction, stroke and so on. The breathing pause time of apnea will have potential to evaluate the obstruction level of airway to monitor OSA deeply.

3.3.4 More validation for AHI detection

Another three all night data from the OSA case and two night data from two young testers are applied to validate the AHI detection method based on time duration of breathing cycles.

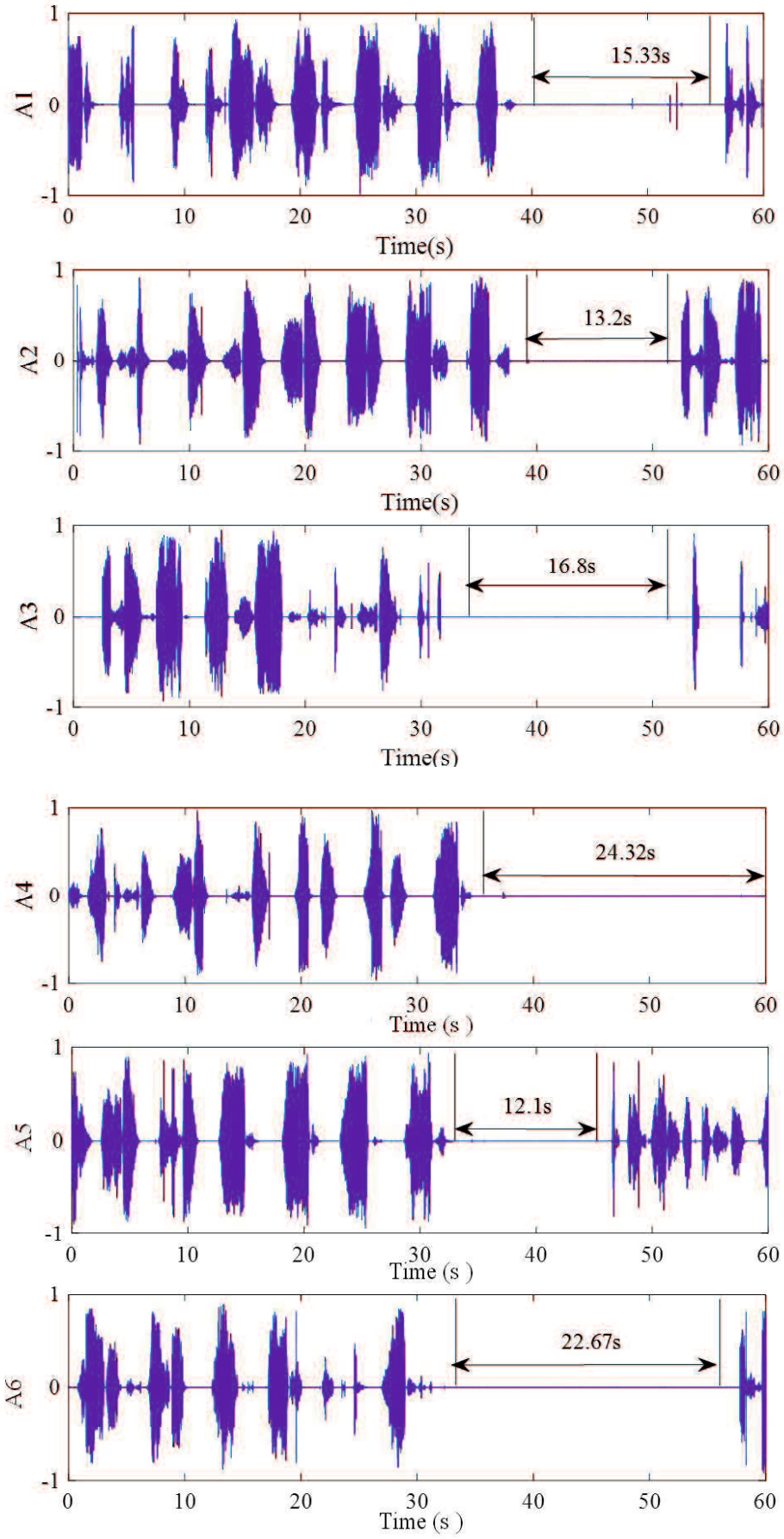

Figure 3.16 Sleep breathing sound signal waveforms with apnea events, A1-A6

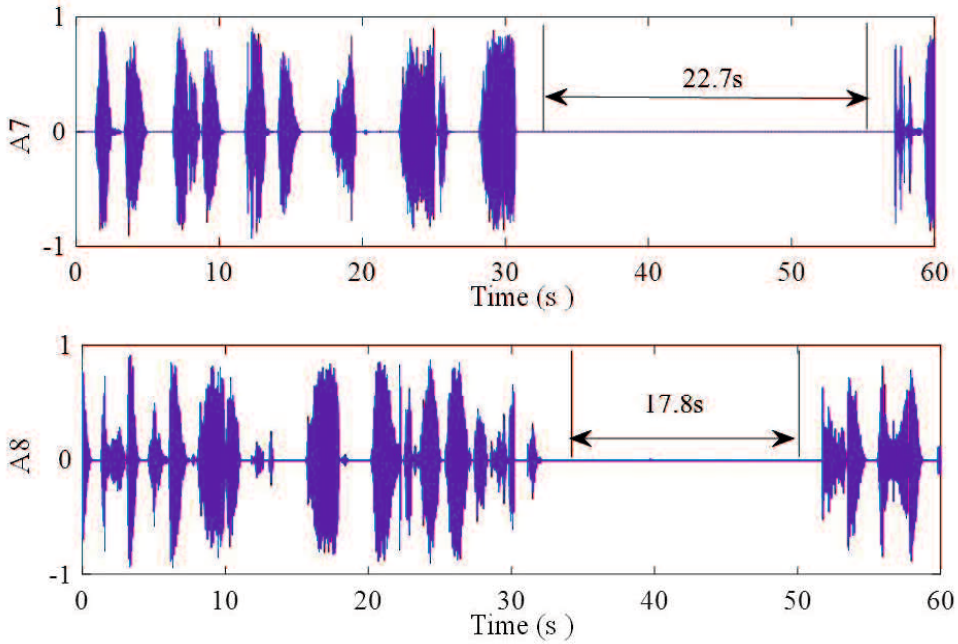

Figure 3.17 Sleep breathing sound signal waveforms with apnea events, A7-A8

Firstly, three all night monitoring results of OSA case are shown in Fig.3.18to 3.23. The threshold value of apnea detection is set as 15 seconds. In the same way, three threshold values are set as 6s, 6.5s and 7s for hypopnea detection.

Table 3.2 AHI detection result of OSA case for the second night monitoring

Hour No.	Apnea	Hypopnea (Thv=6s)	Hypopnea (Thv=6.5s)	Hypopnea (Thv=7s)	AHI (Thv=6s)	AHI (Thv=6.5s)	AHI (Thv=7s)
1	6	17	8	5	23	14	11
2	1	17	9	5	18	10	6
3	3	13	10	6	16	13	9
4	0	13	7	4	13	7	4
5	1	17	7	4	18	8	4
Total	11	77	41	24	88	52	35

The average value of AHI is 17.6 times/hour while Thv=6s, 10.4 times/hour while Thv=6.5s, 7 times/hour while Thv=7s.

According to the AHI detection in Tab.3.2, there are 11 apnea events. The apnea events monitored by threshold value are displayed orderly in Figs.3.20, 3.19. In each plot, X-axis is the time, Y-axis is the amplitude. The time durations

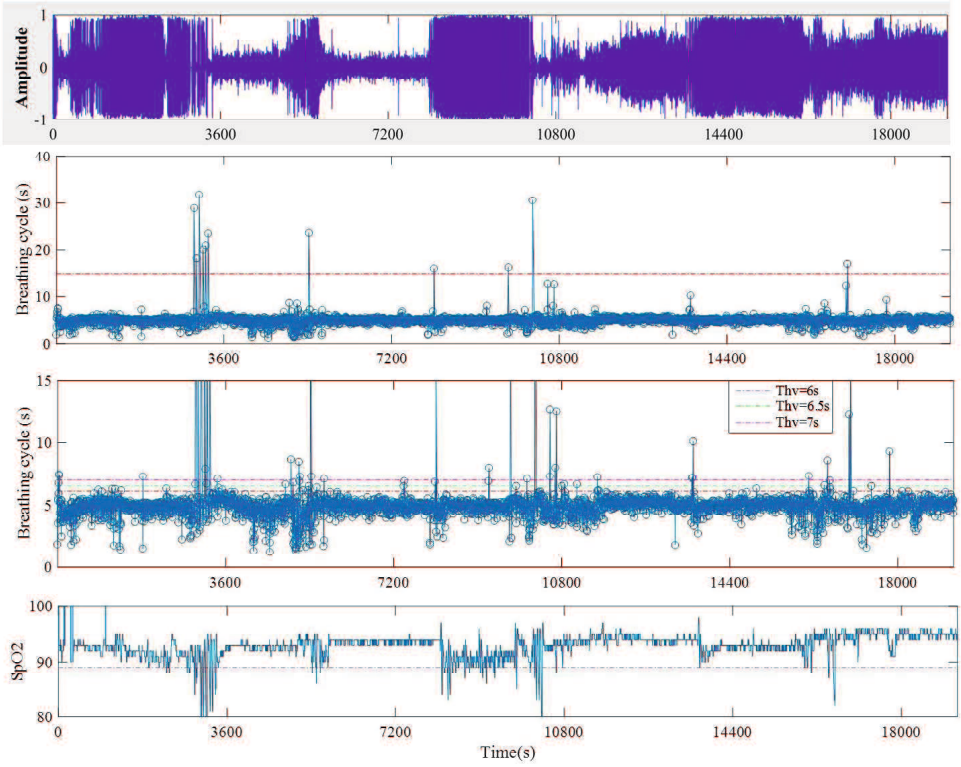

Figure 3.18 AHI monitoring for OSA during the second night

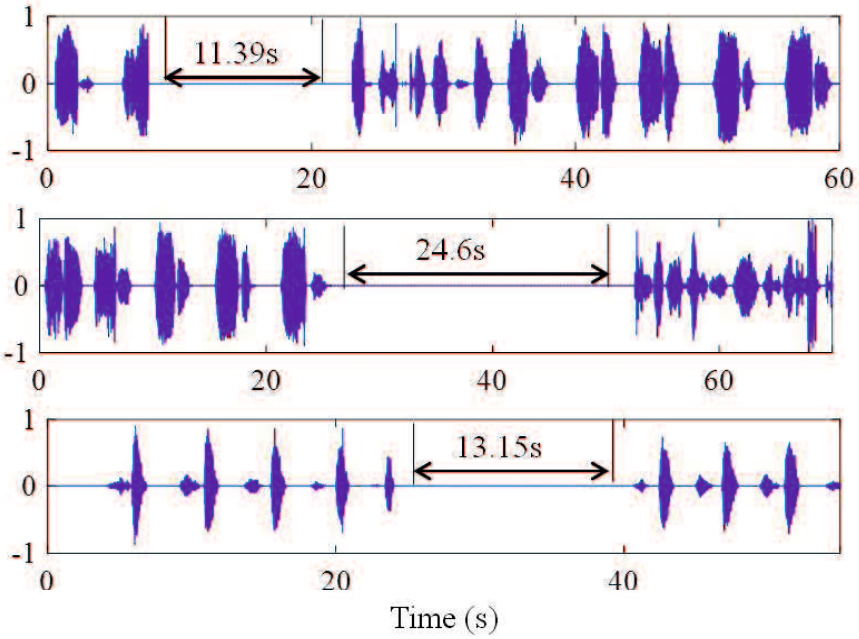

Figure 3.19 Apnea events for OSA during the second night (part 1)

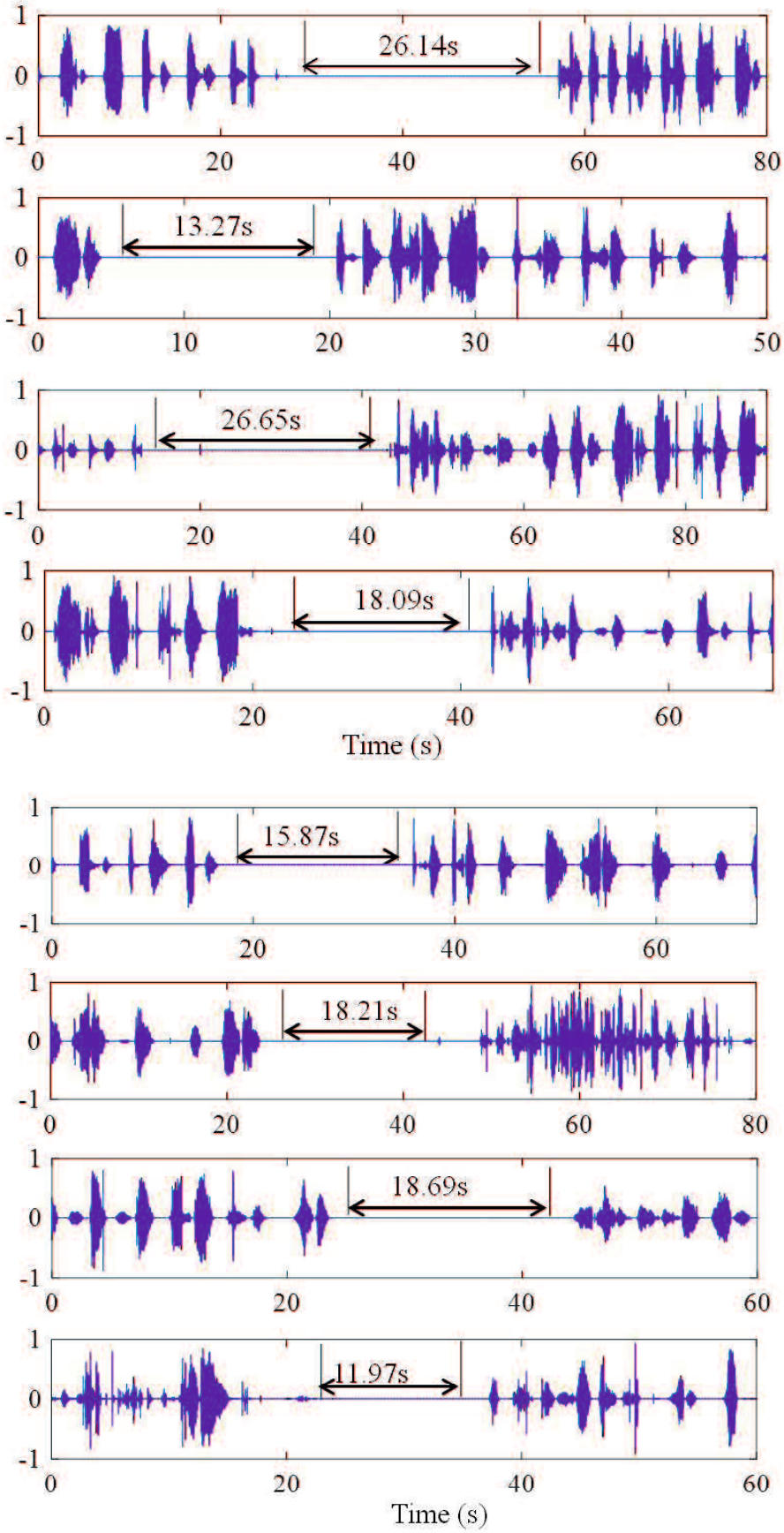

Figure 3.20 Apnea events for OSA during the second night (part 2)

of breathing pause for each apnea are calculated and shown in these figures. The longest breathing pause lasts near half a minute appearing in the first hour of sleep.

The monitoring result of SpO2 is shown in the bottom ofFig.3.18. The median value of SpO2 is 93%, so the value less than 89% represents the apnea and hypopnea. Compared with the SpO2, the location of the hypopnea and apnea events detected by the proposed method is reliable.

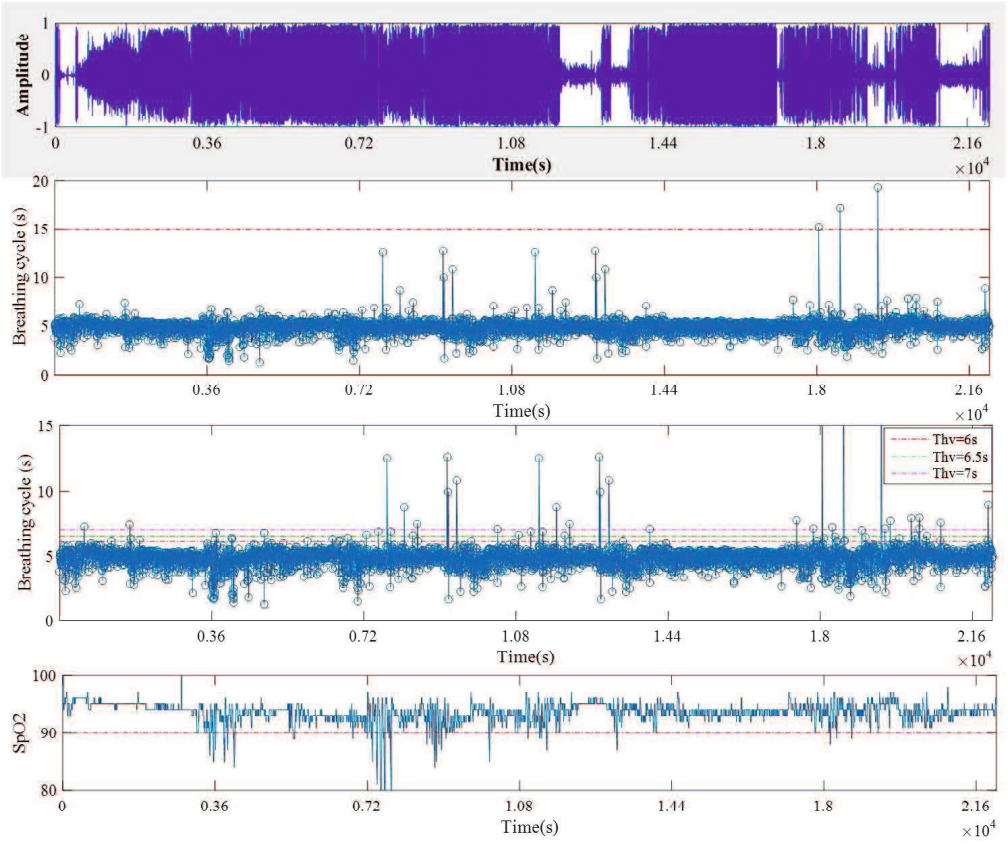

Figure 3.21 AHI monitoring for OSA during the third night

According to the Tab.3.3, the average value of AHI is 11.8 times/hour while Thv=6s, 7.0 times/hour while Thv=6.5s, 4.8 times/hour while Thv=7s.

The apnea events are shown in Fig.3.22. There are three apnea events detected in the sixth hour of sleep. The longest breathing pause of apnea lasts about 15s.

The monitoring result of SpO2 is shown in the bottom ofFig.3.21. The median value of SpO2 is 94%, so the value less than 90% represents the apnea and hypop-

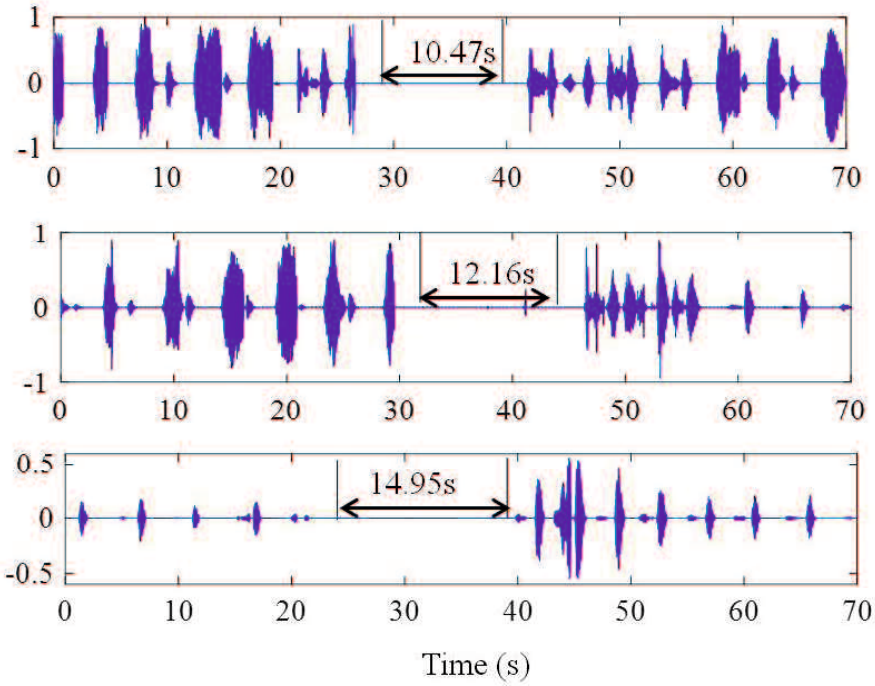

Figure 3.22 Apnea events for OSA during the third night

Table 3.3 AHI detection result of OSA case for the third night monitoring

Hour No.	Apnea	Hypopnea (Thv=6s)	Hypopnea (Thv=6.5s)	Hypopnea (Thv=7s)	AHI (Thv=6s)	AHI (Thv=6.5s)	AHI (Thv=7s)
1	0	5	2	2	5	2	2
2	0	11	2	0	11	2	0
3	0	13	11	7	13	11	7
4	0	13	11	7	12	11	7
5	0	3	2	2	3	2	2
6	3	23	11	8	25	14	11
Total	3	68	39	26	71	42	29

nea. The detection results of hypopnea and apnea matches with the monitoring of SpO2.

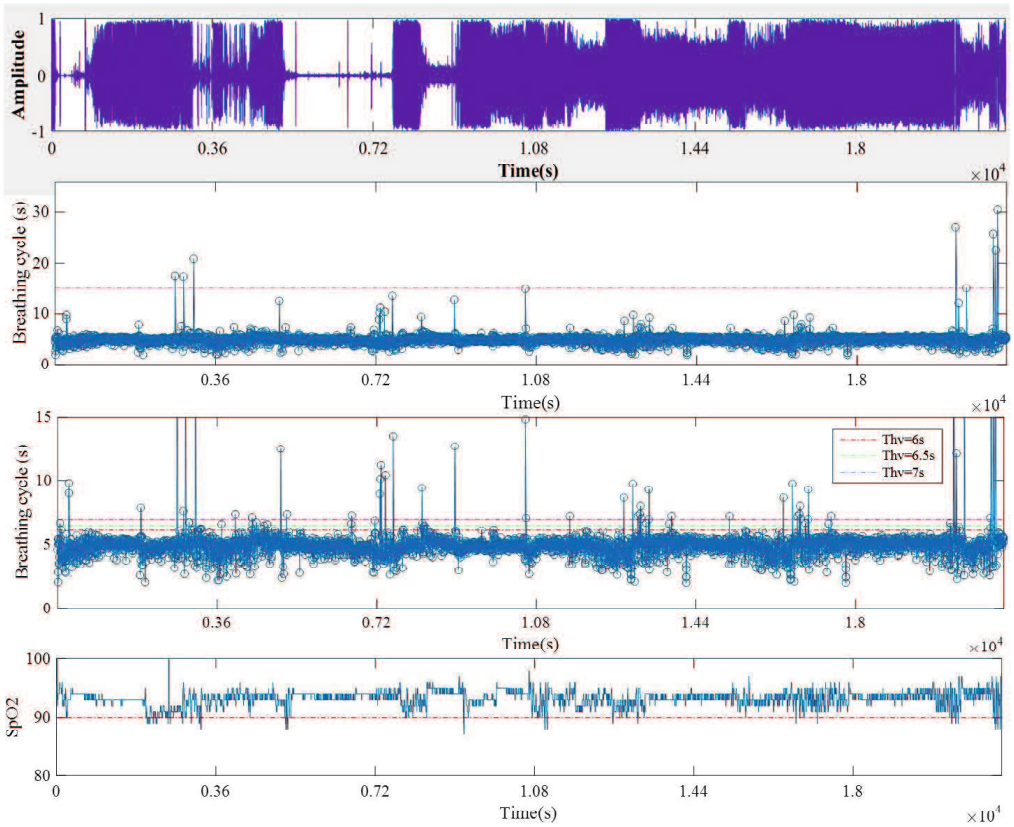

Figure 3.23 AHI monitoring for OSA during the fourth night

Table 3.4 AHI detection result of OSA case for the fourth night monitoring

Hour No.	Apnea	Hypopnea (Thv=6s)	Hypopnea (Thv=6.5s)	Hypopnea (Thv=7s)	AHI (Thv=6s)	AHI (Thv=6.5s)	AHI (Thv=7s)
1	3	15	7	4	18	10	7
2	0	20	11	5	20	11	5
3	0	22	11	9	22	11	9
4	0	14	12	9	14	12	9
5	0	14	12	9	14	12	9
6	5	9	3	2	14	8	7
Total	8	94	56	38	102	64	46

According to the Tab.3.4, the average value of AHI is 17 times/hour while Thv=6s, 10.7 times/hour while Thv=6.5s, 7.7 times/hour while Thv=7s.

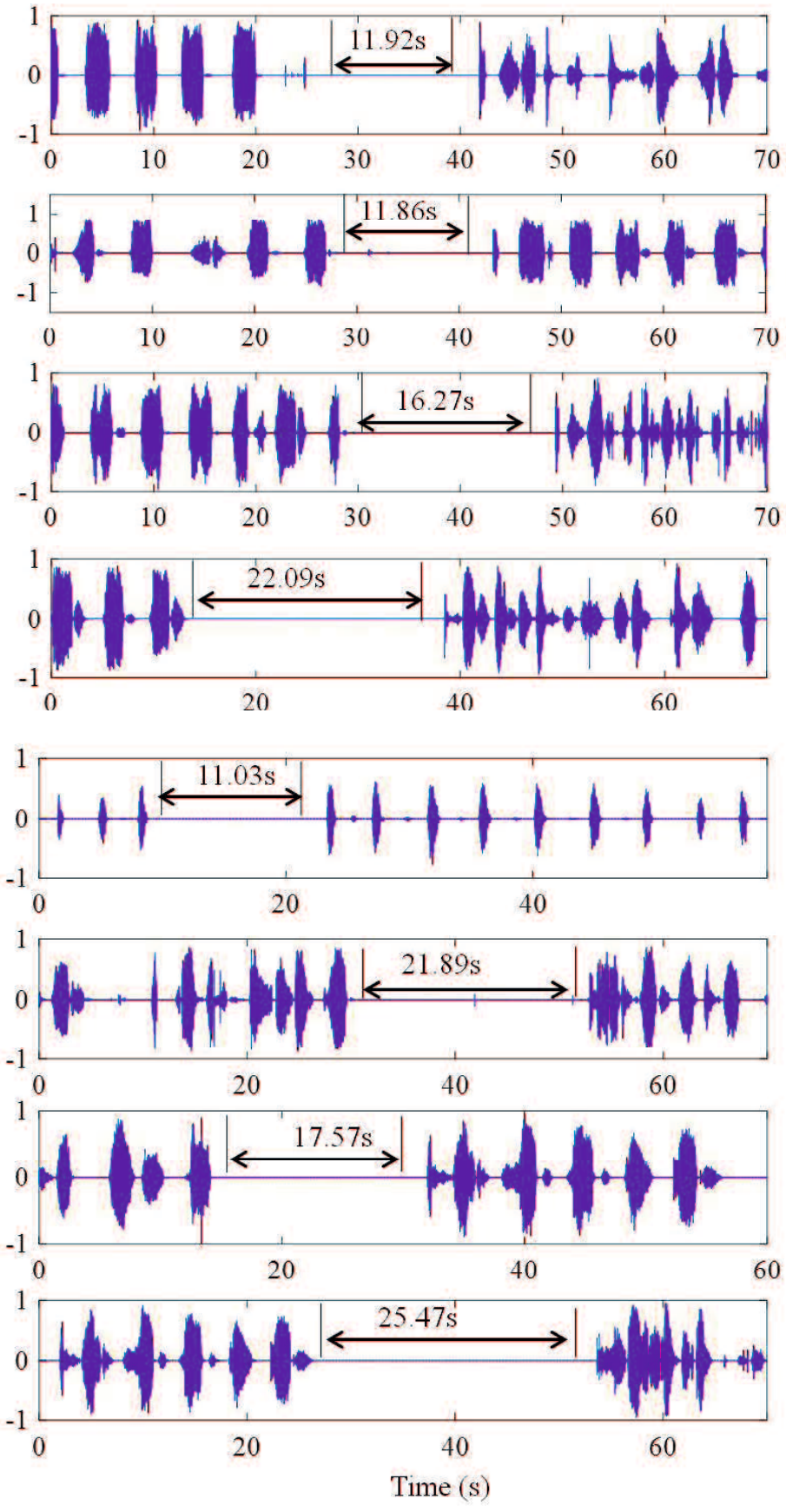

Figure 3.24 Apnea events for OSA during the fourth night

The apnea events detected are shown in Figs.3.24. There are eight apea events during the whole night. The longest time duration of breathing pause is more than 25s.

The monitoring result of SpO2 is shown in the bottom of Fig.3.23. The median value of SpO2 is 94%, so the threshold value is set as 90% to represent the apnea and hypopnea. The detection results of hypopnea and apnea is accord with the monitoring of SpO2.

In the same way, the time duration values $dd(i)$ of each breathing cycle for a young test A is shown in Fig.3.25. The stable breathing cycle lasts about 4 seconds. So the threshold value of apnea detection is set as 14 seconds. Three threshold values are also set as 6s, 6.5s and 7s for hypopnea detection.

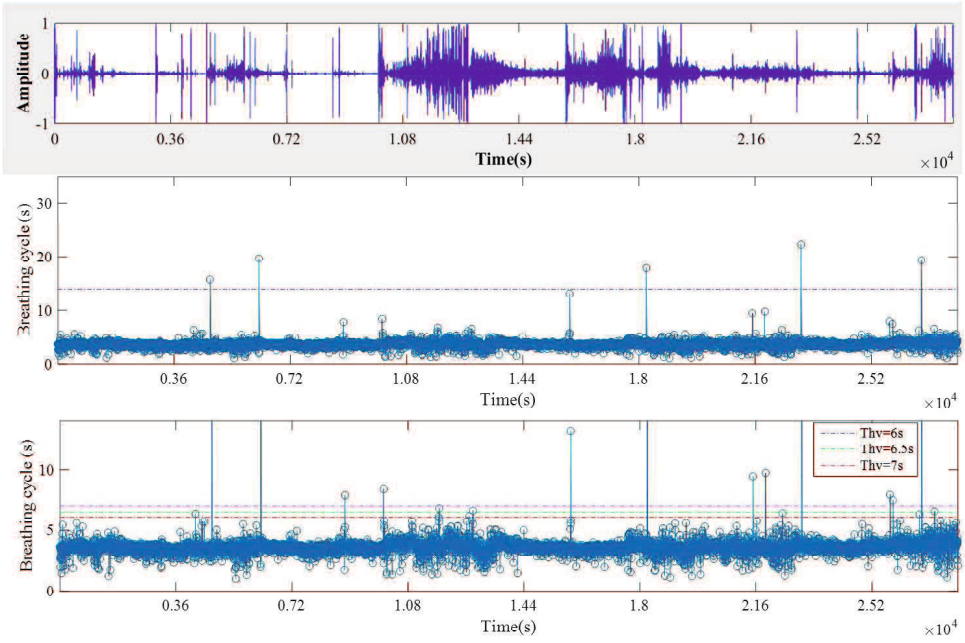

Figure 3.25 AHI monitoring for a young tester A

According to the Tab.3.5, the average value of AHI is 2.5 times/hour while Thv=6s, 1.9 times/hour while Thv=6.5s, 1.5 times/hour while Thv=7s. The tester A can be identified as normal case.

The apnea events detected are shown in Figs.3.26. There are five apnea events during the whole night. The longest time duration of breathing pause is more than 20s.

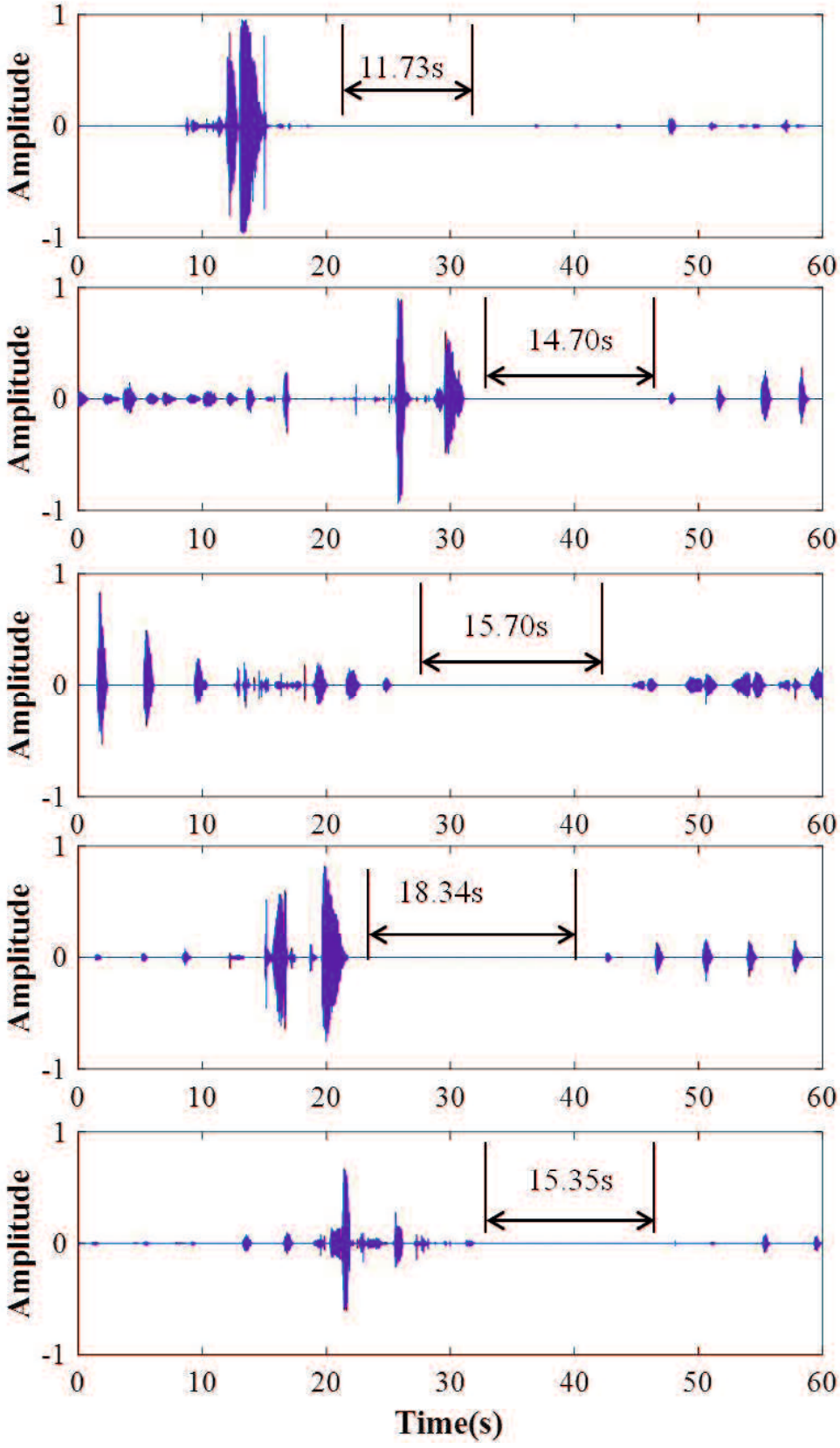

Figure 3.26 Apnea events detected for a young tester A

Table 3.5 AHI detection result of the young tester A during whole night monitoring

Hour No.	Apnea	Hypopnea (Thv=6s)	Hypopnea (Thv=6.5s)	Hypopnea (Thv=7s)	AHI (Thv=6s)	AHI (Thv=6.5s)	AHI (Thv=7s)
1	0	0	0	0	0	0	0
2	2	1	0	0	3	2	2
3	0	2	2	2	2	2	2
4	0	4	2	0	4	2	0
5	0	1	1	1	1	1	1
6	1	1	1	1	2	2	2
7	1	2	1	1	3	2	2
8	1	4	3	2	5	3	3
Total	5	15	10	7	20	15	12

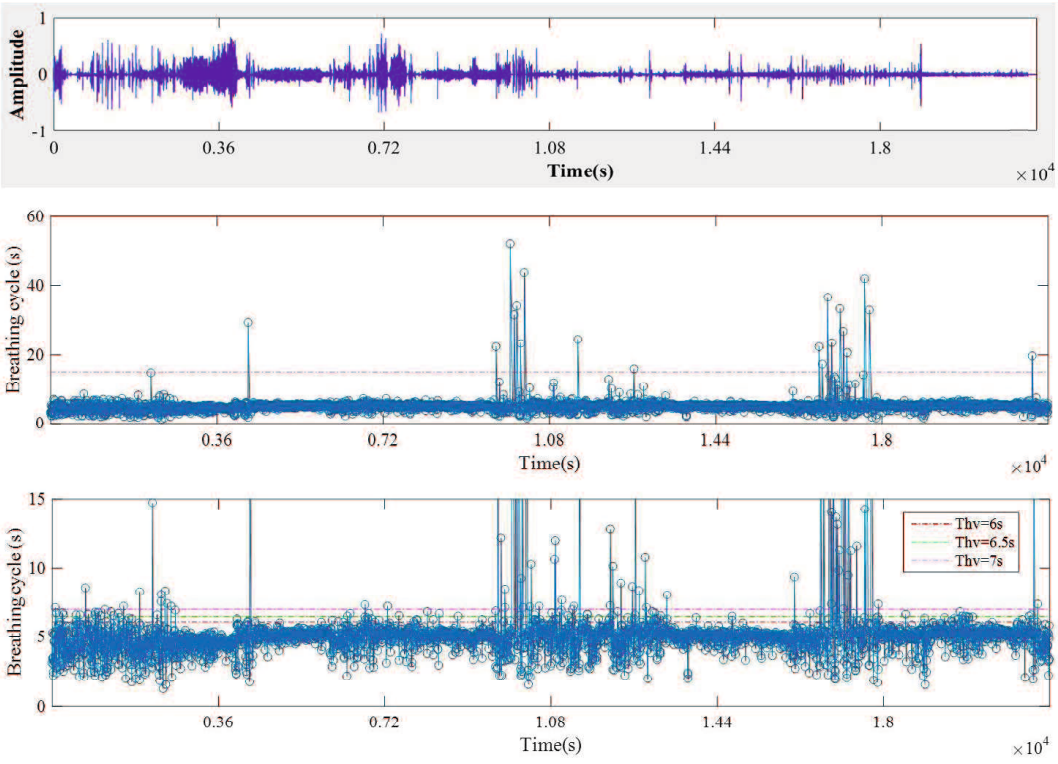

Figure 3.27 AHI monitoring for a young tester B

For another young tester B, the time duration values of each breathing cycle is shown in Fig.3.27. The stable breathing cycle lasts about 5 seconds. So the threshold value of apnea detection is set as 15 seconds. Three threshold values are set as 6s, 6.5s and 7s for hypopnea detection.

According to the Tab.3.5, the average value of AHI is 35.5 times/hour while Thv=6s, 19.2 times/hour while Thv=6.5s, 11.2 times/hour while Thv=7s. The longest breathing pause reaches to 48s. The tester A can be identified as moderate or severe OSA.

Table 3.6 AHI detection result of the young tester B during whole night monitoring

Hour No.	Apnea	Hypopnea (Thv=6s)	Hypopnea (Thv=6.5s)	Hypopnea (Thv=7s)	AHI (Thv=6s)	AHI (Thv=6.5s)	AHI (Thv=7s)
1	0	33	26	10	33	26	10
2	1	20	4	1	21	5	2
3	6	34	16	9	40	22	15
4	2	53	26	14	55	28	16
5	9	33	17	13	42	26	22
6	1	21	7	1	22	8	2
Total	19	194	96	48	213	115	67

Tester B is a 21-year old student. Although he is young, there are many apnea and hypopnea events during sleep. It will affect the health condition if it continues during a long time. Hence, the sleep monitoring is necessary for daily healthcare not only for the aging but also for common adults.

3.4 Conclusion

AHI is the key indicator to diagnose and evaluate OSA. To acquire the AHI, the apnea and hypopnea are defined by the time duration of breathing cycle and breathing phase. According to the definition, the time duration of each breathing cycle can provide exact results for apnea identification. For identification of hypopnea, the results are depend on the threshold value. And the pause time of apnea can also be calculated based on TCW and CMW. It has potential to evaluate the condition of apnea will be studied deeply in future.

The sleep breathing monitoring for OSA case during four nights and two young testers during one night separately are applied to validate the efficiency

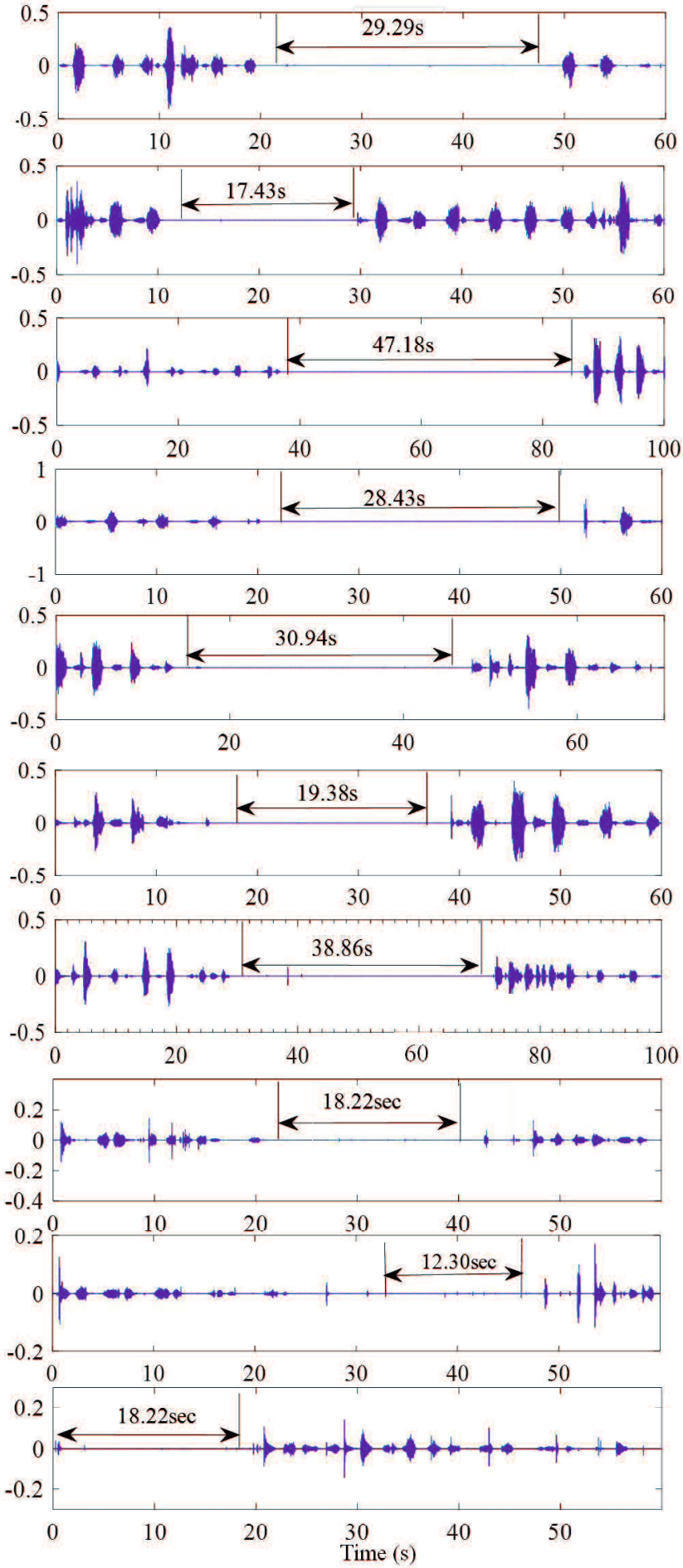

Figure 3.28 Apnea events of tester B (part 1)

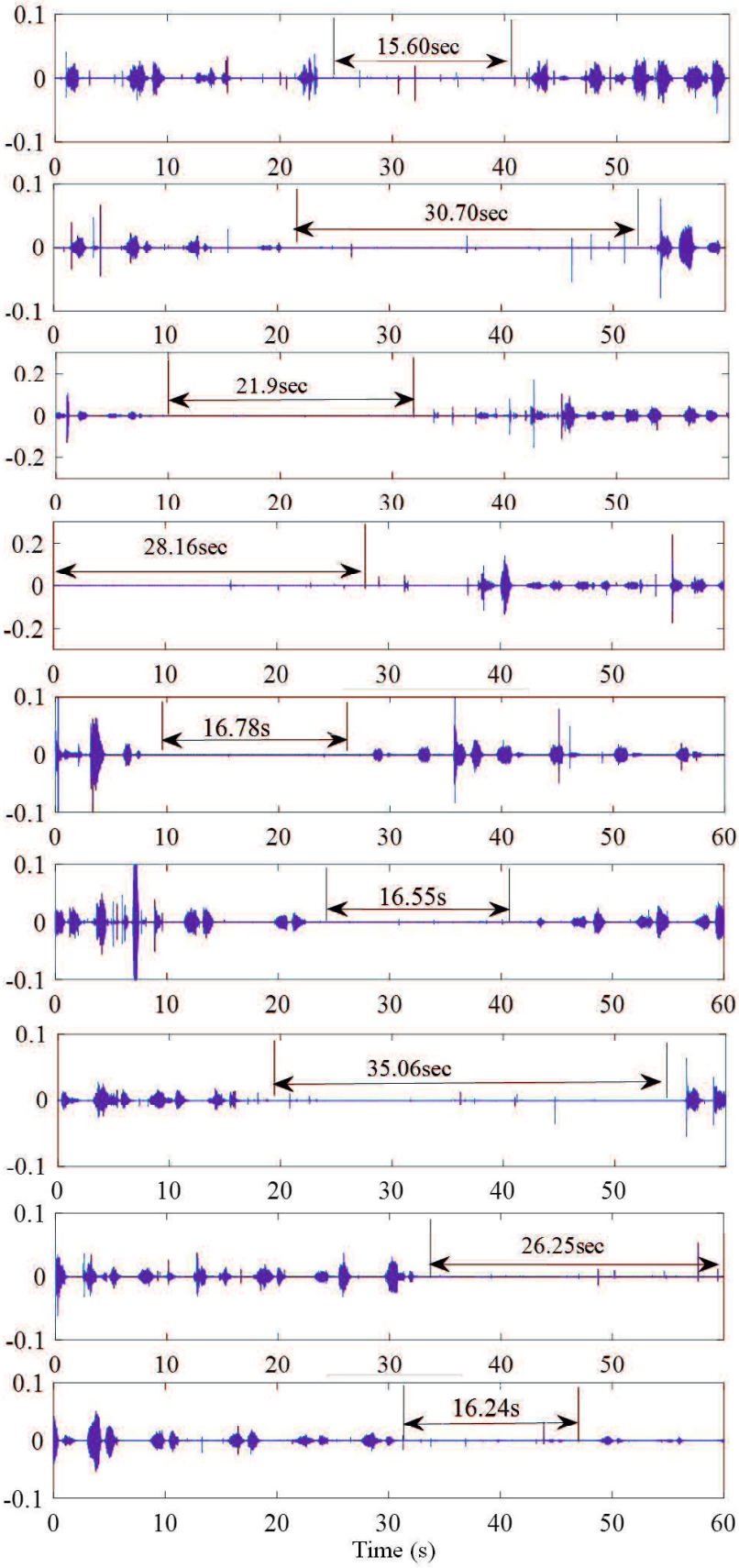

Figure 3.29 Apnea events of tester B (part 2)

of the proposed detection method. Compared with the monitoring results of blood oxygen saturation, the efficiency of the proposed detection method can be validated. The detected AHI value can be provided as a useful reference for individual healthcare and OSA monitoring.

Chapter 4

Breathing state identification by Mel cepstrum analysis

4.1 Abnormal breathing states related to OSA

With the help of time-domain parameter, the apnea can be detected correctly. For parts of hypopnea events, snore as shown in Fig.4.1 and other abnormal breathing signals as shown in Fig.4.2 which are meaningful for OSA monitoring can not be identified in time domain. The blue boxes show the breathing with noise caused by movement of nose and mouth. The orange boxes show the labored breathing.

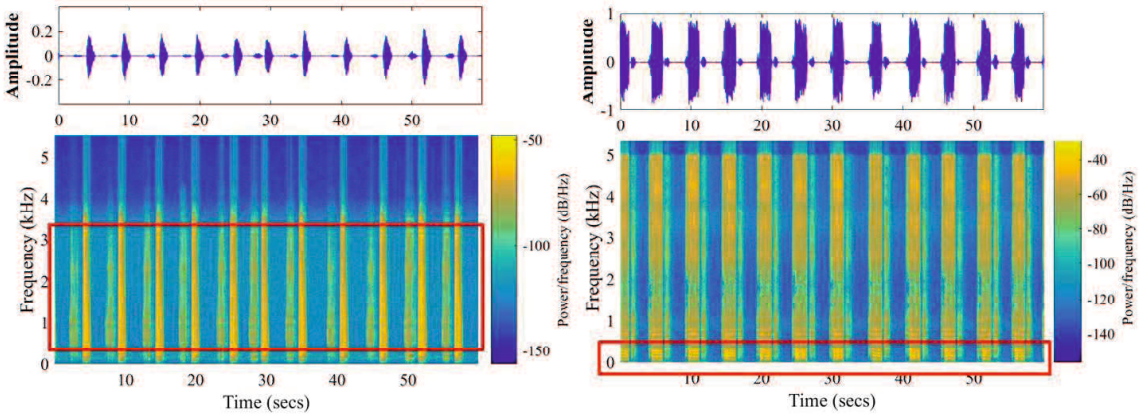

Figure 4.1 Frequency analysis of normal breathing and snoring

As shown in Fig.4.1, breathing frequency is stable for both of two parts of signals. Actually, the left is normal breathing and the right one is snoring. They have different frequency energy distribution as shown in the frequency spectrum by short-time Fourier transform. So we will discuss the different breathing states in frequency domain.

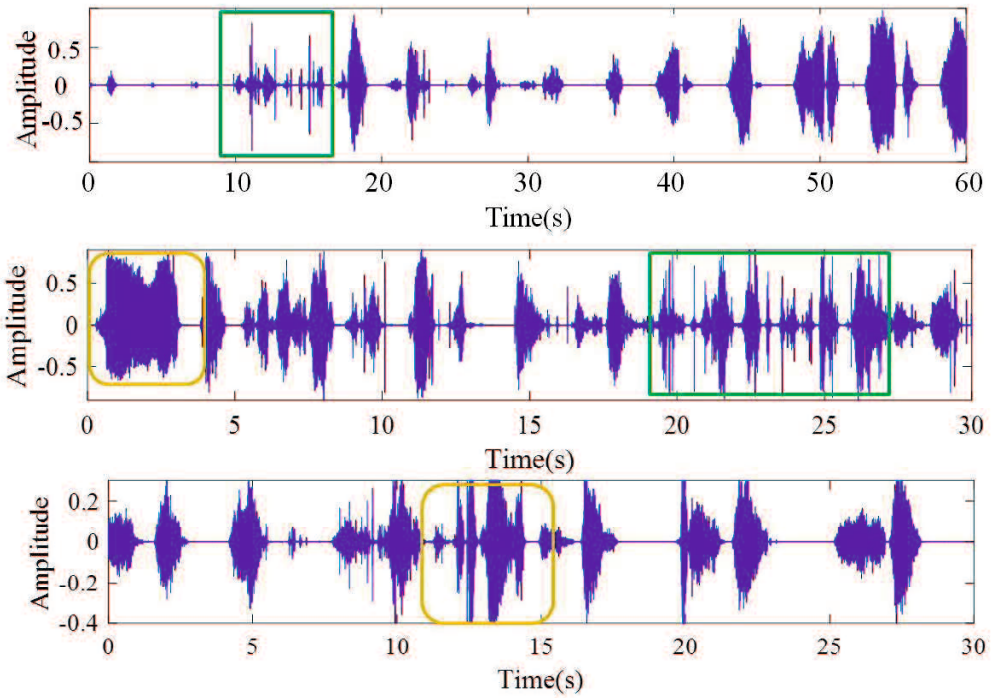

Figure 4.2 Abnormal complex breathing states

4.2 Parameter extraction method based on Mel frequency spectrum analysis

4.2.1 Introduction of Mel frequency spectrum

Psychophysical studies have shown that human perception of the frequency content of sounds does not follow a linear scale and the Mel scale cepstral analysis is very similar to perceptual linear predictive analysis of sound [57].

Mel frequency cepstrum coefficients (MFCCs) are derived from the short time

spectrum of a signal and widely used both for speech and speaker recognition [58]. It is simulating perceptive identify of the human ear to frequency components of the sounds [59]. Speech signal is recognized by the critical frequency band of human ears. To realize the speech reorganization, the frequency is transformed by the Mel-scale, and a triangle filter bank is applied to segment the Mel frequency domain into several bands. MFCCs have already been applied to extract features of respiratory sound in combination with learning machines to recognize the wheeze for respiratory disorders [60, 61].

The procedure of the conventional MFCC algorithm is illustrated by following steps:

Step 1: Framing and windowing. Firstly, framing has been done with frame shift which is the interaction part between frames, and the length of frame shift is about 1/2 1/3 of a frame usually. Framing can keep smooth and continuous between frames. And then assign a window to each individual frame to reduce the leakage of spectral energy [62].

Step 2: Translated the signal of each frame into frequency domain by FFT. Compute the energy spectrum.

Step 3: Filter the energy signal by Mel-scale filter bank. Mel-scale comes from Eq.4.2 which used to transform the real frequency to Mel frequency.

$$Mel(f) = \frac{1000 * ln(1 + \frac{f}{700})}{ln(1 + \frac{1000}{700})}. \tag{4.1}$$

where f is the real frequency and $Mel(f)$ is the Mel-scale frequency. 1000 is a key parameter to determine the relationship of f and $Mel(f)$, which is almost linear below 1kHz and nonlinear over 1kHz. 700 is a parameter which can affect the change trend of relationship between f and $Mel(f)$.

For frequencies under 1000 Hz, the Mel scale can be approximated with a linear scale, MFCC can represent the low frequency region more accurately than the high frequency region and it can capture formants which lie in the low frequency range [63].

The filter bank methods are grouped into two sections, i.e. MFCC contours and subband spectral centroids. The choice of MFCC contours number and filters number used to compute the coefficients is a compromise between information

measured by entropy with consistency of the estimation measured as standard deviation. The number of MFCC should be larger than six and the number of contours used in the literature ranges from 12 to 36 coefficients and 12 is selected commonly [64]. The Mel filter bank composed of 20 triangle band-pass filters is used to extract 12 MFCC coefficients.

The Mel filter bank distributes uniformly in Mel scale and non-uniform in original spectrum, simulating the critical frequency bands of the human ear. The center of each triangle window is the starting of the next one, shown in Fig.4.3.

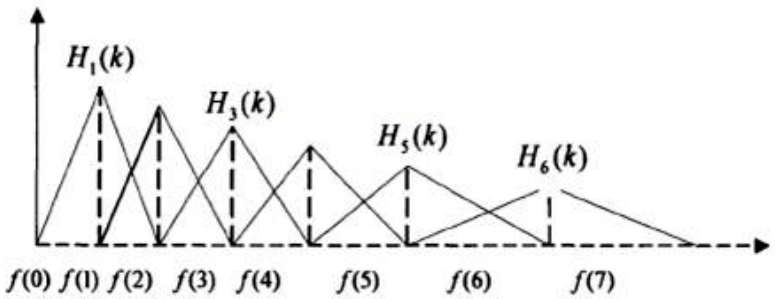

Figure 4.3 The triangle filter in real frequency domain

Step 4: Apply the logarithm to the output of the Mel filter bank.

The logarithm is used to compress the components above 1000Hz. And it can translate the multiplicative components into the additive ones and reduce the computation complexity.

In fact, logarithm can provide the frequency energy distribution on one time-point in the form of addition. It will very important for defining the breathing pattern.

Step 5: Discrete cosine transform is used to transform the signal into the time domain and the 12 coefficients comes like Eq.4.2.

$$MFCC_i = \sum_{k=1}^{K} X_k \cdot cos(i \cdot (k - \frac{1}{2}) \cdot \frac{\pi}{K}), i = 0, 1, ...N \tag{4.2}$$

where N is the dimension of MFCC, k is the number of filters in filter bank.

4.2.2 Parameter extraction based on Mel frequency spectrum analysis algorithm

The focus is the relationship of the frequency energy distribution in time domain, hence the processing results after logarithm should be paid attention. So the Mel frequency spectrum analysis algorithm is proposed for parameter extraction as shown in Fig.4.4. Compared with the classical MFCC algorithm, the FFT is replaced by power spectrum density and the discrete cosine transform is deleted.

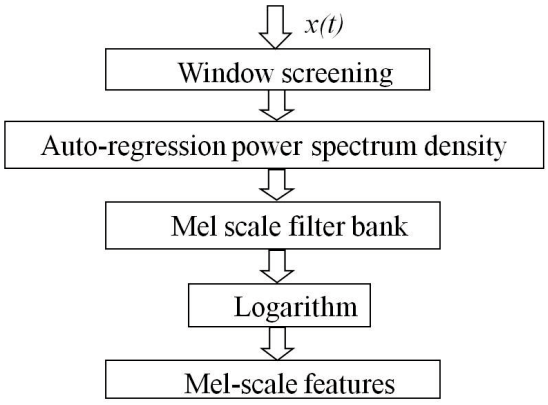

Figure 4.4 The flow chart of the modified MFCC features

The essence of MFCC algorithm is a serious of transforms in the frequency domain. Hence in the beginning of the proposed method, the breathing sound signal is translated from the time domain to frequency domain. In classical MFCC algorithm, the FFT is applied and its waveform has lots of burrs. The burrs will cause the mistakes in continuous steps, so a smoother frequency envelope is necessary. Because the energy spectrum is computed in the classical MFCC algorithm before applying filter bank, the power spectrum density is considered to take the place of FFT.

The power spectrum density estimation is an important part of the modern signal processing and reflect the energy distribution of the frequency component of the signal [65]. Autoregressive method is the most frequently used parametric method because the estimation of AR parameters can be done easily by solving linear equation. Here Yule-Walker's method is used to make the power spectrum density instead of the energy of the FFT result. The order of an autoregressive prediction model for the signal is set as 32.

And the frequency bands of each Mel filter in filterbank are listed in Table4.1. It is easy to find that more details will be discussed in the lower frequencies and

the trend of energy will also be displayed in higher frequencies.

Table 4.1 Frequency bands decided by Mel filterbank

Filter Number	Frequency Band (Hz)	Filter Number	Frequency Band (Hz)
1	0 ~ 161.8	11	1279.7 ~ 1737.3
2	76.7 ~ 256.2	12	1496.6 ~ 2004.3
3	161.8 ~ 361	13	1737.3 ~ 2300.6
4	256 ~ 477.2	14	2004.3 ~ 2629.4
5	361 ~ 606.2	15	2300.6 ~ 2994.1
6	477.2 ~ 749.3	16	2629.4 ~ 3398.9
7	606.2 ~ 908.1	17	2994.1 ~ 3847.9
8	749.3 ~ 1084.3	18	3398.9 ~ 4346.2
9	908.1 ~ 1279.7	19	3847.9 ~ 4899.1
10	1084.3 ~ 1496.6	20	4346.2 ~ 5512.5

A normal breathing cycle is taken for an example shown in the top of Fig.4.5. 20 Mel scale parameters are extracted by the above steps. The length of frame affect the efficiency of Mel scale features greatly. Here the frame is set as about 100ms according to the reference and experiments. The length of frame is set as 1024 points for the fast computation while the sampling frequency is 11025Hz. Fig.4.5 displays the set of Mel scale features.

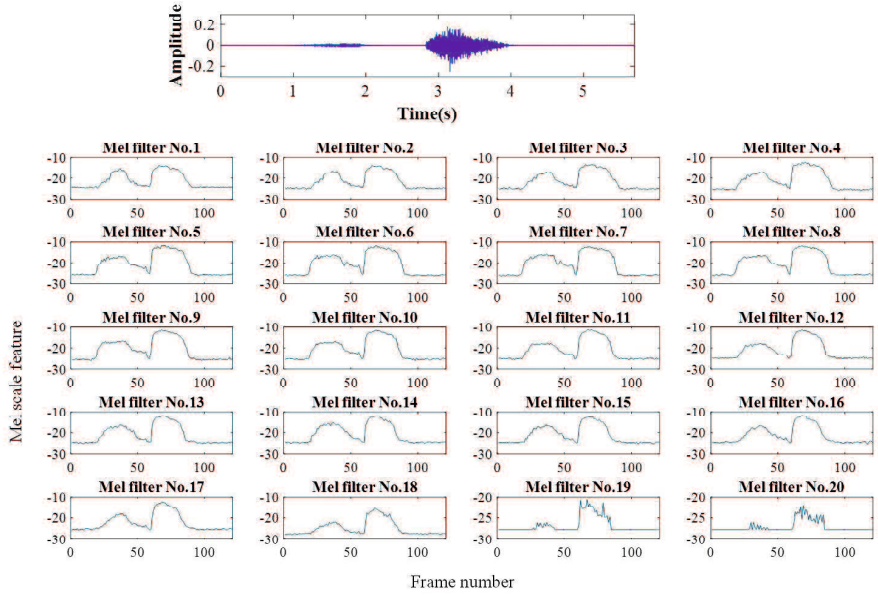

Figure 4.5 The Mel scale features while the length of frame is 1024 points

To stand out the frequency energy distribution of each frame, the Mel scale label L_i has been determined by the maximum value of the Mel-scale features in each frame. It means the main frequency energy in time. Take the above breathing cycle for the example, the Mel scale label is detected and shown in the right plot of Fig.4.6. The present times of each Mel scale label can be counted and shown by bar char in the left of Fig.4.6.

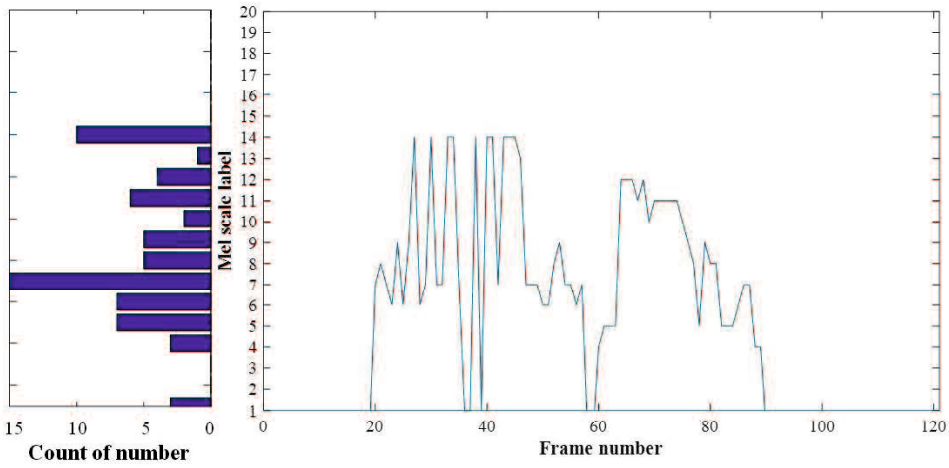

Figure 4.6 The Mel frequency spectrum analysis of a stable breathing cycle

4.3 Sleep breathing state detection by Mel frequency spectrum analysis

The Mel scale labels can be extracted by Mel frequency spectrum analysis for each breathing cycle in last section. The counting number of each Mel scale label during one night monitoring is shown in Fig.4.7 and 4.8. X-axis is the monitoring time, one point means one segmented breathing cycle, marked by the beginning time. Y-axis is the counting number of each Mel scale label for each breathing cycle. It shows the energy distribution in the fixed frequency range during the all night monitoring.

Checking up the original breathing sound data, it is found that the No.2 Mel scale label represents the snore components. No.4 to No.7 Mel scale labels represent the normal breathing components. The abnormal breathing components are marked by No.15 to 17 Mel scale labels.

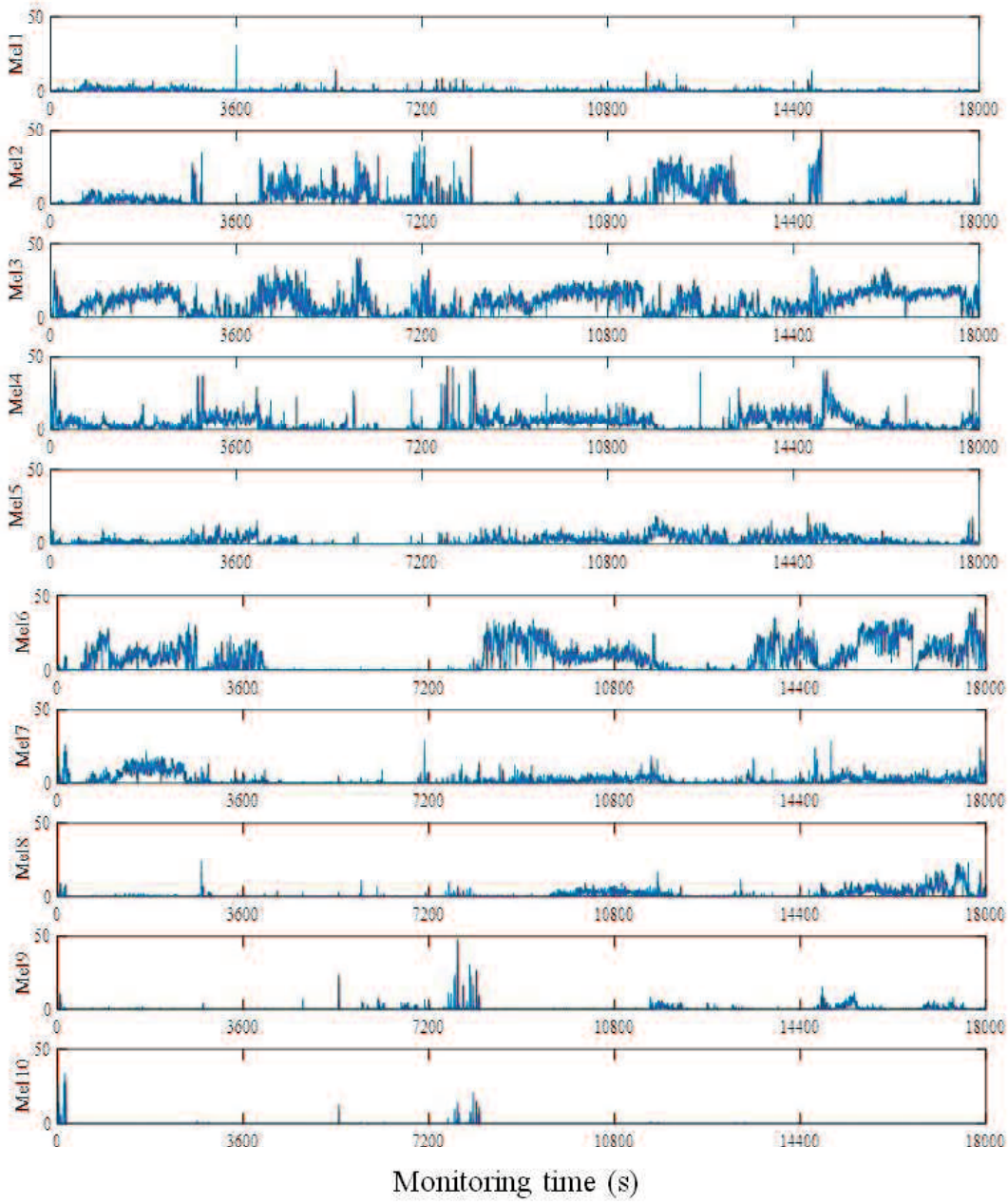

Figure 4.7 Monitoring results of each Mel scale features (1-10)

The threshold values for FM and FH are set by 40% of total present times of Mel scale labels. As the inspiration and expiration last about 2.5 seconds in one breathing cycle, the total present times is about 50, that is the number of shift frames. And the threshold value for FM and FH is 20 times.

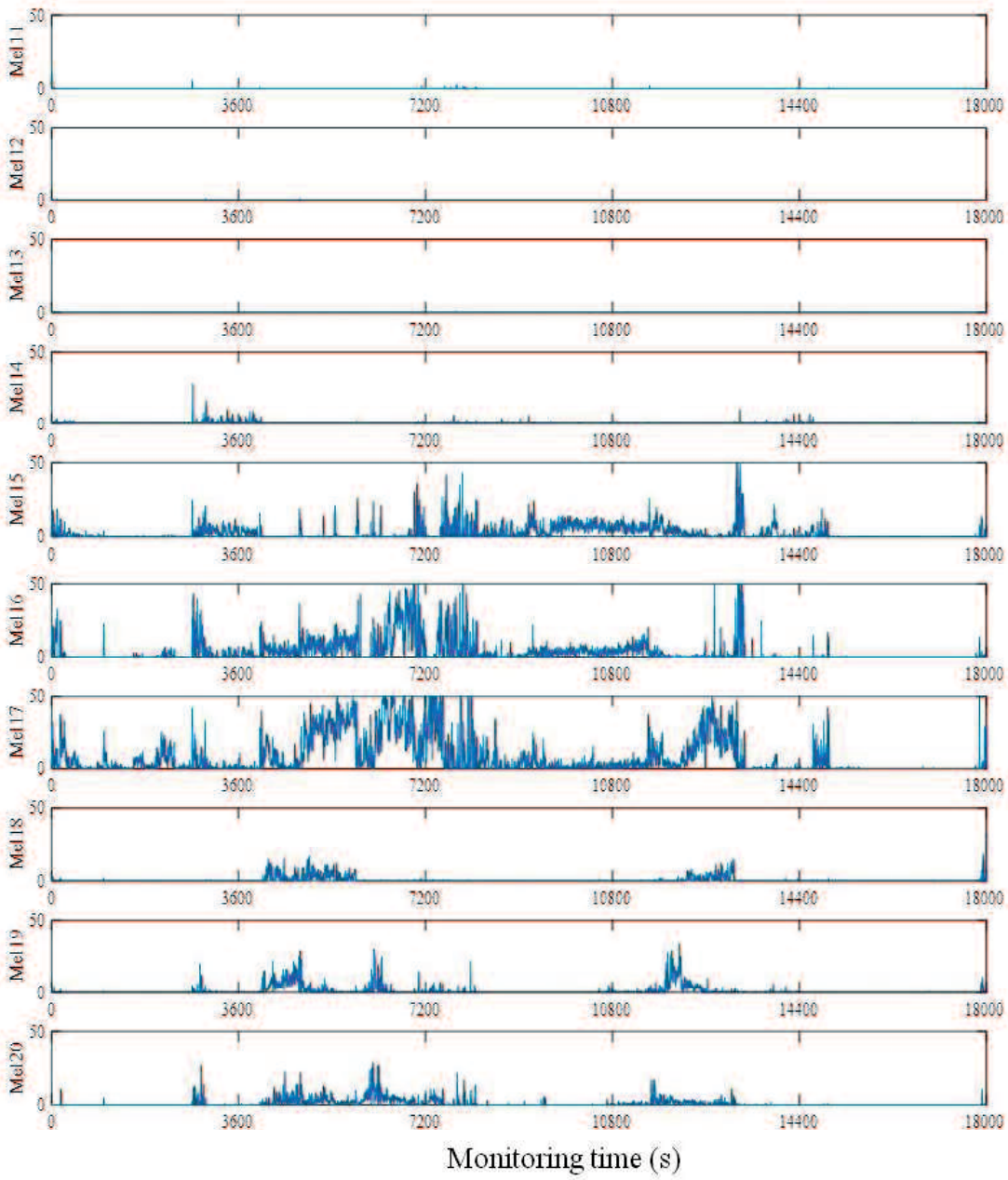

Figure 4.8 Monitoring results of each Mel scale features (11-20)

The threshold value for FL is set by 20% of total present times of Mel scale labels, 10 times.

According to the above analysis, three Mel scale label sets are proposed in this

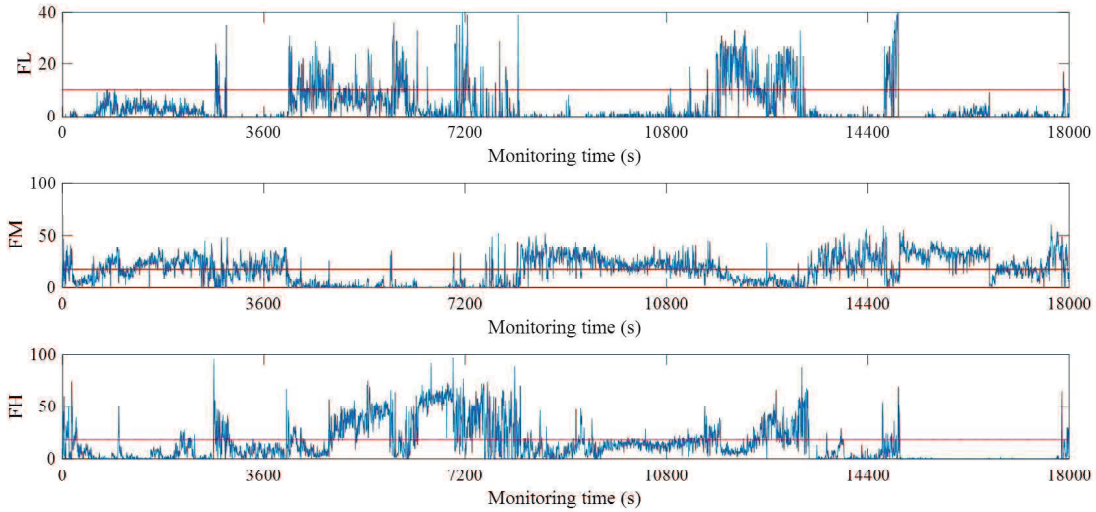

Figure 4.9 Identification results by Mel scales

case marked with FL, FM, FH. The Total counting numbers of each Mel scale set are shown in Fig.4.9. The threshold value is set by mean value of each waveform shown as red line in each plot. The snore component of each breathing cycle is identified by the counting number of each Mel scale set larger than the threshold value. It is the same way for identification of normal breathing component and abnormal breathing component. The identification rules are set as following.

If the cycle has large value in FM and small value in FH at the same time, the cycle identified as normal breathing.

If the cycle has large value in FH and small value in FM at the same time, the cycle identified as abnormal breathing.

If the cycle has large values in FM and FH at the same time, the cycle identified as abnormal breathing.

If the cycle has small values in FM and FH at the same time, it is identified as normal breathing.

The identification results by Mel scale labels are shown in Fig.4.10. Fig.4.10(a) shows the identification of normal/abnormal sleep state. The abnormal sleep breathing cycle is denoted by '1', the normal sleep breathing is '0'. It is easy to compute the time duration of normal and abnormal breathing during whole night. For this case, the normal breathing lasts 2.8 hours, the abnormal breathing

lasts 2.2 hours. In this evening, the normal sleep state takes 56% of sleep.

Fig.4.10(b) shows the identification of snore. The breathing cycle with snore is marked with '1'. The snore lasts 1.8 hours.

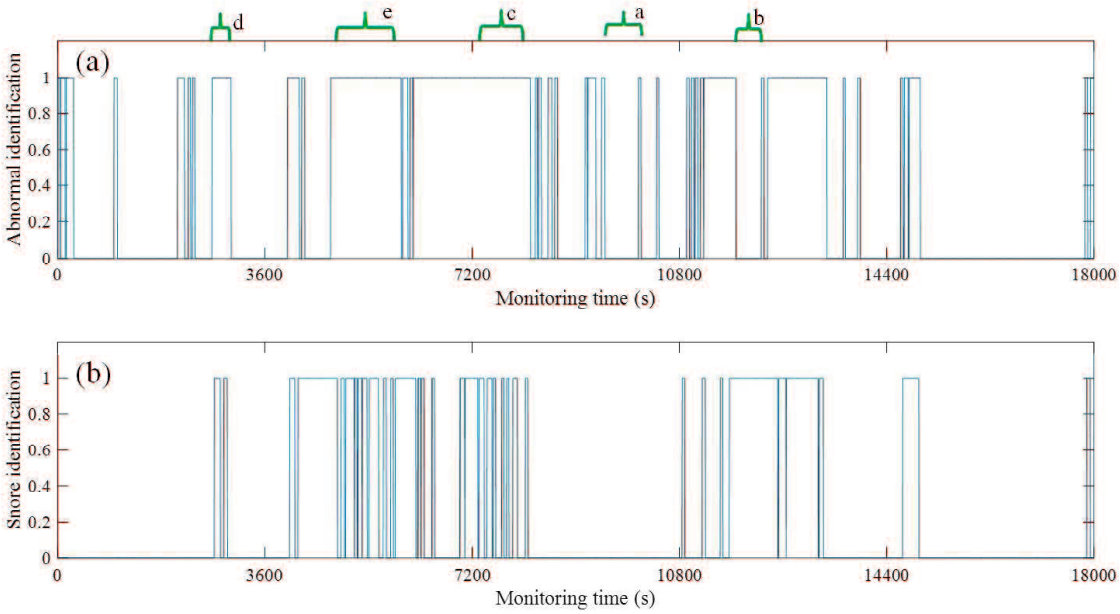

Figure 4.10 Monitoring results by Mel scale label sets for OSA case

To validate the efficiency of the monitoring results, five sections, *a* to *e* marked in Fig.4.10(a), are selected and checked by FFT as a reference. Section (a) belongs to normal breathing, (b) is normal snore, (c) to (d) are abnormal breathing with snore.

From the original breathing waveforms shown in figure 4.11 and 4.12, the two sections are normal stable breathing. There are large energy in middle frequency range, 500-1000Hz. And the large frequency energy distributes below 500Hz is the feature of snore in section (b).

The sections (c) to (e) include apnea, hypopnea and noise according to the original waveforms. According to the FFT results, there are larger energy below 500Hz and in the high frequency range. These three sections all belong to the state of abnormal breathing with snore.

The results of checking match with monitoring results by Mel scale label sets. The efficiency and adaption of Mel frequency spectrum analysis will be validation

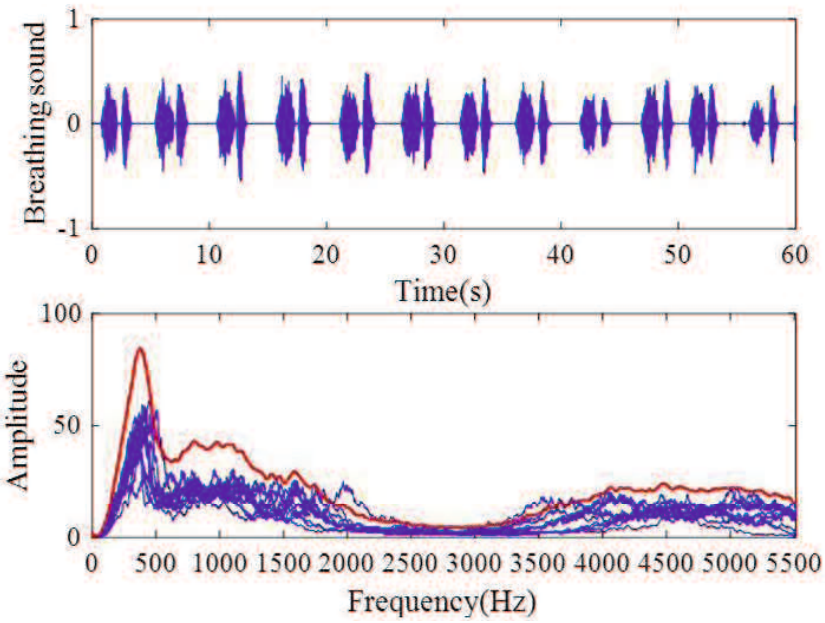

Figure 4.11 Breathing signal of section (a)

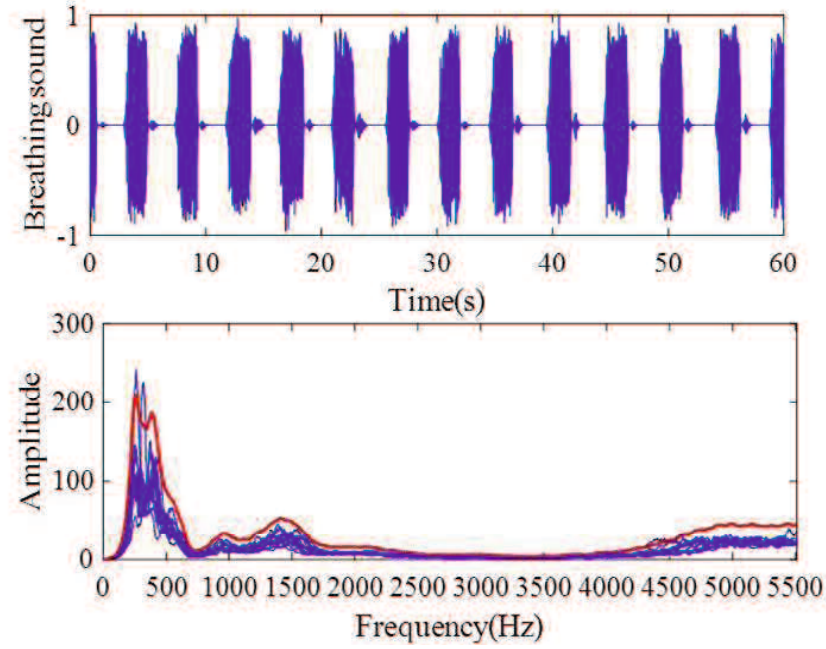

Figure 4.12 Breathing signal of section (b)

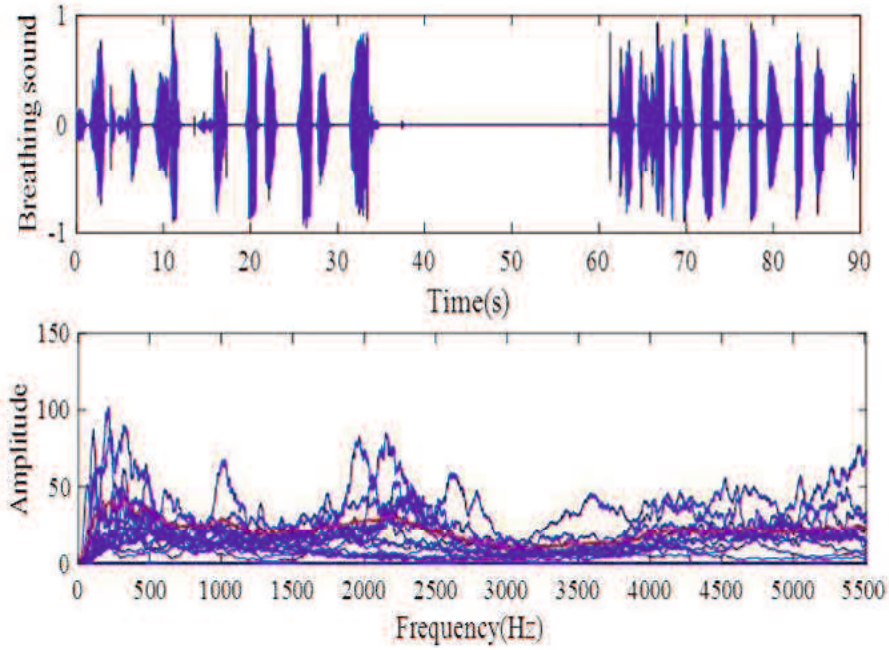

Figure 4.13 Breathing signal of section (c)

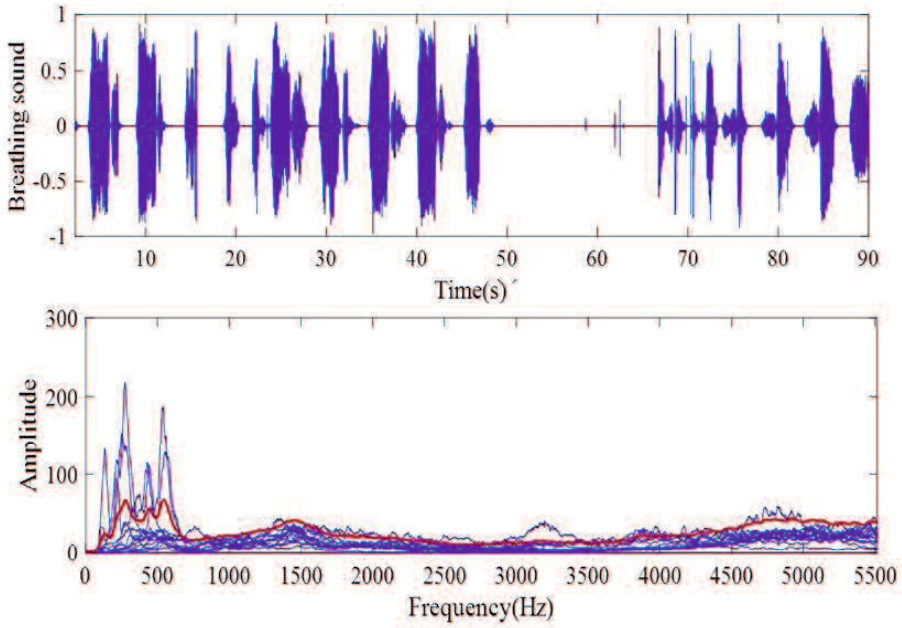

Figure 4.14 Breathing signal of section (c)

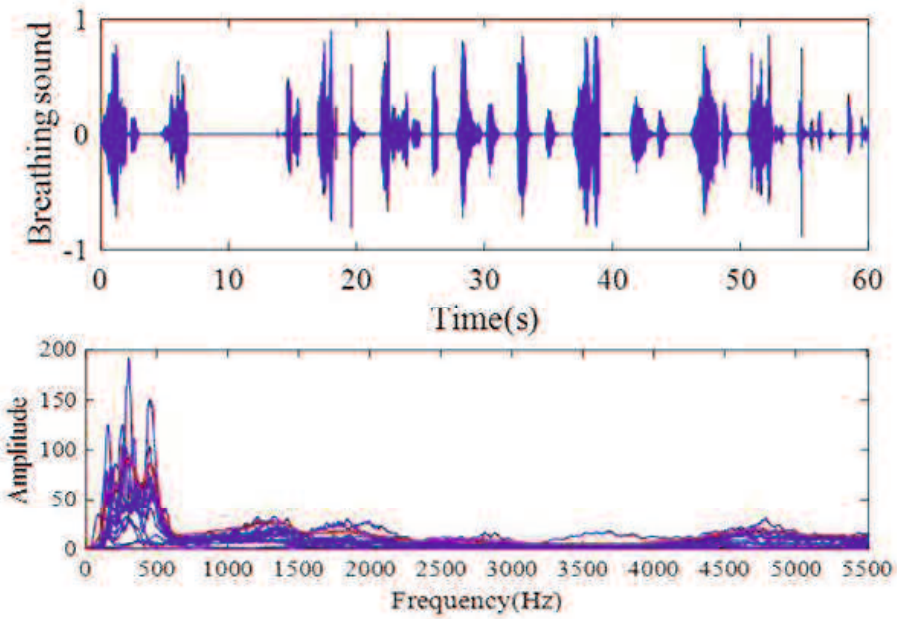

Figure 4.15 Breathing signal of section (d)

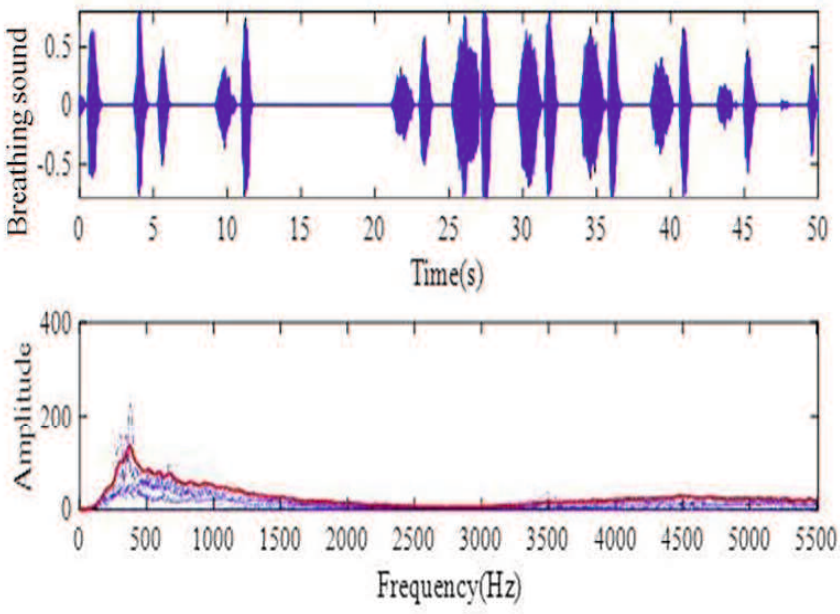

Figure 4.16 Breathing signal of section (d)

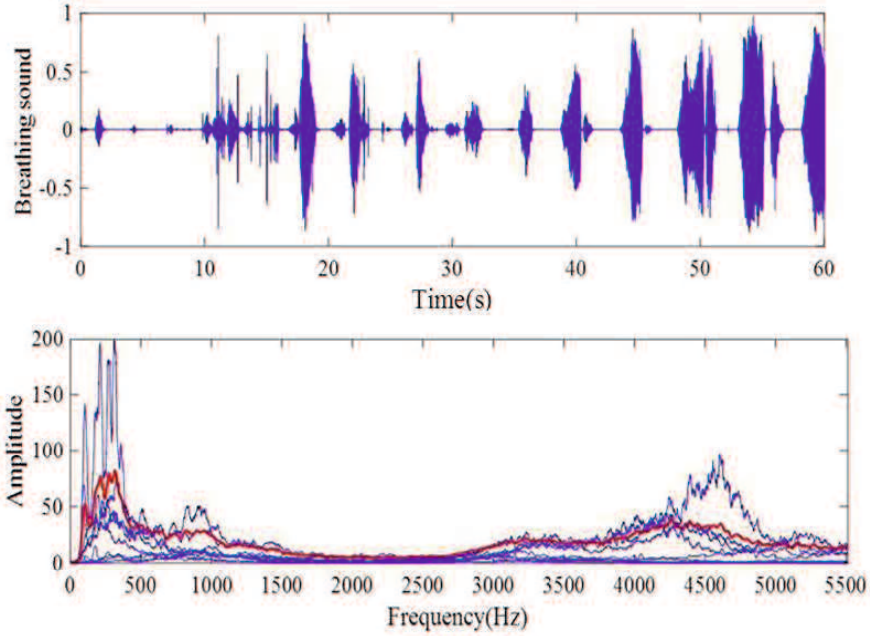

Figure 4.17 Breathing signal of section (e)

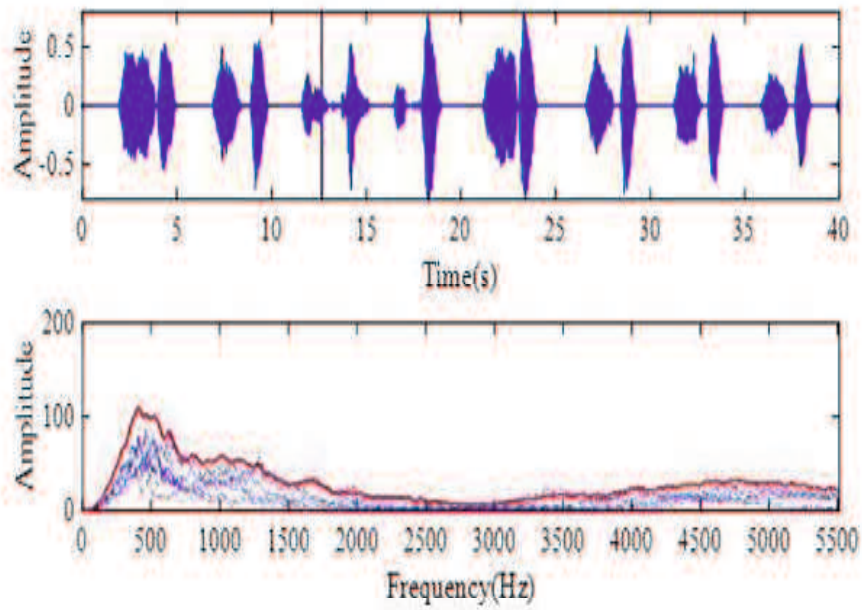

Figure 4.18 Breathing signal of section (e)

by other several cases.

4.4 More monitoring results based on Mel frequency spectrum analysis

For the second night of OSA case, the monitoring results of each Mel scale features are shown in Figs.4.19 and 4.20. Fig.4.19 displays No.1 to 10 Mel scale labels and Fig.4.20 displays No.11 to 20 Mel scale labels.

According to Fig.4.19 and Fig.4.20, FL includes No.2 Mel scale label, FM includes No.4 $\sim$ 7 Mel scale labels, No.15 $\sim$ 20 Mel scale labels belong to FH. The threshold values for FL, FM, FH are set as same as the first night.

The monitoring results in the second evening is shown in Fig.4.22. Based on the identification of normal/abnormal sleep state shown in Fig.4.22(a), the normal breathing states lasts 2.33 hours and abnormal breathing lasts 3 hours. The normal sleep state takes 44% of sleep.

The snore lasts 2 hours according to the identification results shown in Fig.4.22(b).

For the third night of OSA case, the monitoring results of each Mel scale features are shown in Fig.4.23 and 4.24.

According to Fig.4.23 and Fig.4.24, FL includes No.2 Mel scale label, FM includes $No.4 \sim 7$ Mel scale labels, $No.15 \sim 20$ Mel scale labels belong to FH. The threshold values for identification in each Mel scale label set are set as above.

The monitoring results in the third evening is shown in Fig.4.26. Based on the identification of abnormal sleep state shown in Fig.4.26(a), the normal breathing states lasts 2.1 hours and abnormal breathing lasts 4 hours. The normal sleep state takes 34.7% of sleep.

The snore is identified as shown in Fig.4.26(b). In this evening, snore lasts 3.2 hours.

For the fourth night of OSA case, the monitoring results of each Mel scale features are shown in Figs.4.27 and 4.28.

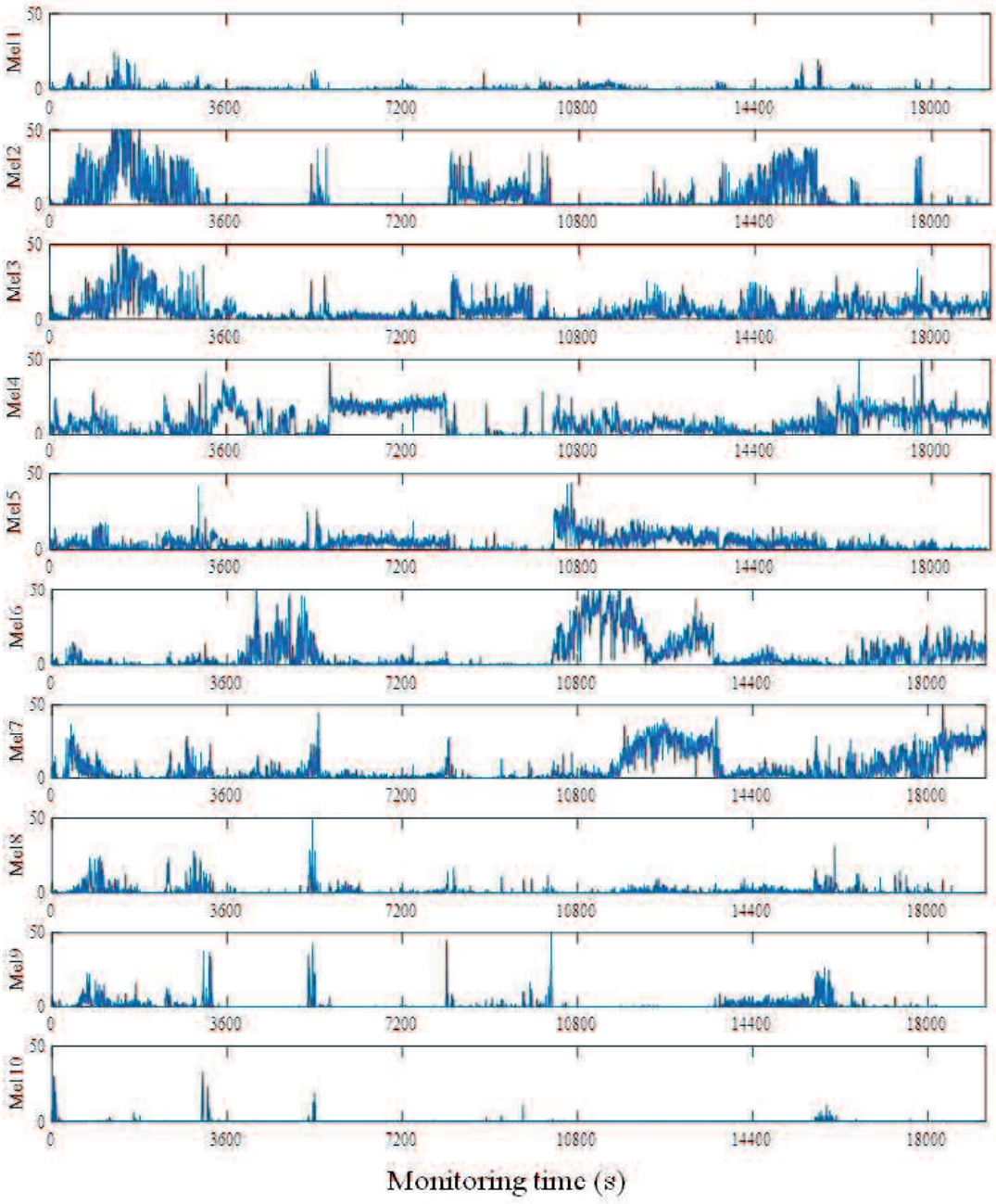

Figure 4.19 Monitoring results of each Mel scale features for OSA case in the second evening (1-10)

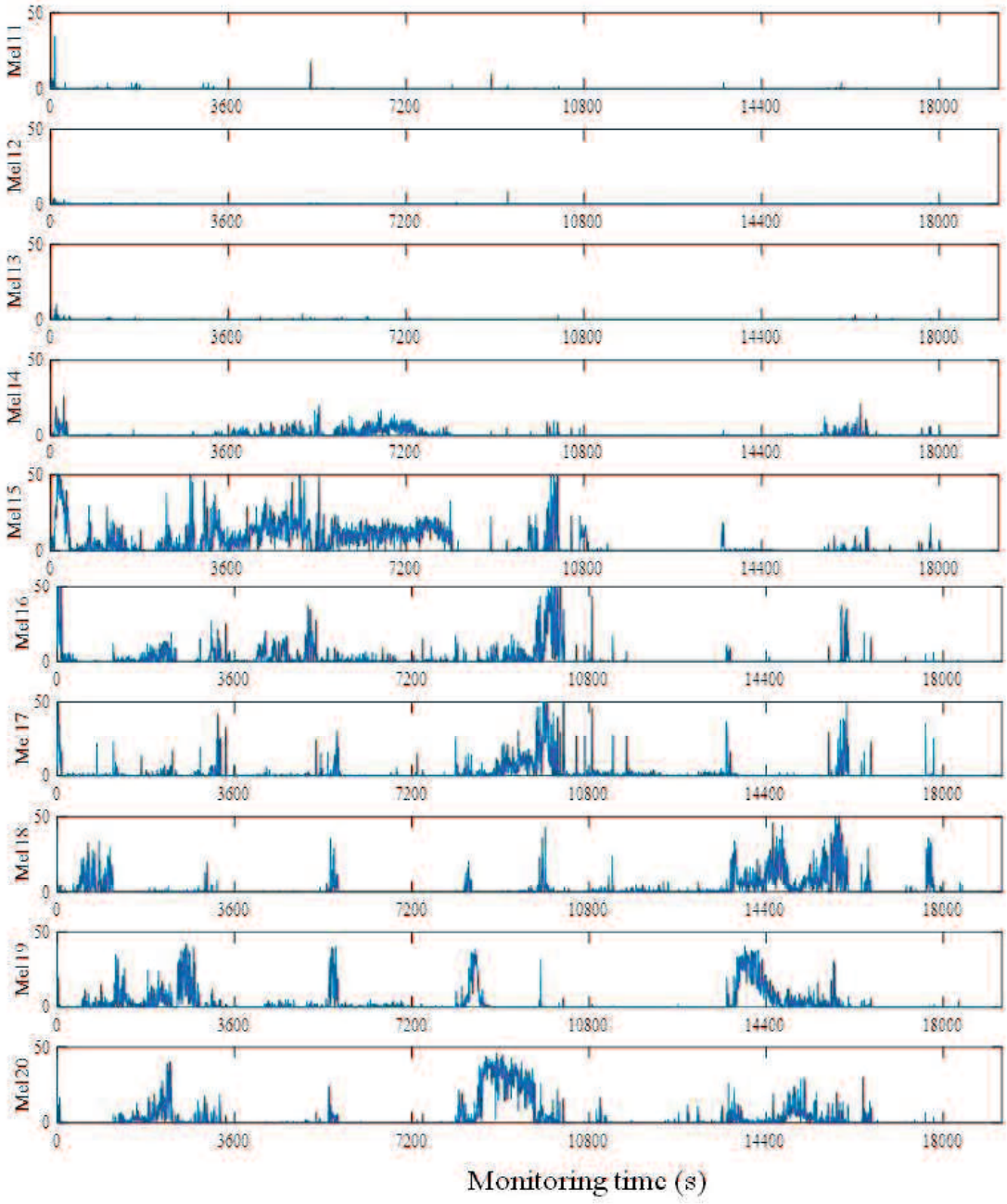

Figure 4.20 Monitoring results of each Mel scale features for OSA case in the second evening (11-20)

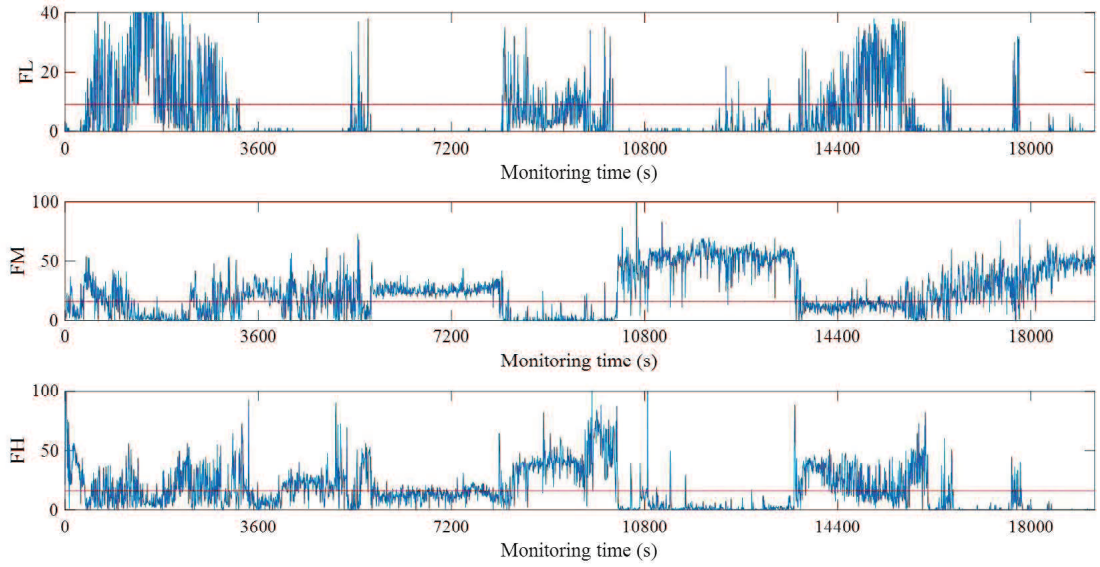

Figure 4.21 Identification results by Mel scales for the second night of OSA case

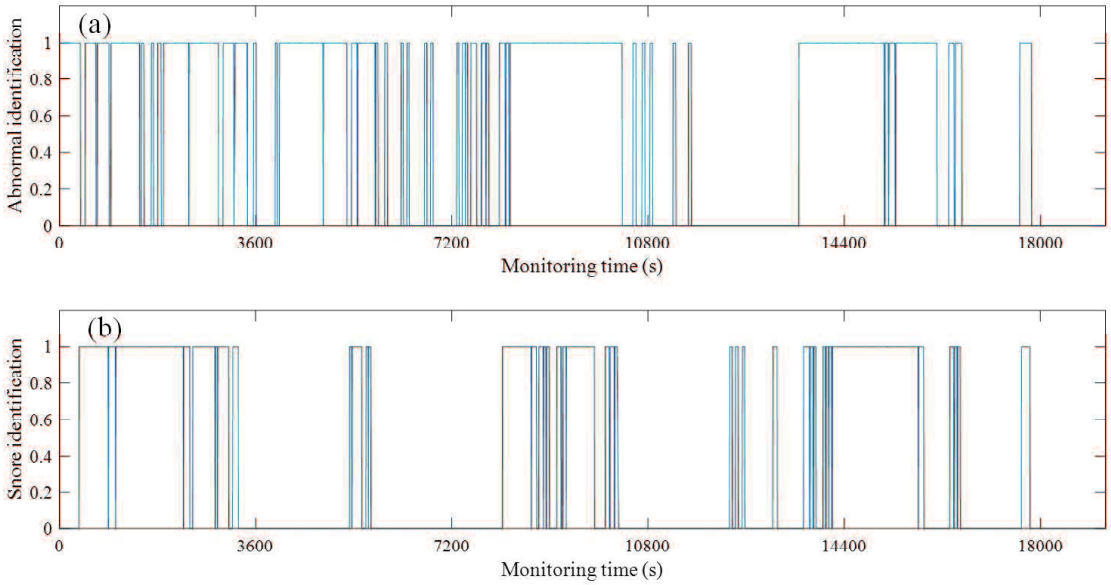

Figure 4.22 Monitoring results for OSA case in the second evening

According to Fig.4.27 and Fig.4.28, FL includes No.2 Mel scale label, FM includes No.4 ~ 7 Mel scales, No.15 ~ 18 Mel scales belong to FH. The threshold values for identification in each Mel scale label set are set as 10, 20, 20 times.

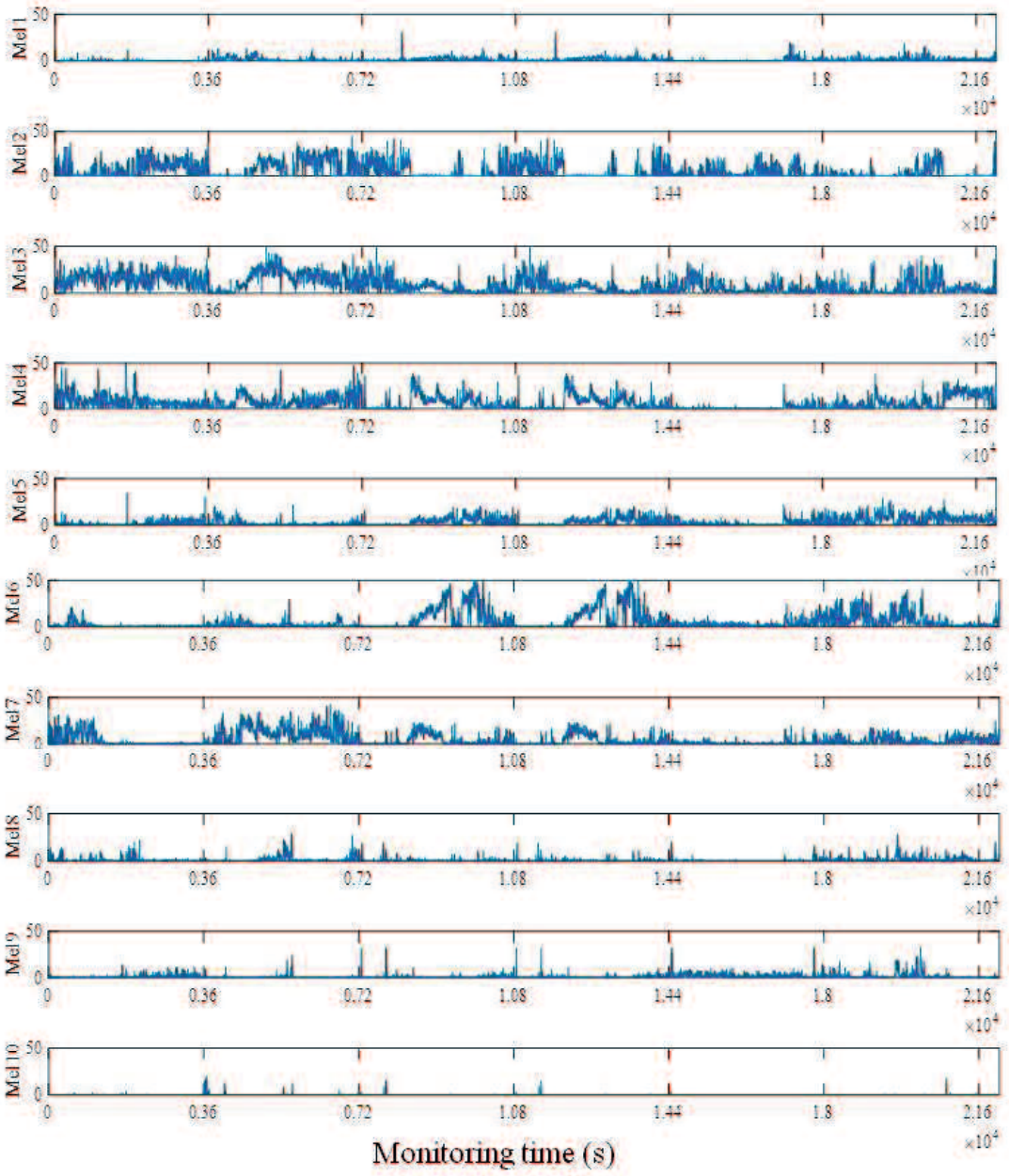

Figure 4.23 Monitoring results of each Mel scale label for OSA case in the third evening (1-10)

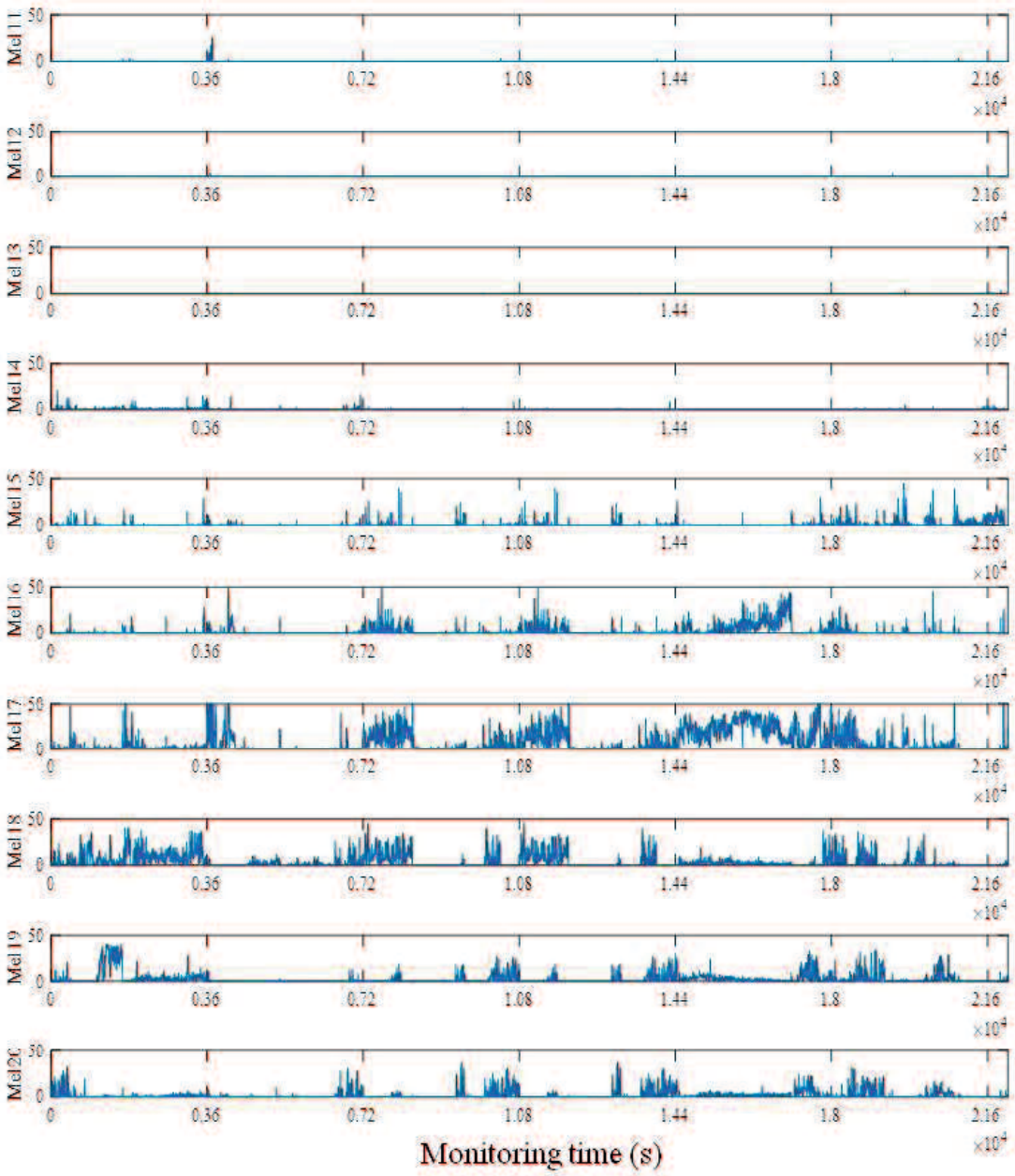

Figure 4.24 Monitoring results of each Mel scale label for OSA case in the third evening (11-20)

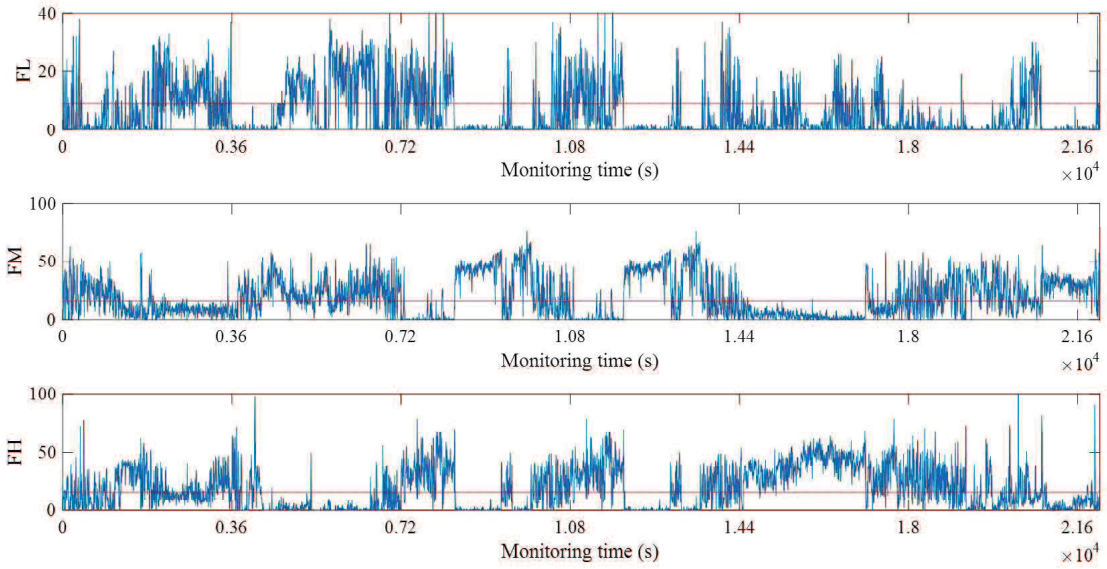

Figure 4.25 Identification results by Mel scales for the third night of OSA case

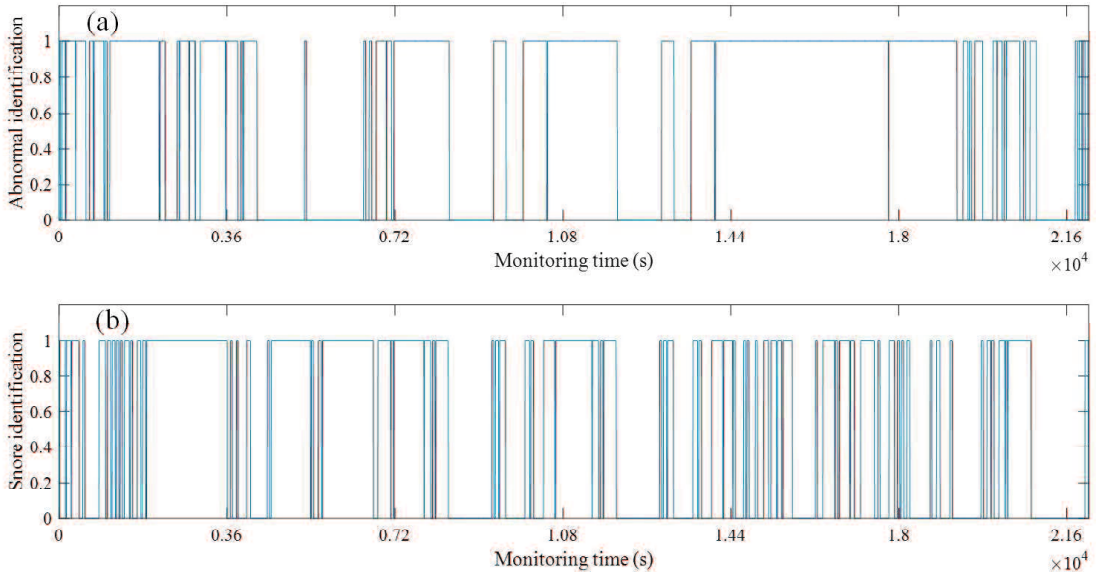

Figure 4.26 Monitoring results for OSA case in the third evening

The monitoring results in the fourth evening is shown in Fig.4.30. Based on the identification of abnormal sleep state shown in Fig.4.30(a), the normal breathing states lasts 3.2 hours and abnormal breathing lasts 2.7 hours. The normal sleep state takes 54.4% of sleep.

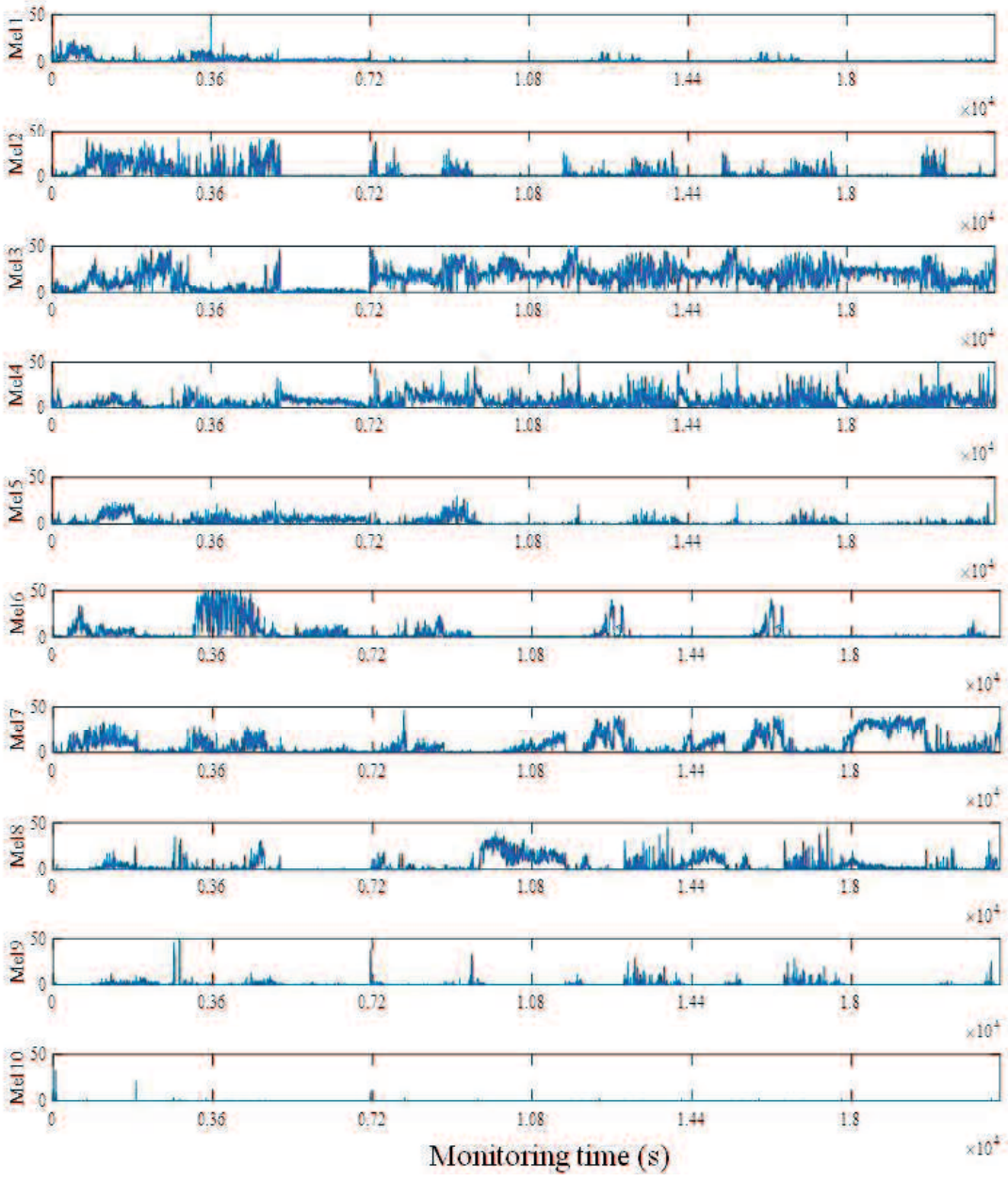

Figure 4.27 Monitoring results of each Mel scale features for OSA case in the fourth evening (1-10)

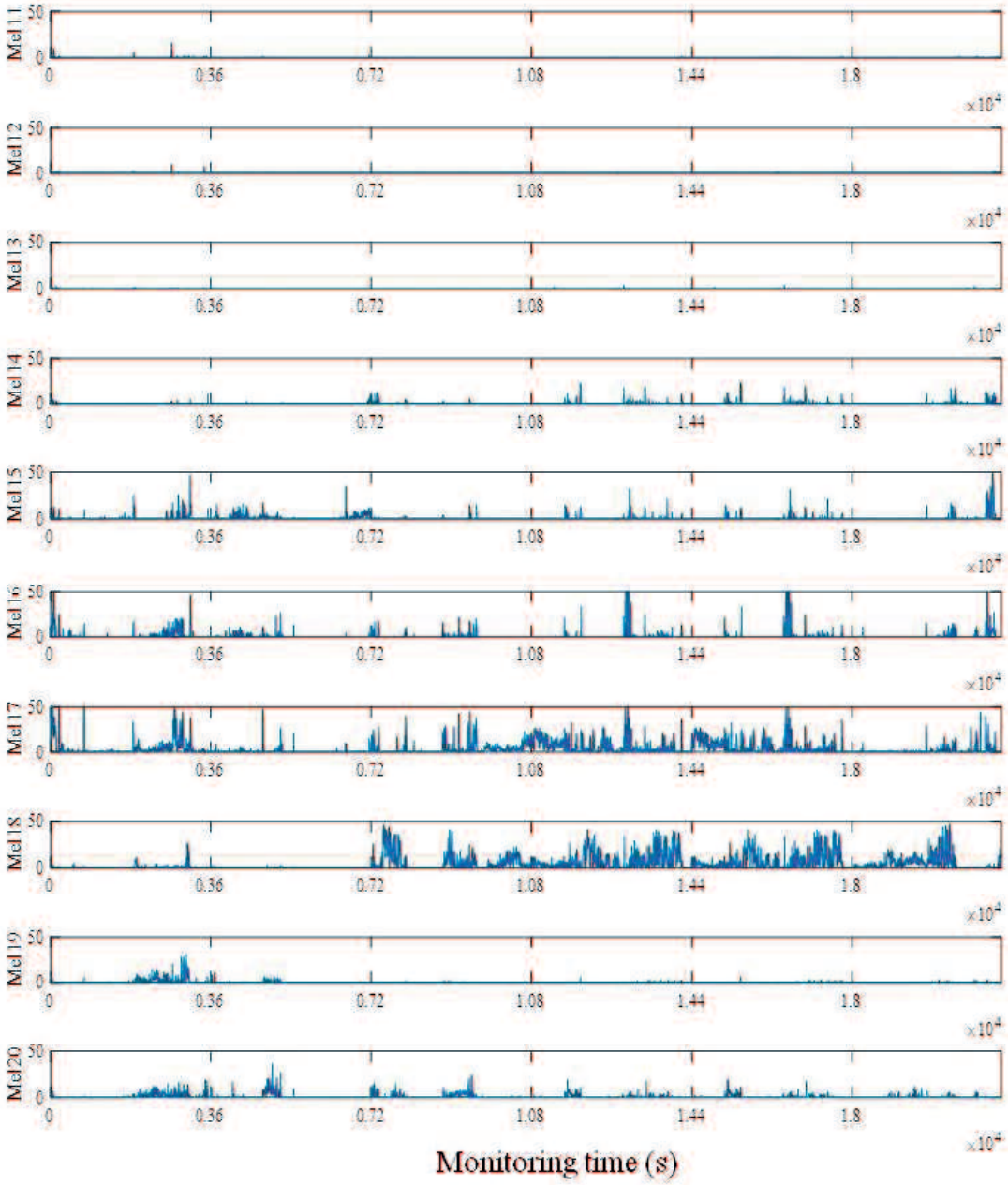

Figure 4.28 Monitoring results of each Mel scale features for OSA case in the fourth evening (11-20)

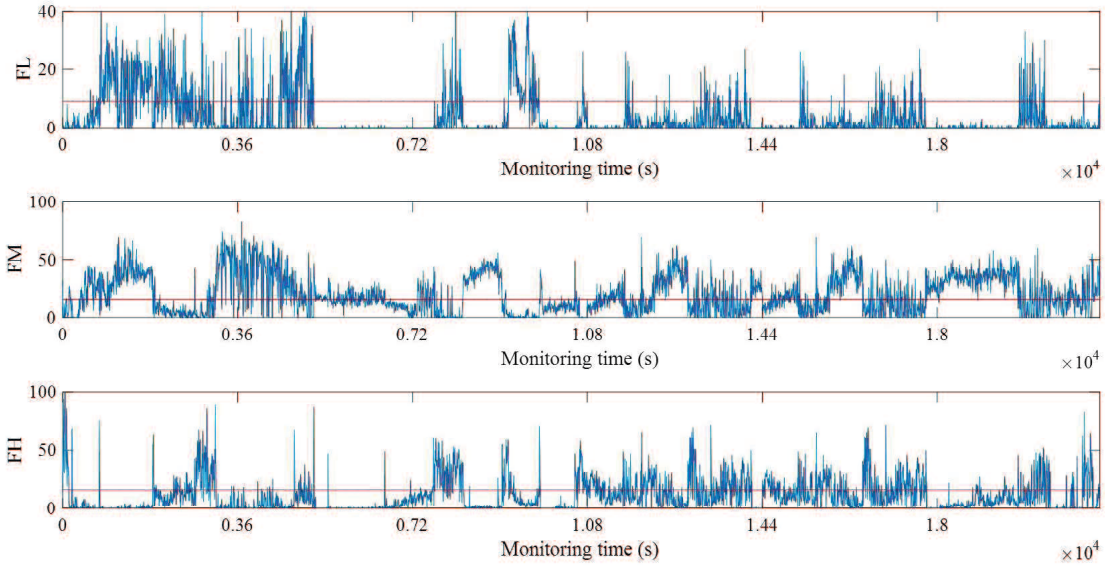

Figure 4.29 Identification results by Mel scales for the fourth night of OSA case

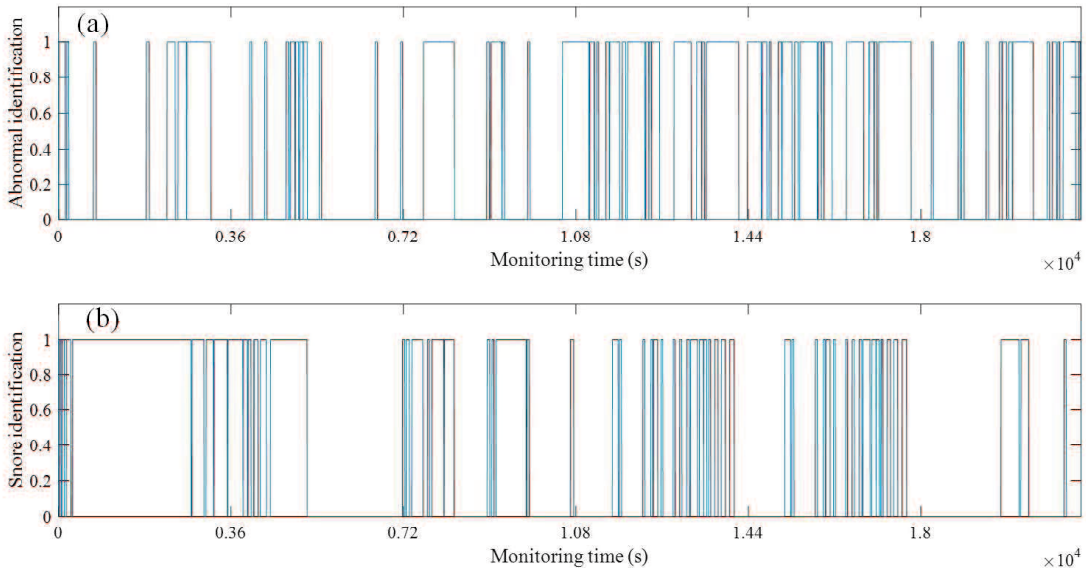

Figure 4.30 Monitoring results for OSA case in the fourth evening

Based on the identification result shown in Fig.4.30(b), the snore lasts 2.1 hours during the sleep overnight.

Based on the identification results of the OSA tester during 4 nights, the monitoring of sleep state is shown in Figs.4.31 and 4.32. The bar chart of Fig.4.31

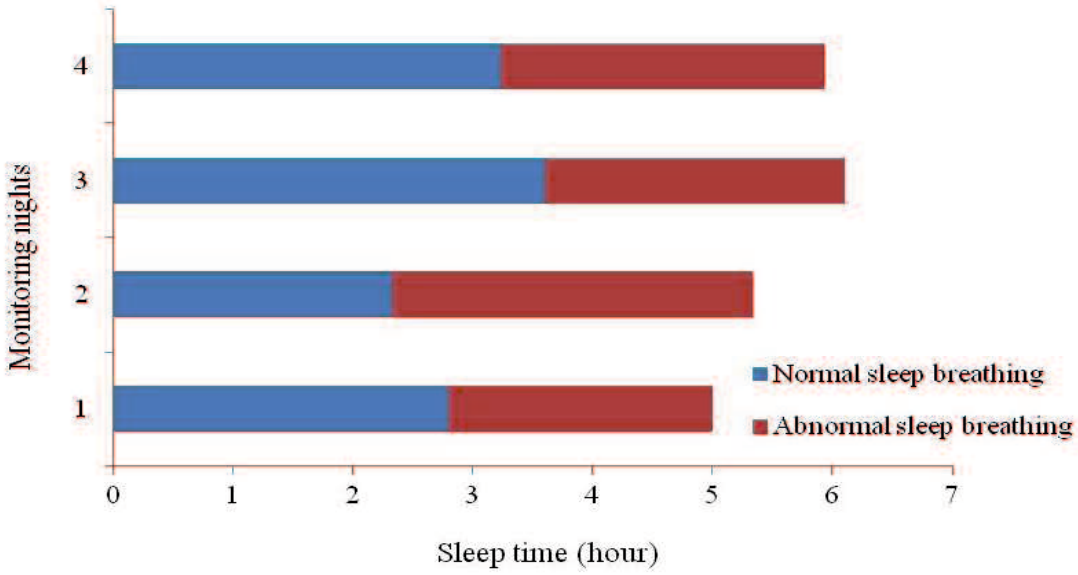

Figure 4.31 Monitoring of sleep state for the OSA tester (1)

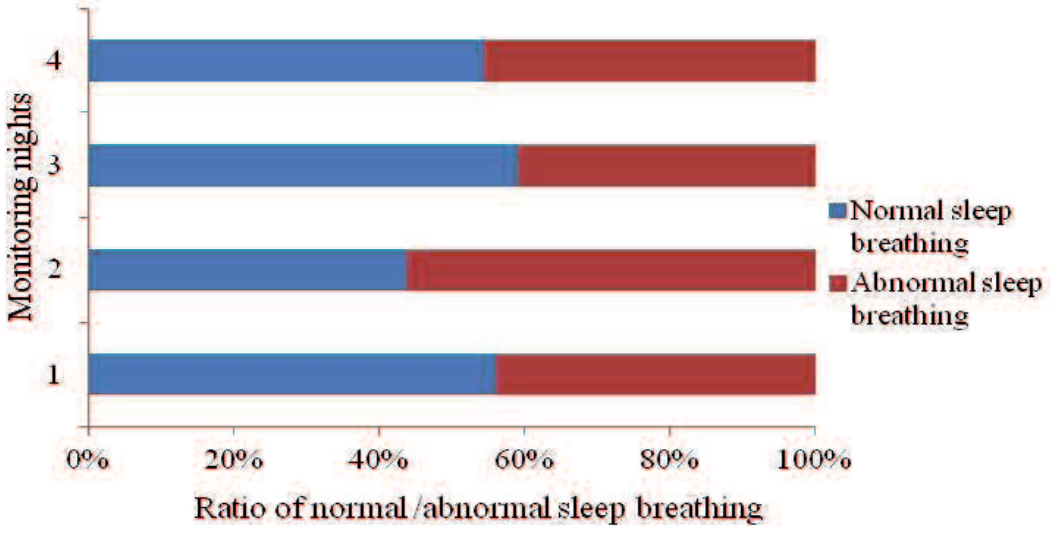

Figure 4.32 Monitoring of sleep state for the OSA tester (2)

shows the real time of sleep and normal sleep state. The X-axis is the monitoring time, Y-axis is the number of monitoring night. The bar chart of Fig.4.32 displays the ratio of the normal sleep state during the whole night sleep. From Figs.4.31 and 4.32, it is easy to found the proportion of normal sleep state and abnormal sleep state during sleep overnight. The normal sleep state takes 43.7 $\sim$ 56% of sleep overnight. The apnea, hypopnea and other unstable breathing lead to the large proportion of abnormal sleep state for OSA case.

For the young tester A, the monitoring results of each Mel scale features are shown in Fig.4.33 and 4.33.

According to Figs.4.33 and 4.34, FL includes No.1 Mel scale, FM includes No.3 $\sim$ 6 Mel scales, No.15 $\sim$ 17 Mel scales belong to FH. The stable breathing cycle lasts about 4 seconds, the inspiration and expiration lasts about 2 seconds. Hence the threshold values for FL, FM, FH are set as 8, 16, 16 times.

According to Fig.4.35, the abnormal sleep state and snore state are monitored as shown in Fig.4.36.

Based on the identification of normal/abnormal sleep state shown in Fig.4.36(a), the normal breathing state lasts 6 hours and abnormal breathing lasts 1.7 hours. The normal sleep state takes 77.9% of sleep.

There is few snore according to the identification results shown in Fig.4.36(b).

For the young tester B, the monitoring results of each Mel scale features are shown in Figs.4.37 and 4.38.

According to Figs.4.37 and 4.38, FL includes No.1 $\sim$ 2 Mel scale labels, FM includes No.4 $\sim$ 7 Mel scale labels, No.13 $\sim$ 17 Mel scale labels belong to FH. The threshold values are set as the OSA case as the breathing cycle lasts the similar time with OSA case.

Based on the identification of abnormal sleep state shown in Fig.4.40(a), the normal breathing states lasts 1.9 hours and abnormal breathing lasts 4.1 hours. The normal sleep state takes 31.7% of sleep. The proportions of normal and abnormal sleep states is close to the detection results of OSA case. As introduced in chapter 3, the AHI detected for tester B more than 30 times/hour. It is necessary to take the PSG examination as early as possible for tester B.

There is one-hour snore according to the identification result shown in Fig.4.40(b).

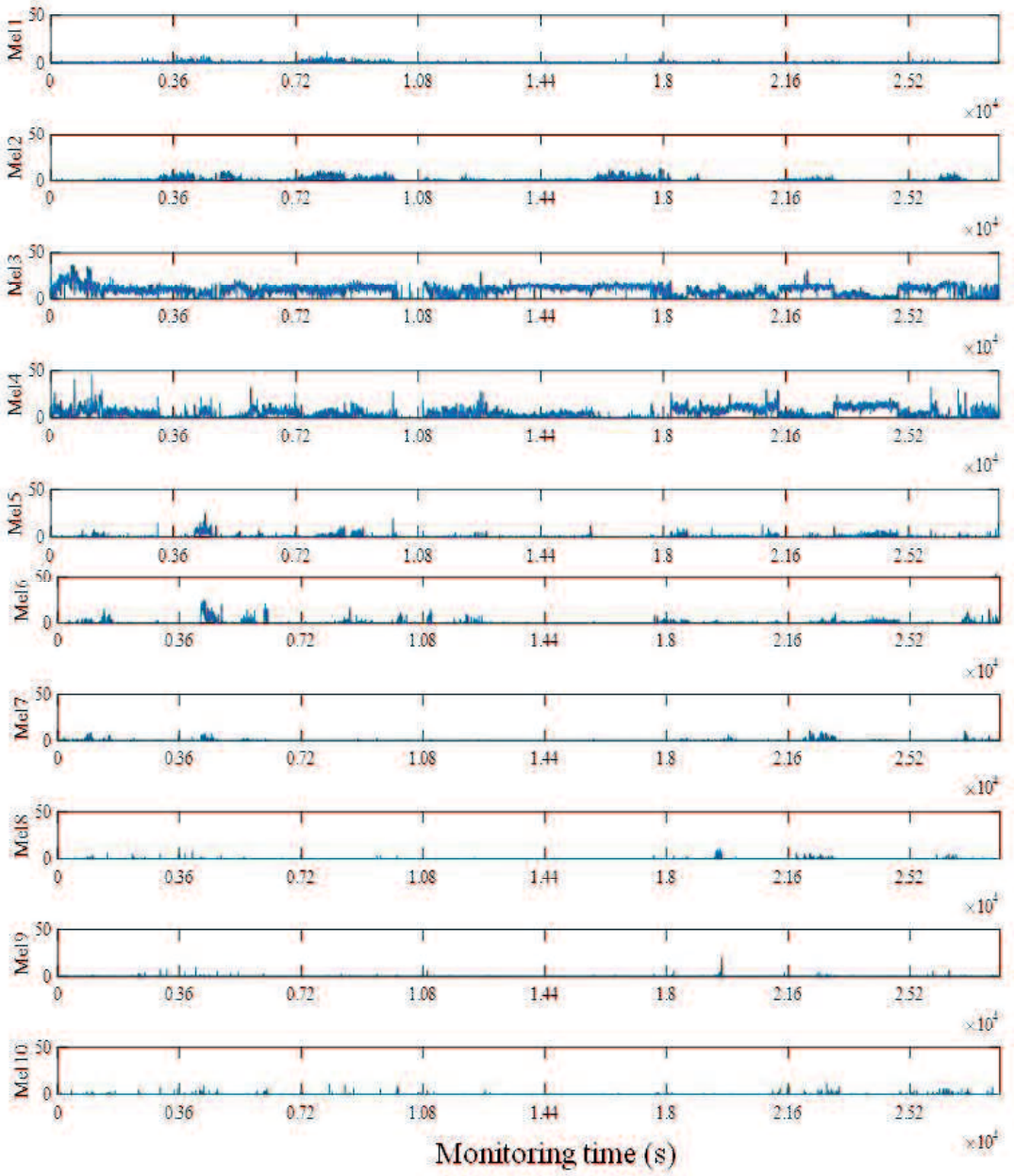

Figure 4.33 Monitoring results of each Mel scale features for the young tester A (1-10)

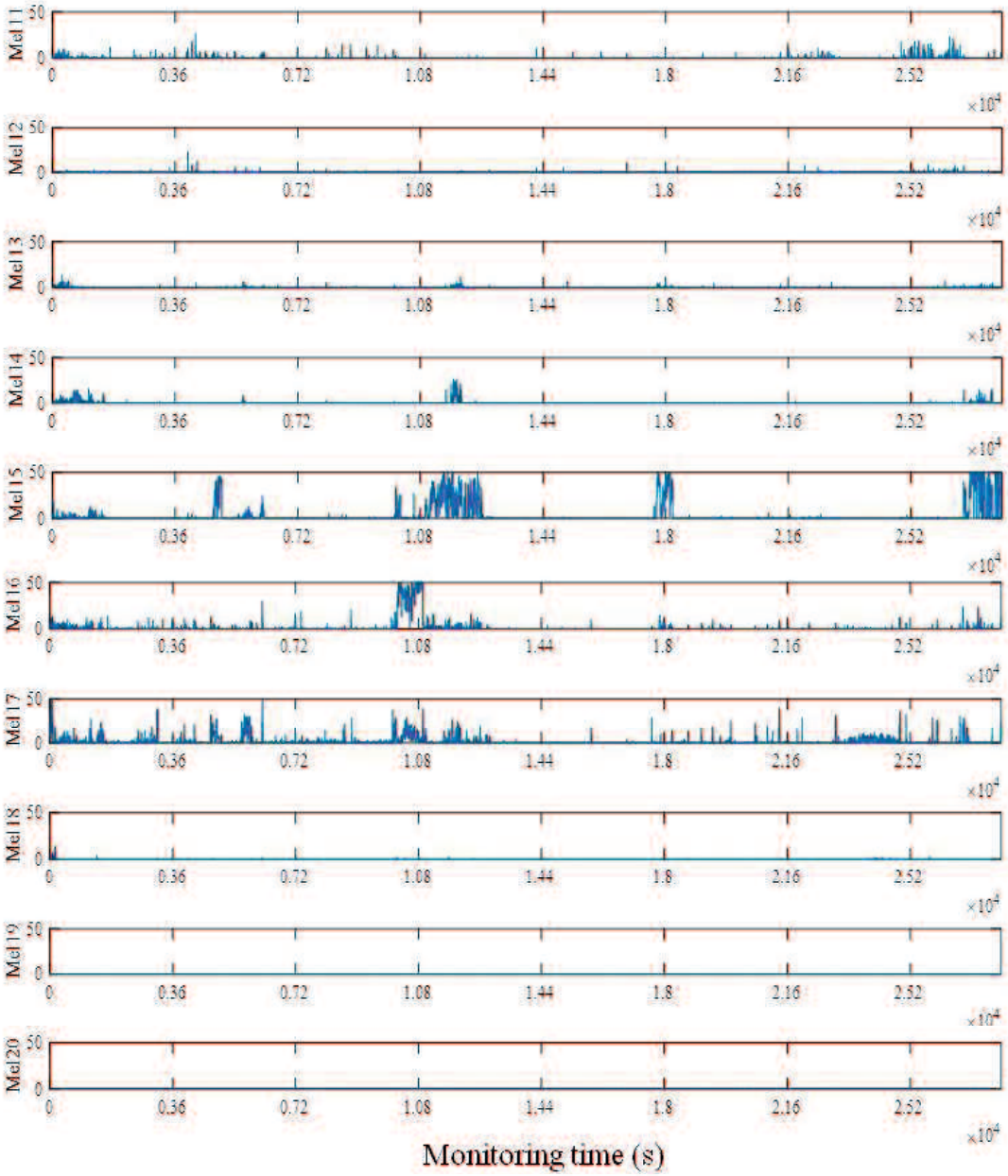

Figure 4.34 Monitoring results of each Mel scale features for the young tester A (11-20)

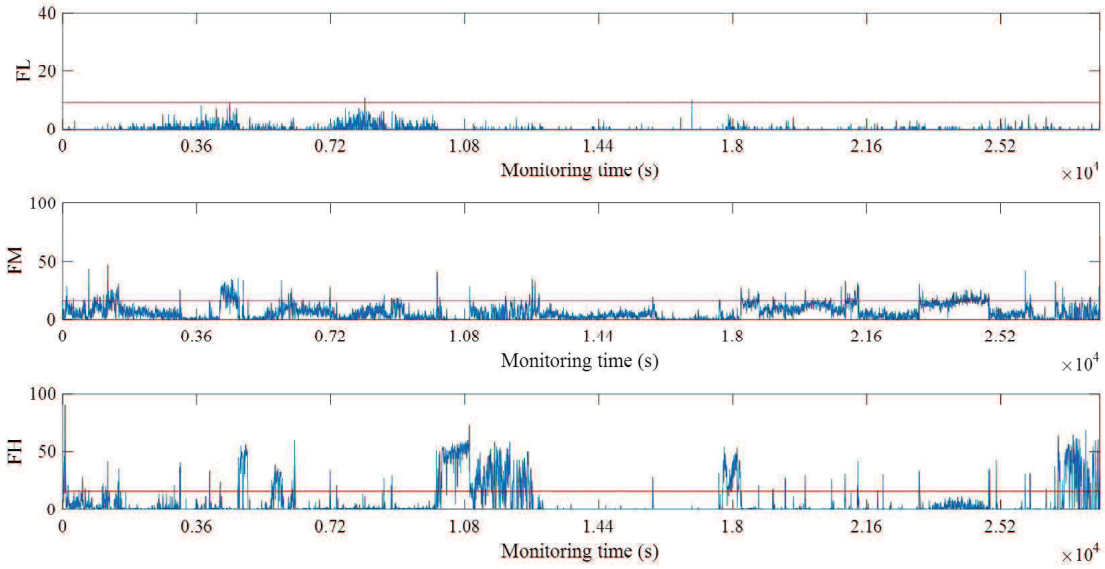

Figure 4.35 Identification results by Mel scales for the young tester A

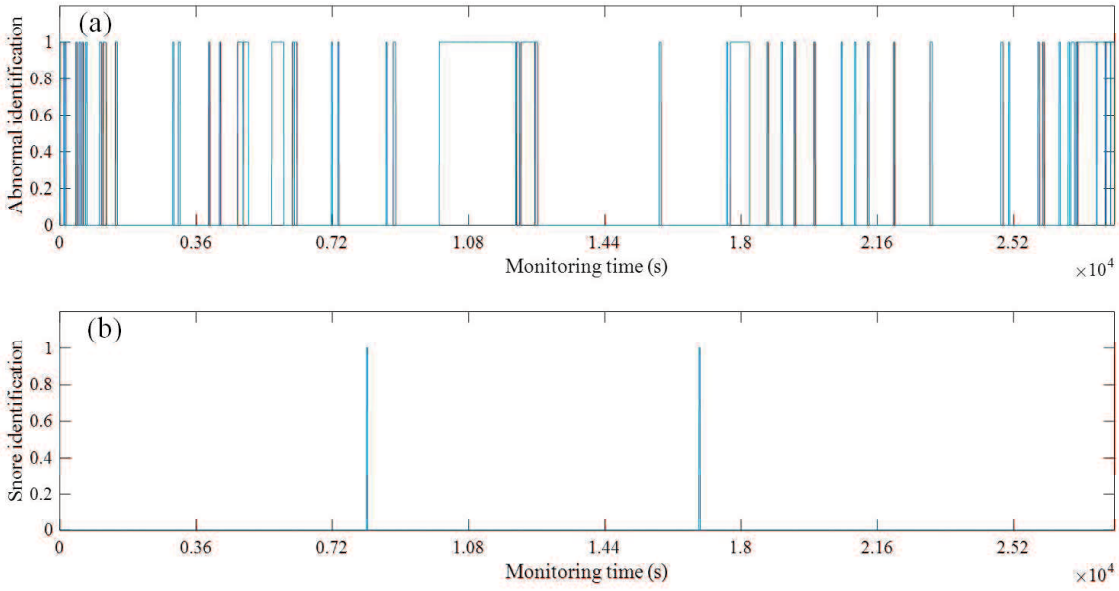

Figure 4.36 Monitoring results for the young tester A

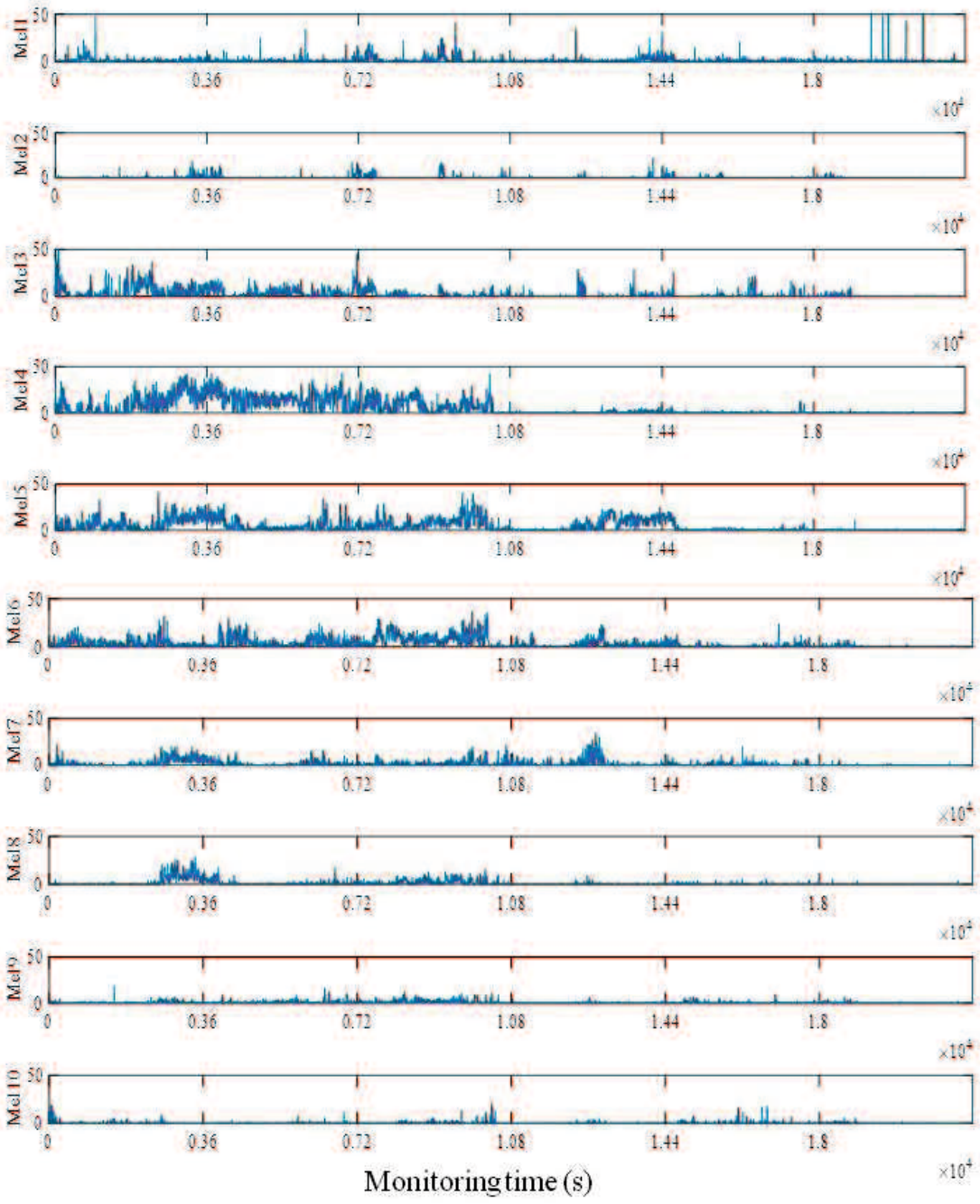

Figure 4.37 Monitoring results of each Mel scale features for the young tester B (1-10)

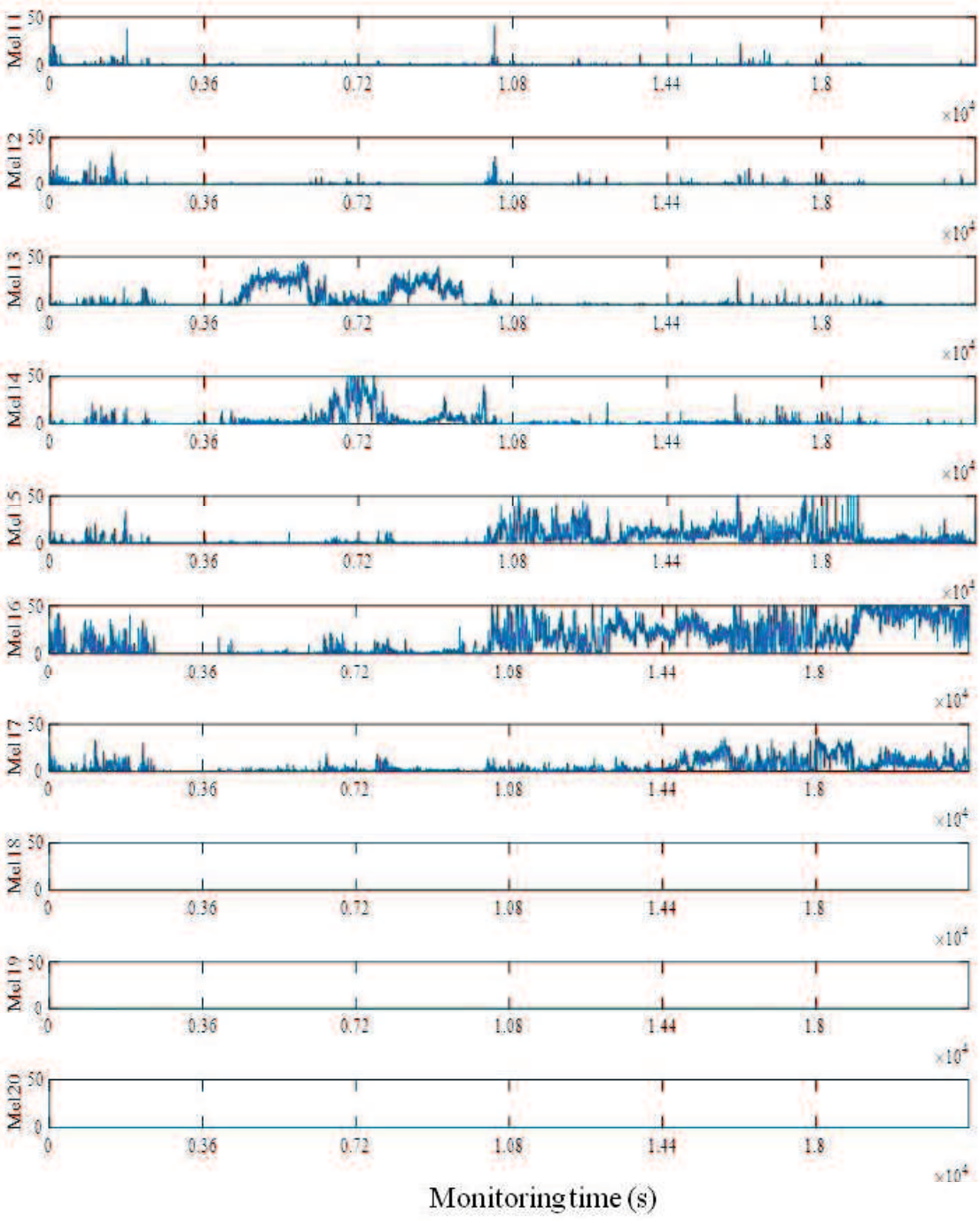

Figure 4.38 Monitoring results of each Mel scale features for the young tester B (11-20)

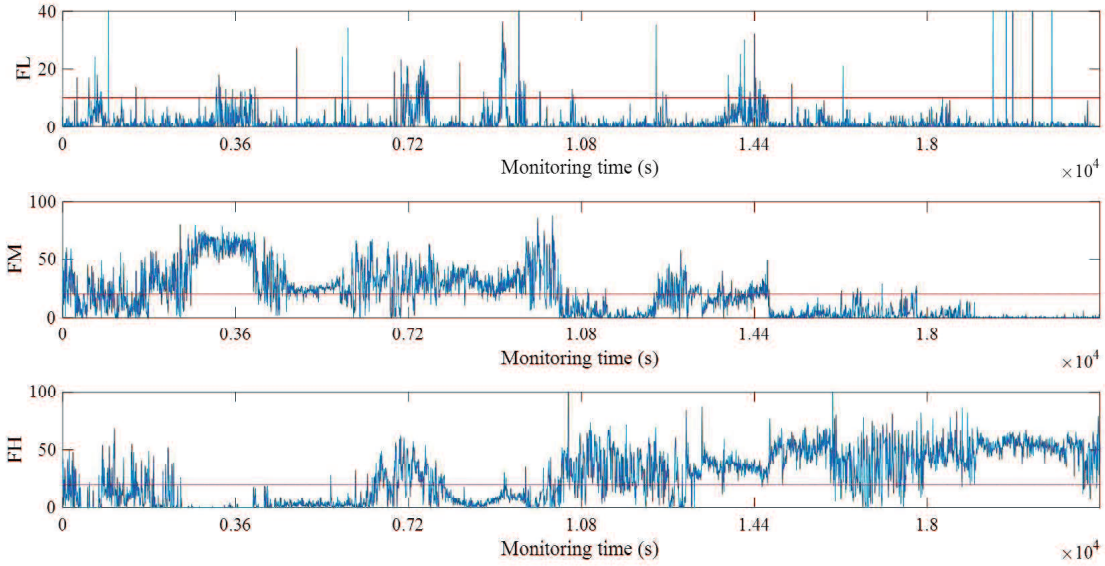

Figure 4.39 Identification results by Mel scales for the young tester B

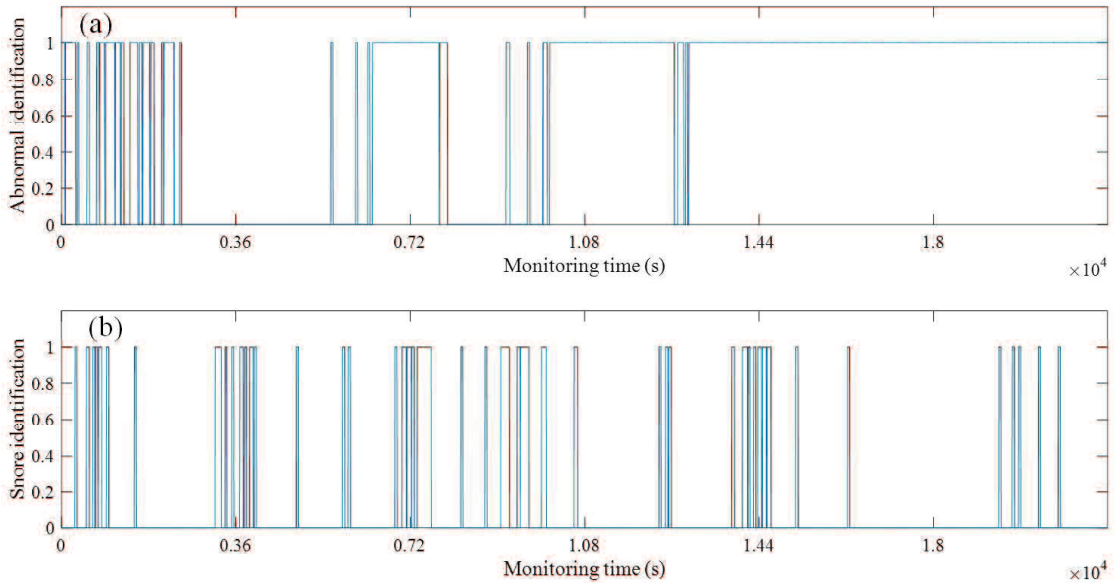

Figure 4.40 Monitoring results for the young tester B

4.5 Conclusion

Mel frequency spectrum is introduced from speech signal processing to identify snore and other abnormal sleep states from the sleep breathing sound signal. The core of the Mel analysis method is reflecting the relationship between the time and the frequency energy simulating the acoustic character of human ear. For each frame in time domain, the Mel scale label is extracted by finding the maximum value of frequency energy in each Mel scale. The present times of each Mel scale label is computed to show the frequency energy distribution. Then the normal breathing, abnormal breathing and snore energy can be identified based on the selected Mel scale label set. The normal breathing energy can be commonly marked by No.4 $\sim$ 7 Mel scale labels, FM. The abnormal breathing energy can be commonly marked by No.15 $\sim$ 17 Mel scale labels, FH. The snore energy can be commonly marked by No.1 $\sim$ 2 Mel scale labels, FL. With the suitable threshold values, the abnormal sleep and snore states can be identified successfully.

The monitoring results of three testers are applied to validate the efficiency of the proposed Mel frequency spectrum analysis. The proportion of the normal breathing state during sleep has been proposed as a new index to evaluate the condition of ventilation. It will be helpful for OSA monitoring and individual healthcare management.

For different individual, the frequency distributions have some changes. Long time monitoring and big data analysis are necessary in the future work.

Chapter 5

Application on heart state monitoring

5.1 Heart sound and heart murmurs

Cardiovascular disease has became one of the main reasons threatening the health and causing the death of human being, according to the report of cardiovascular in China 2016 [66]. During the sleep monitoring, heart state monitoring is important to prevent the heart infarction, cerebral infarction, stroke and so on.

Heart is a hollow muscle that pumps blood throughout the blood vessels by repeated, rhythmic contractions. Heart sound is generated by the mechanical vibration of the heart. Heart sound signal can be considered as periodical signal and a cardiac cycle is a period. The cardiac cycle is divided into systole and diastole and mainly contains two main heart sounds, i.e. the first heart sound (S1) which the beginning of the systole and the second heart sound (S2) which is the beginning of the diastole [67, 68].

The heart sound can reflect the condition of the heart working with rich information. When the heart structure or the opening and closing of the valves are not normal, the heart murmurs will be generated by the turbulence of the blood flow and can be detected by stethoscope too. Heart murmurs existing during the heartbeat is the key sign to diagnose the heart disease.

Congenital heart disease (CHD) is one of the typical cardiovascular diseases, which is a congenital defect in the heart structure before birth. And mortality resulted from CHD increases in recent years.

In China, ventricular septal defect (VSD) is 30.4% ~ 59.69%, atrial septal defect (ASD) is 18% ~ 39.8%, patent ductus arteriosus (PDA) is 5% ~ 14.9%, tetralogy of fallot (TOF) is 3.8%, they are typical CHDs. It is a killer for the babies and destroys the stable of the family.

Some single CHDs can be healed up naturally during one year after birth, like the healing probability of the signal VSD is about 20.5 ~ 52.9%. However, if the defects exist for a long time, it will affect the growth of the children and may become much more serious even cause pathological changes.

The defects and abnormalities of heart structure will cause the low oxygenation blood mixed with the rich oxygenation blood and destroy the balance of the pressure of the right and left heart. It can generate heart murmurs which are useful to diagnose the heart diseases. The heart murmurs divide into two types mainly, systolic murmurs and diastolic murmurs.

In this chapter, heart murmurs as an abnormal heart state is analyzed deeply for sleep monitoring based on the segmentation and analysis algorithms proposed for sleep monitoring with good performance.

5.2 Wearable acquisition system

The wearable acquisition of our test system for heart state monitoring include a auscultation vest, stethoscopes and recorders. The auscultation vest can fix the stethoscopes at the four auscultation sites exactly. The heart sound data acquired by the stethoscope is saved by the IC-recorder or smart phone as shown in Fig.5.1. The wearable system can collect heart sound signal fast with high SNR. The analysis will be completed on the computer. The sampling frequency of original heart sound signal is down sampled from 44.1kHz to 2000Hz.

Fig.5.2 displays a normal heart sound signal including the main components, the first heart sound (S1) and the second heart sound (S2). And the systole and diastole are divided by the heart pumping blood and convergent-divergent. The third heart sound (S3) always appear in the early diastole and the fourth heart

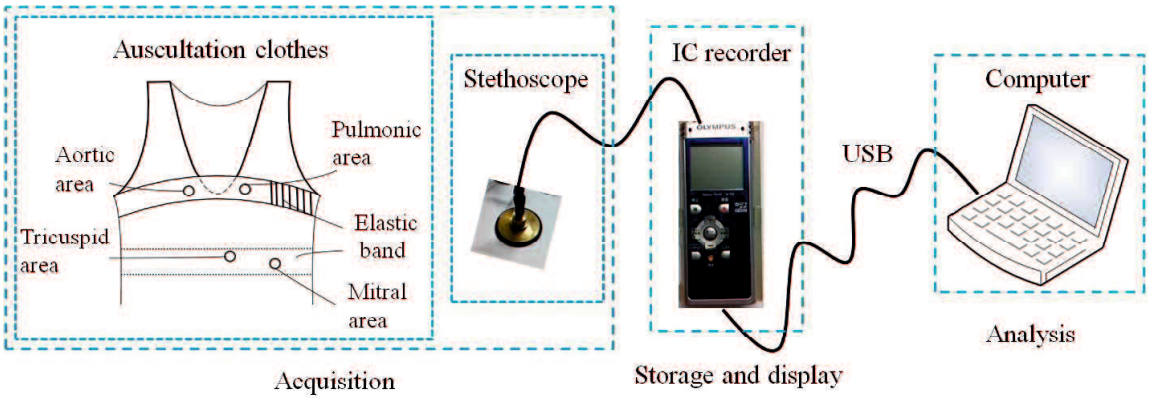

Figure 5.1 Test system of heart sound signal

sound (S4) appear in the late diastole usually. Sometimes the S3 can be found in the healthy person and S4 is a sign of abnormal heart commonly.

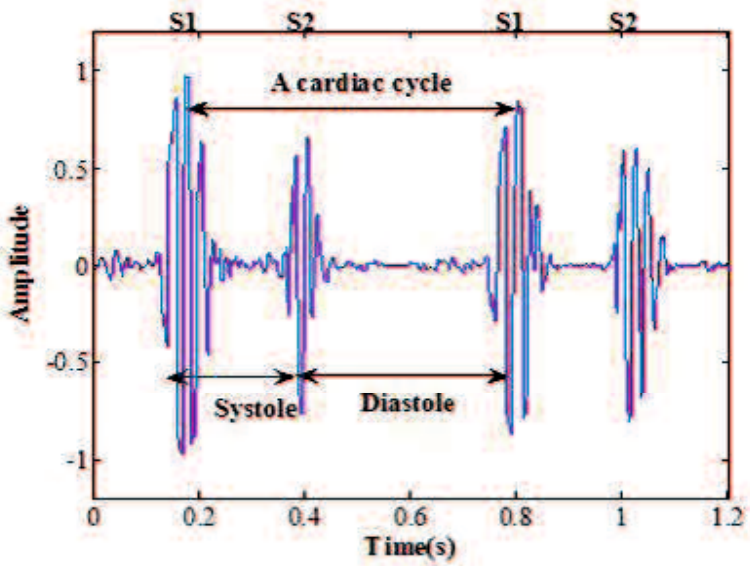

Figure 5.2 The normal heart sound signals

Fig.5.3 shows a part of abnormal heart sound, the murmurs appearing in systole can be distinguished from the normal heart sound signal with eyes obviously. It will be critical for heart monitoring.

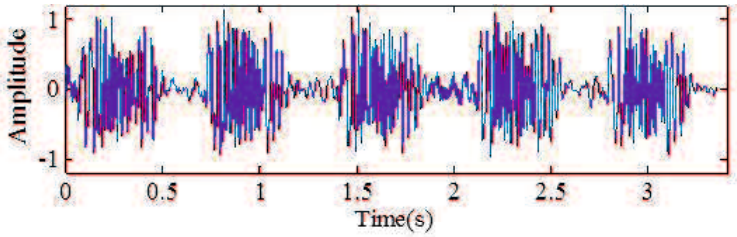

Figure 5.3 Heart sound signal of VSD case with systolic murmurs

5.3 Preprocessing of clinical heart sound signal

At the beginning of analysis, denoising is necessary to stand out the main heart sounds and murmurs for envelope extraction in the next part. The low-pass filter, band-pass filter are commonly applied to reduce the noise by setting a frequency band manually. The denoising methods based on wavelet is widely used as well. In this section, a denoising algorithm based on frequency slice wavelet transform (FSWT) and histogram curve is applied to reduce the surrounding noise and . The details are summarized as follows.

FSWT is defined as a new kind of time-frequency representation (TFR) of a signal [69]. FSWT has better properties than classical wavelet transform, such as symmetry, controllability, easy-to-design, dynamic scale, filter, and the reconstruction independency etc. So FSWT is more flexible to fit ever-changing signals than the classical methods.

In previous research, we have known that the main energy of S1 and S2 mainly distributes in 20 $\sim$ 80 Hz and energy of heart murmurs is in high frequency band. The ambient noises are usually presented in extensive frequency bands randomly and in low energy state on TFR plane. Base on the assumption that each of time-frequency components of PCG are connected at local area on its TFR image, the FSWT can be applied.

For any $f(t) \in L^2(R)$, the Fourier Transform of a window function $p(t)$ exists, and the FSWT is simplified as

$$W_f(t,\omega,\sigma) = \frac{1}{2\pi}\int_{-\infty}^{+\infty} \hat{f}(u)\hat{p}^*(\frac{u-\omega}{\sigma})e^{iut}du \tag{5.1}$$

where scale σ can be a function of ω and t or a constant not equaling 0. $*$ means the conjugate operator. ω and t represent the observed frequency and time, and u

is the assessed frequency. $\hat{p}(\omega)$ is frequency slice function.

While satisfying the condition of $\hat{p}(0) = 1$, the heart sound signal $f(t)$ can be reconstructed by

$$f(t) = \frac{1}{2\pi} \int_{-\infty}^{+\infty} \int_{-\infty}^{+\infty} W_f(\tau, \omega, \sigma) e^{i\omega(t-\tau)} d\tau d\omega \tag{5.2}$$

The damping speed of histogram curve can represent the noisy level of the surrounding. The surrounding is noisier, the damping speed of histogram curve descends more slowly. Noise reduction could be done by adjusting damping speed of histogram curve to modify the time-frequency image computed by FSWT, detail of the algorithm is expressed as below.

$$W_{new}(t, \omega, \sigma) = W_f(t, \omega, \sigma)(1 - e^{\frac{\alpha|W_f(t,\omega,\sigma)|}{M}}) \tag{5.3}$$

where M is the max value of the $W_f(t, \omega, \sigma)$, and α named a adjustment parameter is a constant larger than 0. The signal after denoising can be acquired by bringing $W_{new}(t, \omega, \sigma) =$ into the reconstruction function.

A heart sound data from a 9-year girl who is not suffered from CHD is applied to show the efficiency of the denoising method. It is easy to see that the noise appear around 1.0 second including speak noise, movement noise and strong breath sound.

The planes noted by (a) display the original signal and its time-frequency image. (b)(c)(d) show the time-frequency image after denoising and the reconstructed signal while α equals 0.2, 2 and 20.

The denoising energy ratio, the energy before denoising divides the original signal energy, is used to show the efficiency.

While $\alpha = 0.2, 2, 20$, the denoising energy ratio are 24.84%, 15.84% and 1.16%. As the time-frequency image shown in Fig.5.4 and Fig.5.5 , the smaller α is , the more noise components can be reduced. When $\alpha = 20$, the reconstructed signal still mixes with lots of noise, and when $\alpha = 0.2$, part of useful information has been removed according to test results by ear. Hence, the α is set as 2 to keep the S1, S2 and heart murmurs up for continuous study.

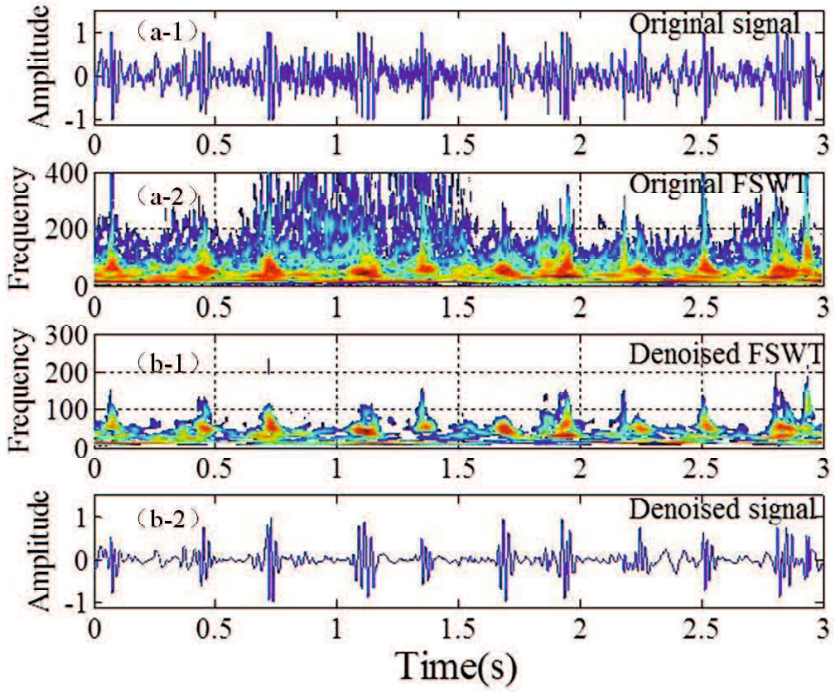

Figure 5.4 The denoising results with different adjusting parameter α (1).

5.4 Application on heart sound segmentation and heart murmur duration extraction

For CHD patients, researchers presented a character frequency band named as Arash-bands [70] to extract the heart sound energy, and then combined with the neural network to identify the normal heart sound and CHD heart sound [71]. The short time power spectrum and regression parameter were applied to extract the heart sound envelope and locate the S1, S2 and the cardiac cycle [72]. Furthermore, the average of the largest envelope of the later heart diastole is proposed to diagnose the PDA murmurs [73].

Researchers begin to focus on the extraction of heart murmurs to analyze heart diseases. The singular spectrum analysis is applied to segment the heart murmurs from the heart sound signal [74, 75]. The heart murmurs also can be located and extracted based on envelop extraction and segmentation [76]. So the duration of heart murmurs should be segmented and extracted firstly.

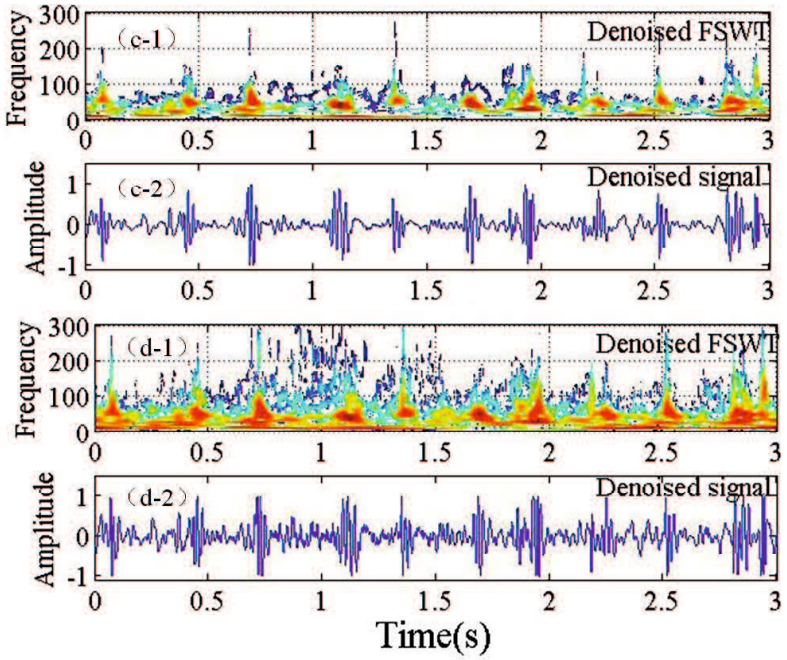

Figure 5.5 The denoising results with different adjusting parameter α (2).

5.4.1 Heart sound segmentation based on moment waveform extraction

The signal waveform segmentation based on moment waveform extraction is an effective method for sleep breathing sound signal. Breathing sound and heart sound are quasi-periodic signals. And a cardiac cycle which is made up of systole and diastole is similar to one breathing cycle including inspiration and expiration. So the proposed segmentation method is applied to segment the heart sound signal.

According to the functions introduced in chapter 2, TCW and CMW extraction have been done. For heart sound, the $\delta = 0.05$ and $l = T/2$ by experiments and try. T is the time duration of a cardiac cycle, it can be detected by finding the peak of the Fourier transform of TCW envelope. Then the local extrame points are computed to segment the systole and diastole.

A clinical data set including normal heart sound data and VSD data is applied in my research. The information of experimental data is listed in Tab.5.1.

Fig.5.6 show the segmentation result of heart sound waveforms based on moment waveform analysis. The first plot is the waveform of heart sound signal after

Table 5.1 The information of experimental data

Data type	Case number	Year	Data length(s)	Number of cycles
Normal	40	4 ~ 28	198	201
VSD	17	3 ~ 17	170	235

denoising. TCW and its local extramum points can be found in the middle plot. CMW and its local extramum points can be found in the last plot. As shown in the first plot. The solid line shows the segmentation of cardiac cycles and the dot line shows the segmentation of S1 and S2.

Fig.5.7 to Fig.5.9 display another 3 segmentation results. The normal heart sound waveform in Fig.5.7 and the VSD heart sound waveform in Fig.5.8 can be segmented correctly. But for the VSD case shown in Fig.5.9, two cycles can not be segmented successfully.

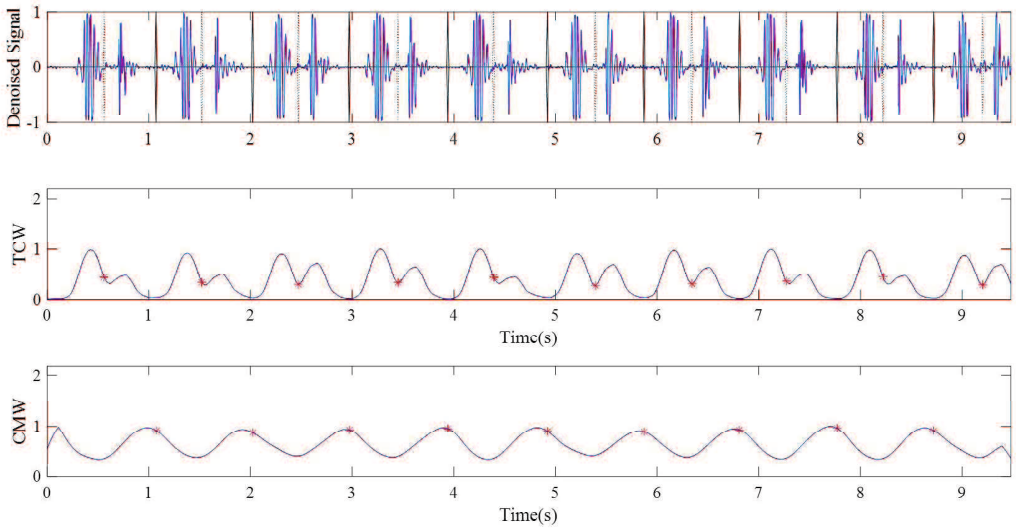

Figure 5.6 Segmentation of heart sound waveform (case 1)

The Segmentation results for clinical heart data set can be found in Table 5.2. It is easy to found that the successful rate of VSD case is lower than that of normal case. For the continues study, the cycles segmented correctly are applied for the following experiments.

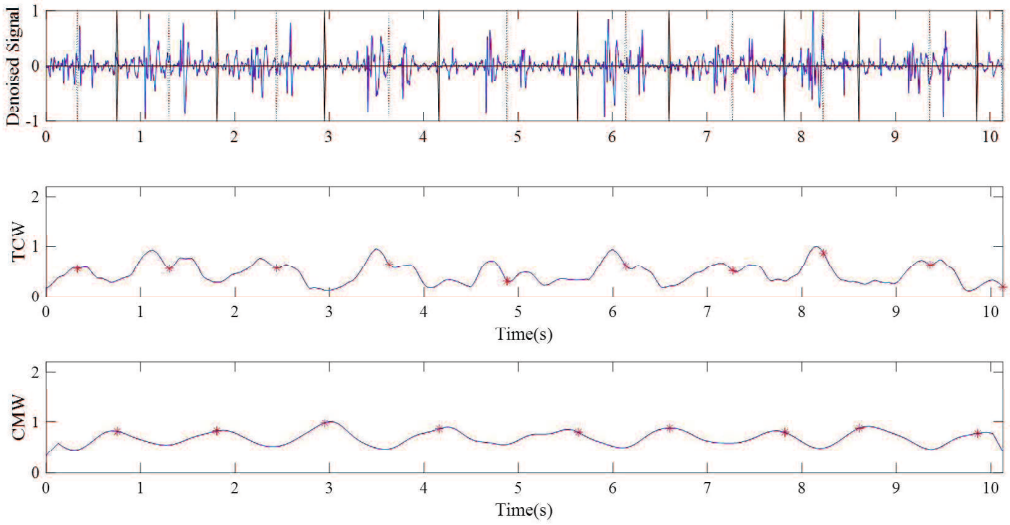

Figure 5.7 Segmentation of heart sound waveform (case 2)

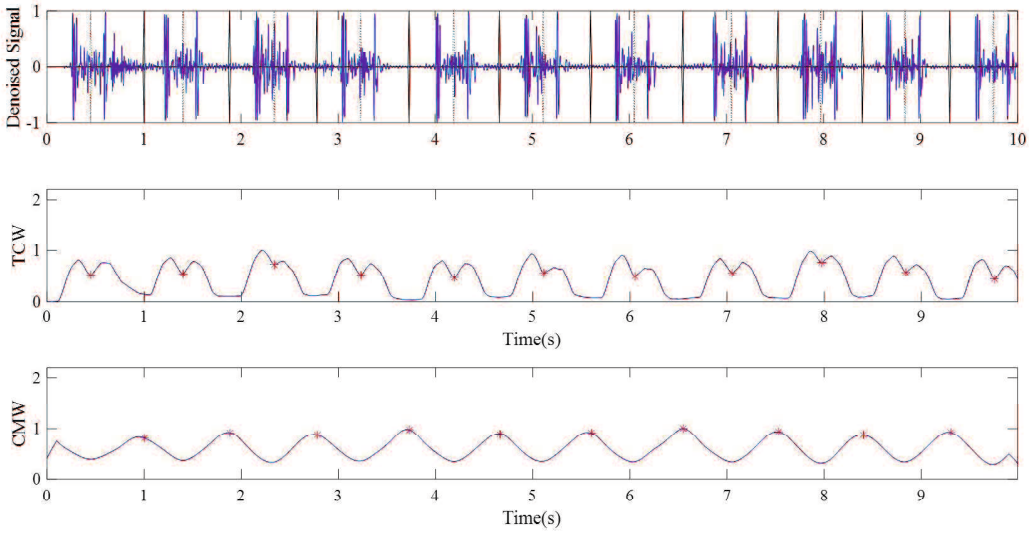

Figure 5.8 Segmentation of heart sound waveform (case 3)

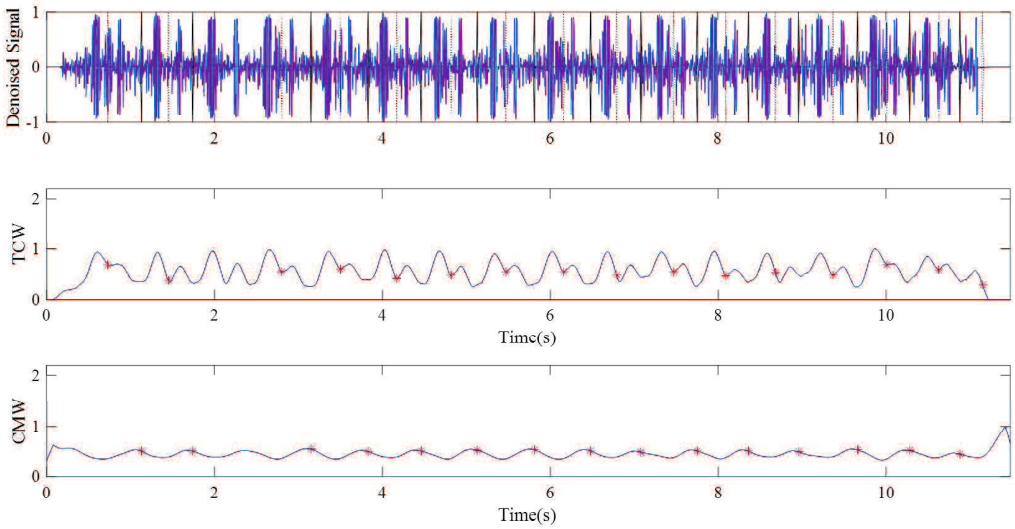

Figure 5.9 Segmentation of heart sound waveform (case 4)

Table 5.2 Segmentation results for clinical heart sound signals

Group	Total cardiac cycles	Segmented cycles	Successful rate
Normal	201	200	99.5%
VSD	235	225	95.74%

5.4.2 Heart murmur duration extraction

Based on the segmentation results, the time duration of heart murmurs can be extracted for further analysis. The sketch map of duration extraction for systolic murmur (SM) and diastolic murmur (DM) is shown in Fig.5.10. In Fig.5.10, the green $\star$ represents the center of DM, the local maximum points of the CMW. The red $\star$ is the center of SM, the local minimum points of the TCW between the two adjacent green stars. On the basis of statistic data of experiments, the time durations of SM and DM last $T/6$ and $T/3$ respectively. The heart murmurs can be extracted with the detection of centers.

For the heart sound signal whose strong murmurs cover the S1 and S2, the segmentation of murmurs based on the location of S1, S2 via envelope and threshold is difficult. So the TCW and CMW which have good performance in previous research is used to extract the heart murmurs.

Fig.5.11 shows the SM and DM duration extraction based on TCW and CMW

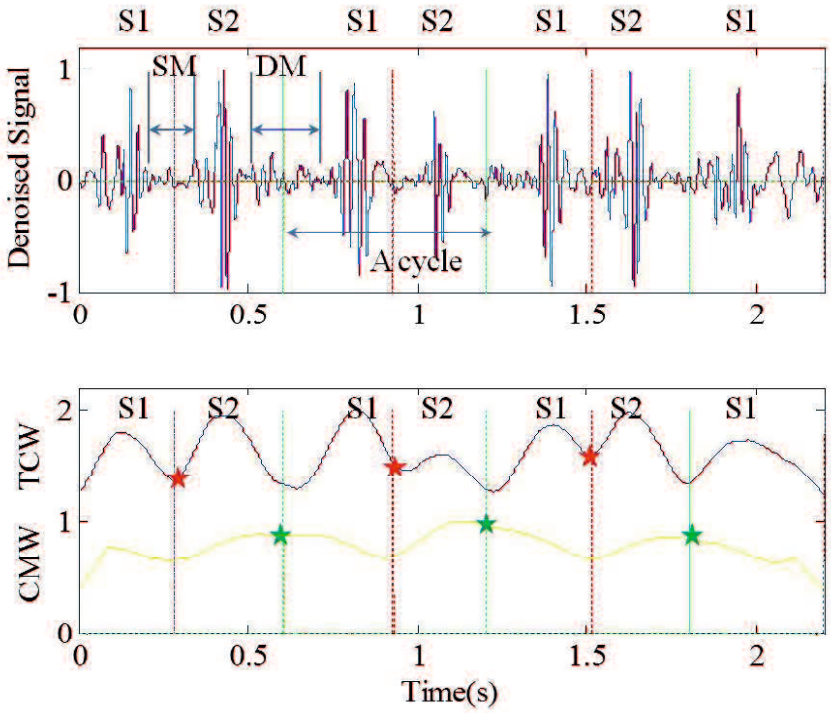

Figure 5.10 Sketch map of SM and DM durations extraction.

for a VSD case. Fig.5.12 displays the signal of DM duration in the middle plot and the signal of SM duration in the bottom plot. There is sysotlic murmurs for VSD case. Fig.5.13 shows the SM and DM duration extraction for a normal case. Using the proposed method, heart murmurs can be also extracted from the filtered heart sound signal successfully.

5.5 Identification of heart murmurs by Mel frequency spectrum analysis

Features extraction of heart murmurs is the key point. In time domain, time durations of heart murmurs are extracted by setting a threshold value on the envelop [77], the energy of murmur are used to discuss the patten of heart diseases [78]. In frequency domain, the peak value and frequency bands are extracted based on Fourier spectrum or power spectral density [79], frequency energy index are proposed via wavelet packet composition [80].

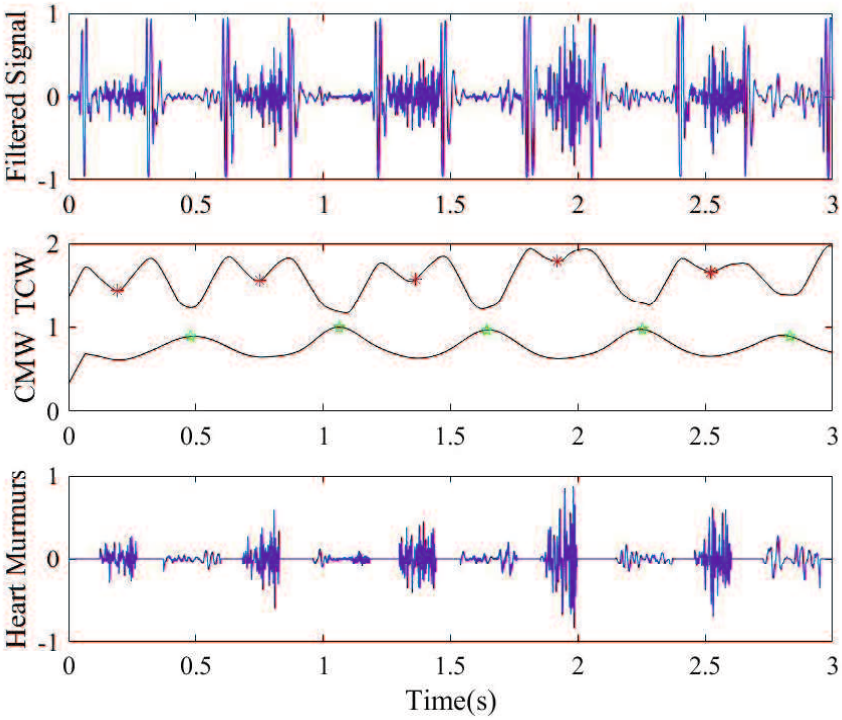

Figure 5.11 SM and DM durations extraction of a VSD case.

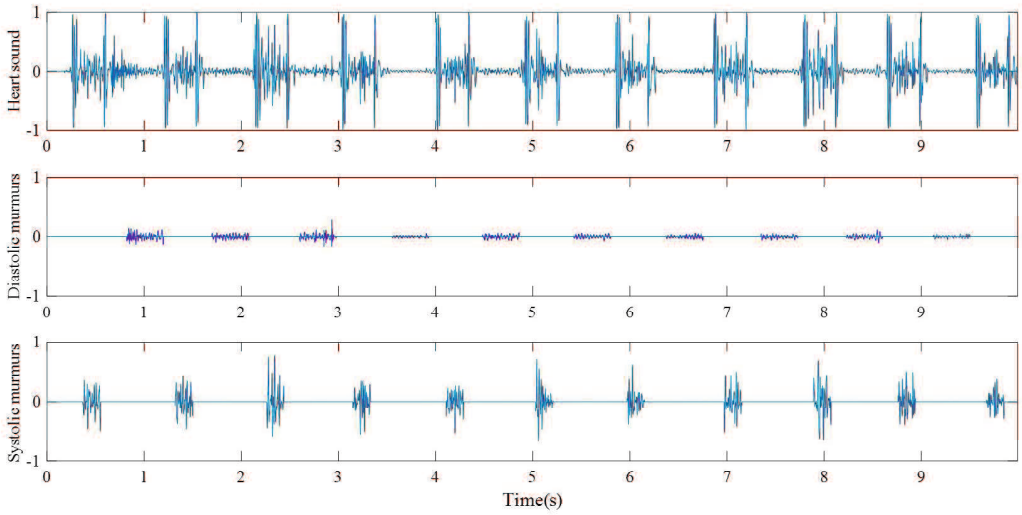

Figure 5.12 SM and DM durations extraction of a VSD case.

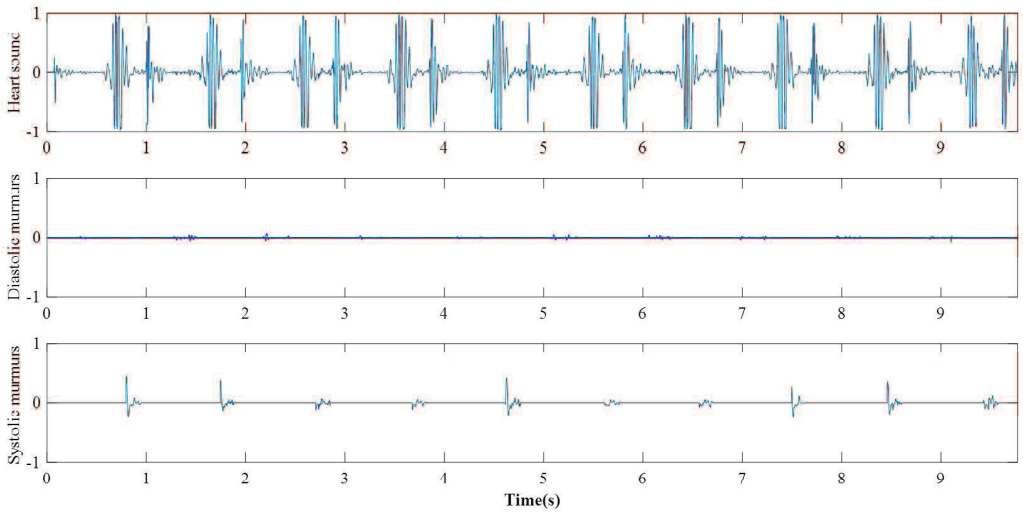

Figure 5.13 SM and DM durations extraction of a normal case.

In our previous study, the MFCC algorithm is applied to analyze the sleep breathing sound signal. To acquire the useful information more directly, a modified MFCC method is proposed and the Mel-scale features are extracted. Part of Mel-scale features are selected to classify the healthy cases and the case who suffered from sleep-related breathing disorders. The experimental results show the efficiency of the selected feature set. Hence it is introduced to heart state monitoring via heart sound signals as a necessary part of sleep monitoring.

The Mel-scale features of heart sound are extracted as following steps.

Step 1: Heart sound framing and windowing. The heart sound is screened by a hamming window, which can minimize the spectral distortion by tapering the signal to zero at the beginning and end of each frame, about 32ms with about 15ms overlapping. For convenience of the computation, the length of window will be the power of 2 and it is set to 64 points with 32 points overlapping.

Step 2: Calculate the power spectral density (PSD) of the signal in each frame. Here Yule-Walker's method is used to make the power spectrum density instead of the energy of the FFT result.

Step 3: Filter the PSD signal by the Mel-scale filter bank. The Mel filter bank is composed of 20 triangle band-pass filters.

Step 4: Apply the logarithm to the output of the Mel-scale filter bank and the

Mel-scale features are extracted.

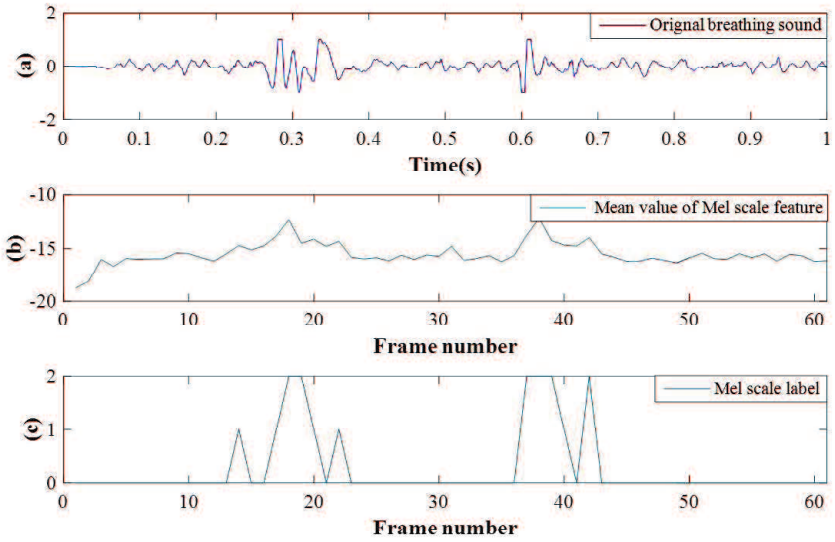

Figure 5.14 Mel frequency spectrum analysis for a cycle of normal heart sound signal.

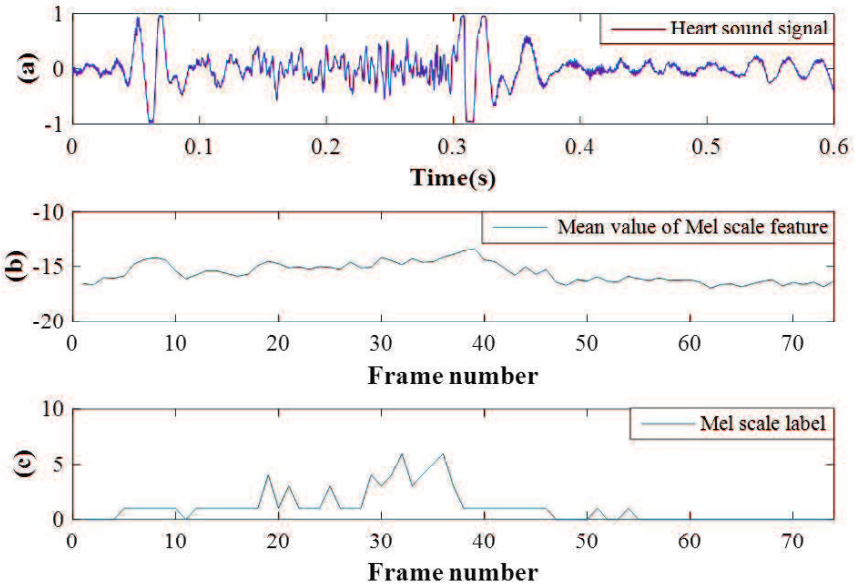

Figure 5.15 Mel frequency spectrum analysis for a cycle of abnormal heart sound signal.

Fig.5.14 is a normal heart sound cycle with clear S1 and S2. Fig.5.15 is a heart sound cycle with systolic murmurs. Fig.5.16 and 5.17 show the frequency

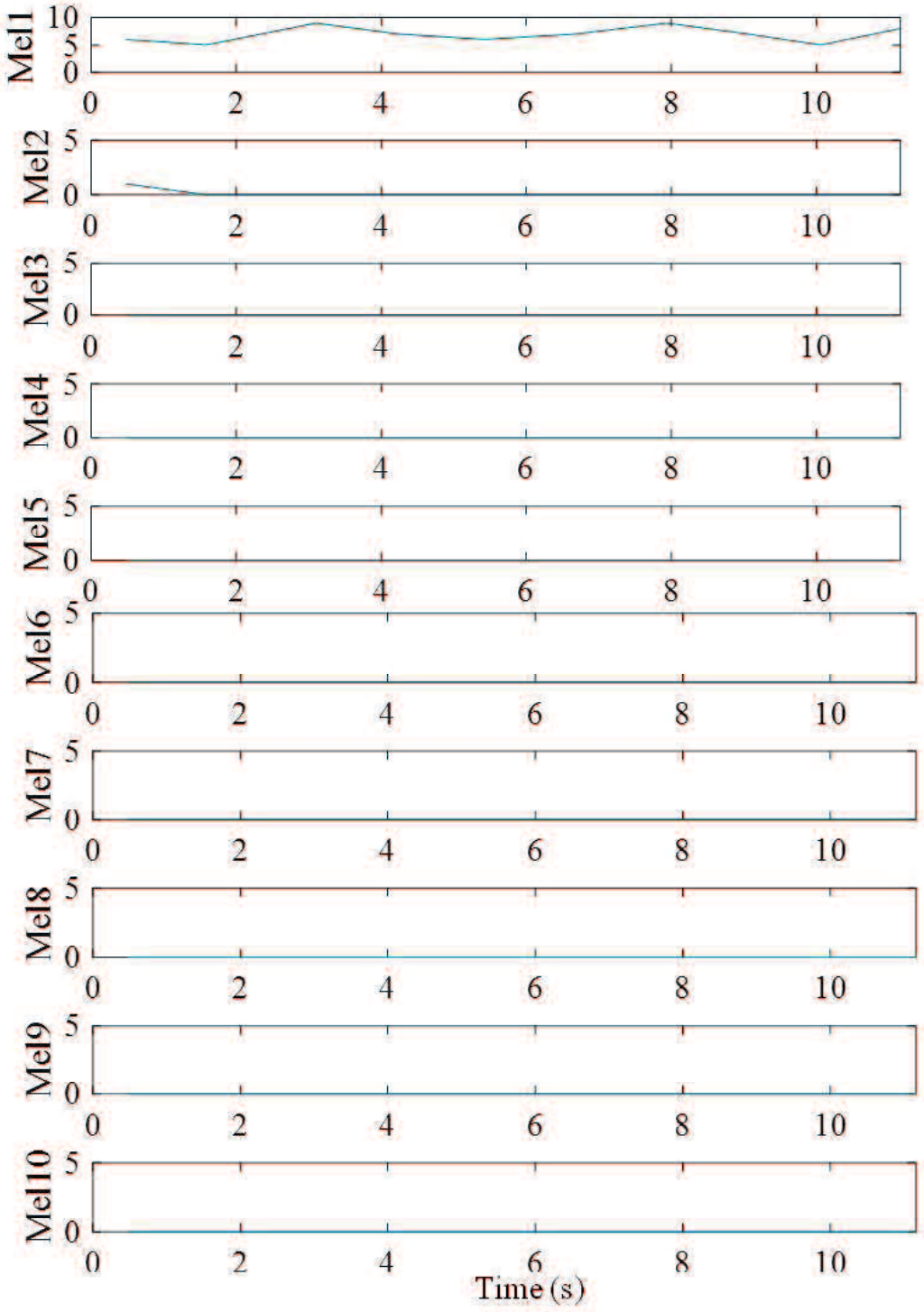

Figure 5.16 Frequency distribution analysis by each Mel scale for normal case in SM duration

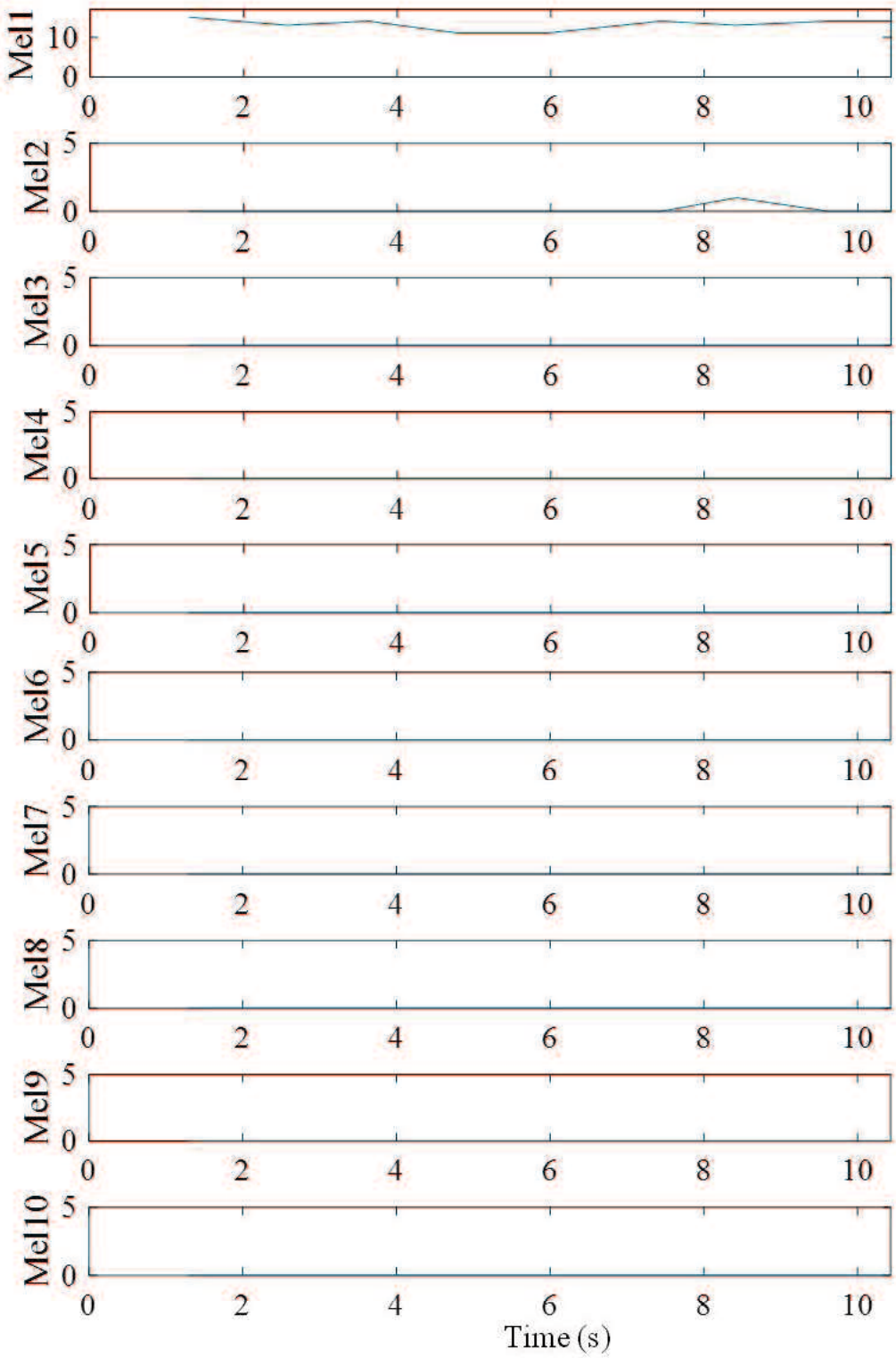

Figure 5.17 Frequency distribution analysis by Mel scales for normal case in DM duration

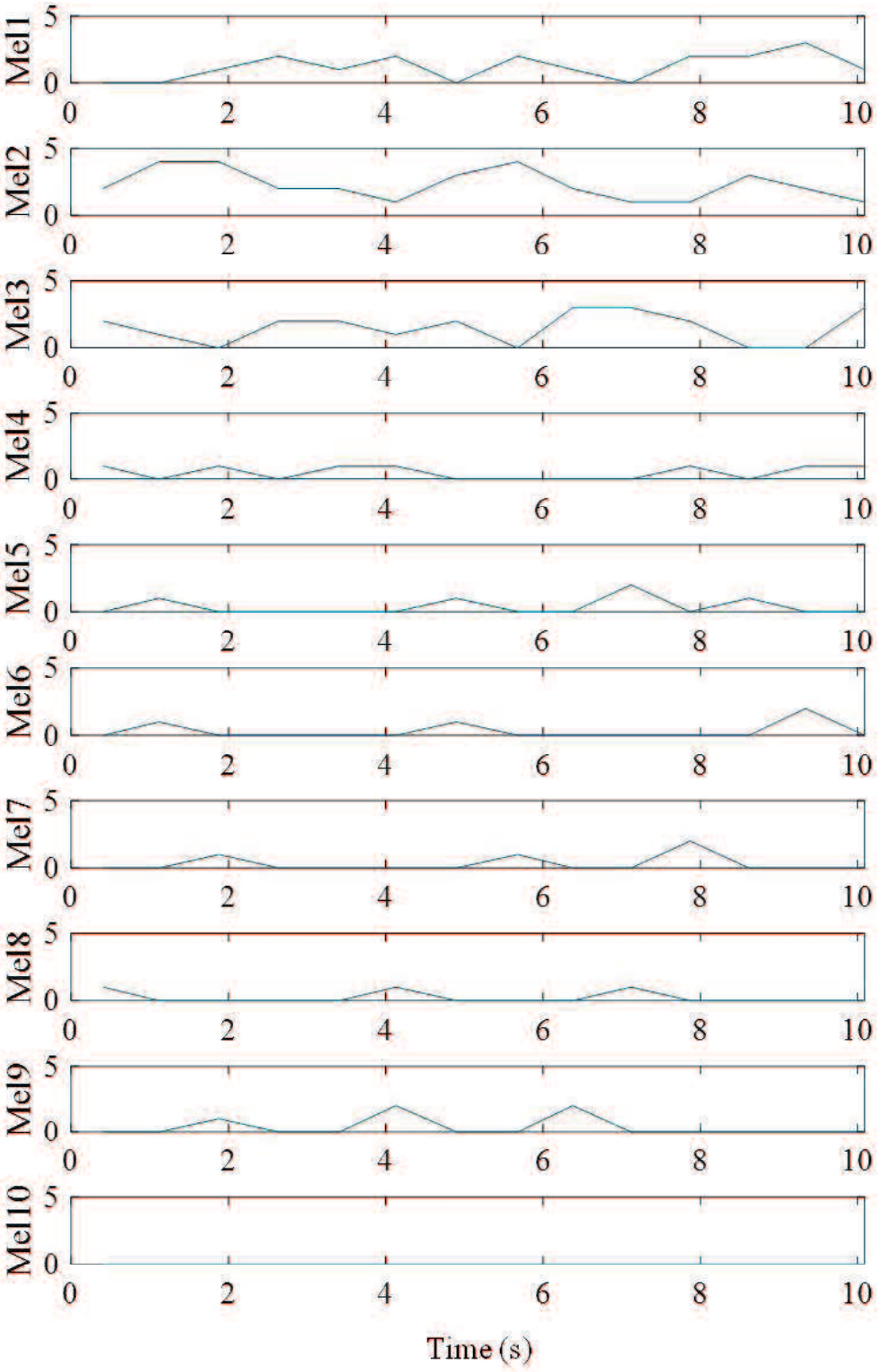

Figure 5.18 Frequency distribution analysis by Mel scales for a VSD data in SM duration

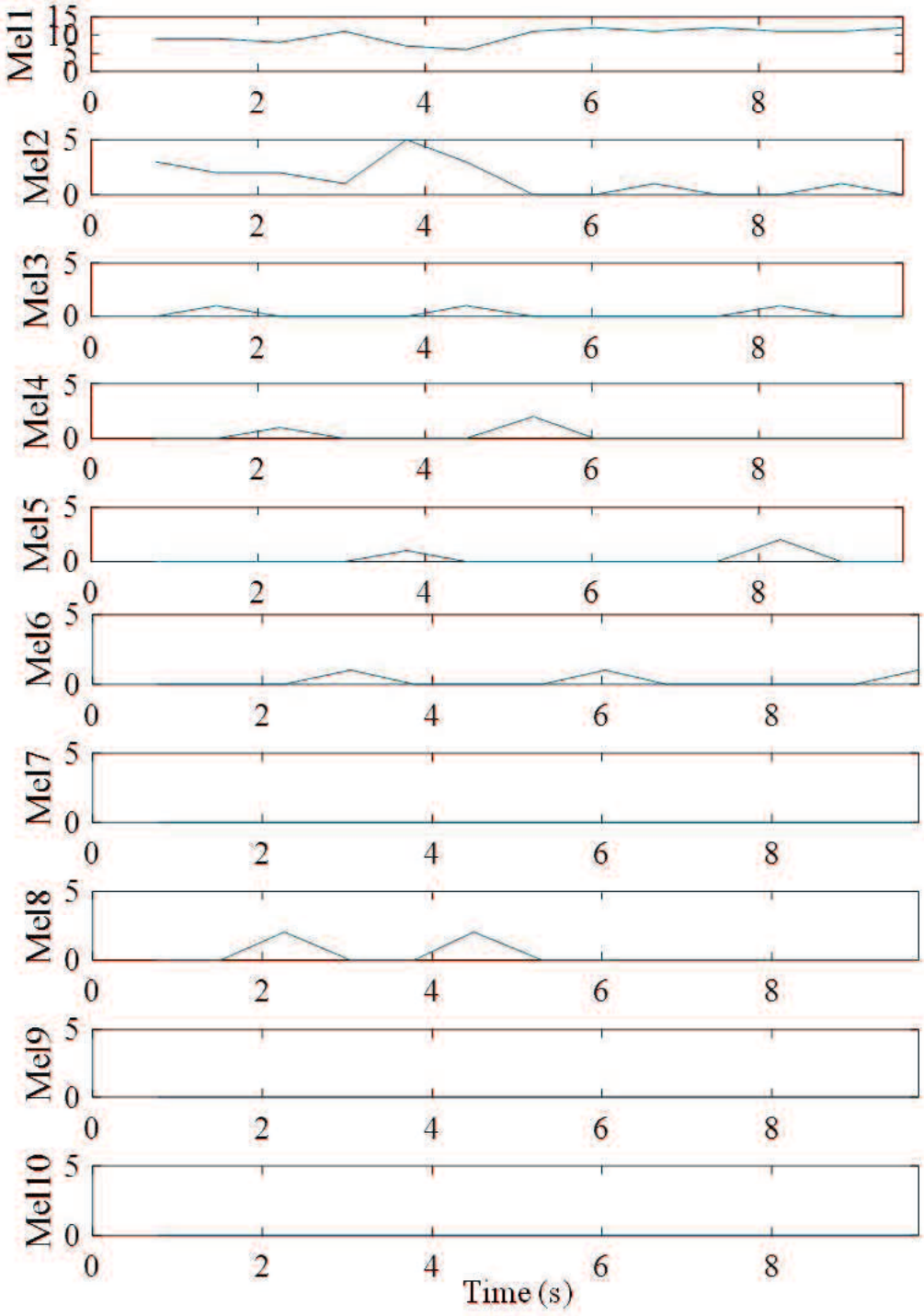

Figure 5.19 Frequency distribution analysis by Mel scales for a VSD data in DM duration

distribution by No.1-10 Mel scales for a normal case in SM and DM duration respectively. In both SM and DM duration, there are larger value in No.1 and 2 Mel scales.

Fig.5.18and 5.19 show the frequency distribution by No.1-10 Mel scales for a VSD case in SM and DM duration respectively. In SM duration, there are larger values of No.1-8 Mel scales. In DM duration, there are larger values of No.1-6 Mel scales.

For the results shown in the above figures, normal heart sound components are mainly marked by the first two Mel scale labels. The murmurs, abnormal heart sound components, have larger value from No.3 to No.8 Mel scale labels.

We focus on VSD case in this stage and the Mel-scale features from third to tenth are selected to identify the heart murmurs of VSD cases in SM and DM duration.

Among the data set, 21 normal case (103 cycles) and 11 VSD cases(156) is selected as training data to build the identify model. The features in SM and DM of each data is extracted and the ranges of Mel scale features are shown in Figs.5.20 and 5.21.

The mean value and the standard deviation of each Mel-scale features are computed to determine the range of the parameters. The red lines is VSD identification range and the blue lines shows the boundaries of the normal identify zone.

The identification model of normal and VSD cases in SM is displayed in the left, the model in DM is shown in the right.

In order to validate the efficiency of identify modes built above, the rest data including 19 normal cases(95 cycles) and 5 VSD cases (69 cycles) are used as test data. More than five features of one test data distribute in normal zone is identified as normal case, and it is the same way for VSD case. The identify results can be summarized in Table 5.3.

Table 5.3 The identify results by Mel-scale features

Experiment data	**Identify results in SM**		**Identify results in DM**	
Classification	Normal	VSD	Normal	VSD
Normal	95	0	80	15
VSD	0	69	0	69

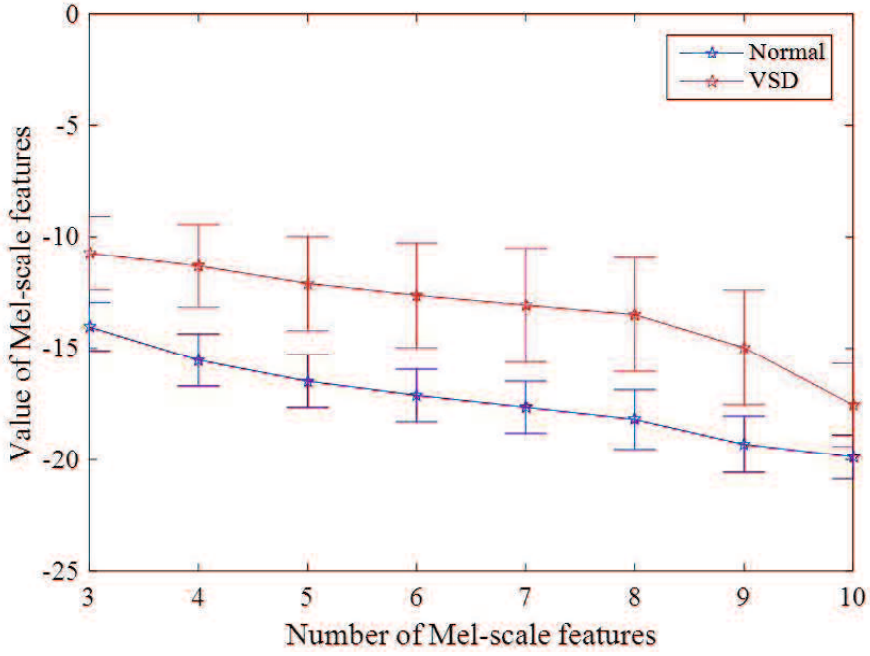

Figure 5.20 VSD identification in SM duration

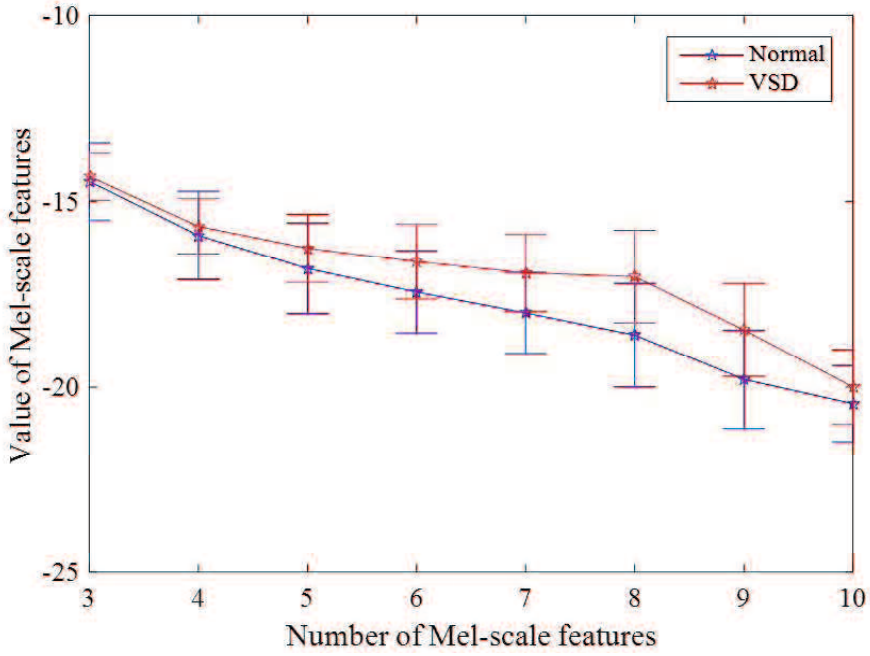

Figure 5.21 VSD identification in DM duration

According to the results shown in Table5.3, the normal and VSD cases can be identified in SM with 100% of the accuracy. The identify accuracy is 90.85% in DM. Besides, because true positive (TP) is 69, false negative(FN) is 0, false positive (FP) is 15 and true negative (TN) is 80 in DM, the sensitivity calculated by $TP/(TP+FN)$ equals 100% and the specificity of two groups gotten by $TN/(FP+TN)$ is 84.21%.

5.6 Conclusion

Heart sound can not only reflect the condition of heart function but also the abnormal of heart structure. Hence heart monitoring is a indispensable part of healthcare, especially for sleep monitoring.

The heart murmurs analysis method based on moment waveform extraction and MFCC algorithm is introduced for abnormal heart state monitoring. The processing method based on FSWT and histogram curve can improve the signal to noise ratio of recorded signal. The durations of heart murmurs is extracted based on TCW and CMW. Mel-scale features are extracted from each murmur duration to build identification model of congenital heart disease. The clinical heart sound data set is applied to test the model's availability. In the duration of systolic murmurs, ventricular septal defect (VSD) can be identified successfully. The sensitivity and specificity are 100% and 84.21% for normal and VSD cases identification in duration of diastolic murmurs.

The proposed analysis method of heart sound signal can identify the abnormal heart murmurs which is meaningful to monitor the heart state during sleep.

Chapter 6

Conclusion

6.1 Summary and Contribution

Healthcare become a social hot issue with the development of aging population, the threat of chronic disease and the increased cost of healthcare. Sleep spending one third of the life is indispensable to support humans' health. The sleep-related disorders affect the sleep quality seriously, increase the complications risk of cardiovascular disease including apnea syndrome, heart failure and so on. Therefore, monitoring and analysis for breathing sound and heart sound during the whole night sleep play a very important role on healthcare.

PSG is the golden standard to evaluate the sleep states and diagnose the sleep respiratory disorders, especially for diagnosing obstructive sleep apnea (OSA). At present only polysomnography (PSG) can provide exact apnea-hypopnea index (AHI) for estimating the severity of OSA. However, PSG should be tested in hospital and is not suitable for daily monitoring at home. So the smart monitoring system which is low-cost and portable is indispensable for daily healthcare.

Compared with PSG, sleep breathing sound signal can be acquired portably. The portable acquisition composed of a smart phone and an earphone is utilized to record, save and analyze the sleep breathing sound signal. It can collect the breathing sound signal during whole night with little influence of sleep quality. Using breathing sound signals, the abnormal breathing state caused by sleep-related breathing disorders can be detected effectively. In this thesis, a research on

parameter extraction and analysis of cardiorespiratory sound for sleep and heart state monitoring is introduced.

In order to guarantee the veracity of the sleep breathing signal analysis, the sleep breathing sound signal should be segmented into cycles first. There are stable and unstable breathing, snore, apnea during the whole night sleep. The segmentation is difficult via common measure because the breathing state changes greatly during the whole night. In my study, a sleep breathing waveform segmentation based on the moment waveform analysis is proposed to segment the breathing cycles and respiratory phases. To reduce the affection of breathing intensity, a preprocessing for decreasing the amplitude contrast has been applied. Then the time characteristic waveform (TCW) and characteristic moment waveform (CMW) is extracted with suitable time-scale parameters. Lastly, the breathing cycles and inspiration/expiration can be segmented successfully by the local extreme points of TCW and CMW. The efficiency of the proposed segmentation method is validated by a set of testers including normal students and a patient suffered from obstructive sleep apnea (OSA) with the manually counting as reference. With the help of proposed preprocessing method, the successful rate of breathing cycle segmentation can reach to 98.4%. For the OSA case, 97.44% of breathing cycle can be segmented correctly. The successful rate of respiratory phase segmentation is more than 95.96%.

Abnormal breathing patterns are important for sleep state monitoring and sleep breathing database. Especially for obstructive sleep apena analysis, the abnormal breathing signal including apnea and hypopnea should be identified to detect the AHI value during the night. Apnea can be defined by breathing pause lasting more than 10 seconds. But the hypopnea estimated by ventilation is less than 50% or breathing cycle lasting more than 6 seconds has not clear definition. The normal breathing pattern, apnea pattern and hypopnea pattern are defined by the time duration of breathing cycles. Apnea can be detected with a threshold value setting as dd_{stable} + 10s exactly. Hypopnea is detected by setting a set of threshold values of the breathing cycle time according to the clinical definition. The detected apnea parts are displayed to validate the efficiency of time-domain parameters. Moreover, the pause time of each apnea is calculated to evaluate the level of obstruction. Then the AHI can be estimated by the number of apnea and hypopnea. Four-night data from the OSA tester and two-night data from two young students are monitored and the AHI values are estimated. The identification results of apnea can be confirmed, but the identification of hypopea is related with the threshold values. The AHI value is detected to provide a useful reference to monitor OSA patients and manage the sleep health for common people.

Mel frequency spectrum is introduced from speech signal processing to monitor the abnormal breathing states which cannot be detected in time domain, such as snore, unstable periodic breathing and so on. The Mel frequency spectrum can show the relationship between the time and the frequency energy simulating the acoustic character of human ear. For each frame in time domain, the Mel scale label is extracted by finding the Mel scale with the maximum value of frequency energy. Then the present times of Mel scale label are counted to show the frequency energy distribution clearly. The normal breathing energy, abnormal breathing energy and snoring energy can be identified by the fixed Mel scale label set. Based on the whole night monitoring results, the snore energy can be represented by No.1 $\sim$ 2 Mel scale labels, the normal breathing energy is commonly represented by No.4 $\sim$ 7 Mel scale labels, the abnormal breathing energy are mainly represented by No.15 $\sim$ 17 Mel scale labels. With suitable threshold values, the normal/abnormal breathing states and snore state can be identified. The time duration of each breathing state can be computed. The proportion of normal/abnormal states has been proposed to reflect the condition of breathing ventilation. It has potential to prevent the cardiovascular diseases as a new evaluation index.

At last, the proposed breathing waveform segmentation method and Mel frequency spectrum analysis method are applied for abnormal heart sound signal detection in chapter 5. The original heart sound data can be recorded and saved by a portable acquisition system. The processing method based on FSWT and histogram curve are used to improve the signal to noise ratio of the original signal in the beginning. The proposed segmentation method based on moment waveform analysis is applied to heart sound signal with adjusted parameters. The efficiency of the proposed segmentation method is confirmed again by segmenting the cardiac cycle and systole/diastole successfully. Moreover the intervals of heart murmurs have been extracted correctly and fast. Mel-scale features are extracted from each murmur intervals. According to the Mel frequency spectrum analysis, No.3 $\sim$ 10 Mel scale features are selected to identify the heart murmurs of ventricular septal defect (VSD). The clinical children's data is applied to test the usefulness of the feature set. In the duration of systolic murmurs, VSD can be identified successfully. The sensitivity and specificity are 100% and 90.85% for normal and VSD cases identification in the duration of diastolic murmurs.

6.2 Future work

In the future, the detection of hypopnea will be improved to get the exacter AHI index for monitoring OSA. With more clinic data, the data base of breathing state patterns will be completed. The identification parameters will be modified and selected for effective sleep monitoring. More useful parameters will be proposed to reflect the condition of breathing ventilation while sleep. It will helpful to prevent Alzheimer's disease and other related diseases.

The monitoring of heart states in time and frequency domain will be studied deeply to prevent cardiovascular disease, such as heart infarction, stroke and so on. The cases with heart diseases and sleep respiratory disorders at the same time will be concerned. The application will be expanded to all night monitoring for abnormal breathing states and heart states.

In addition, the proposed analysis methods in this research will be introduced for other physiology signals. It will improve the function of our monitoring system for healthcare.

Reference

[1] N. Israel, A. Tarasiuk, and Y. Zigel. Nocturnal Sound Analysis for the Diagnosis of Obstructive Sleep Apnea. in Proceedings of the 32nd IEEE International Conference on Engineering in Medicine and Biology Society (EMBS 2010),6146-6149, 2010.

[2] Charalampos Doukas, Theodoros Petsatodis, Christos Boukis, Ilias Maglogiannis. Automated sleep breath disorders detection utilizing patient sound analysis. Biomedical Signal Processing and Control,7:256- 264, 2012

[3] News Conference of World Sleep Day, Beijing, 2017.

[4] HUANG Jun-ying, ZHANG Jin-ru, MAO Cheng-jie, et al.Effects of obstructive sleep apnoea hypopnoea and rapid eye movement sleep behavior disorder on cognitive impairment in Parkinson's disease. J Clin Neurol, 29(6):417-420, 2016

[5] Yoko Komada, Shoichi Asaoka, Takashi Abe, Yuichi Inoue. Short sleep duration, sleep disorders, and traffic accidents. IATSS Research, 37:1-7, 2013

[6] Quanying He. OSAHS is An Important Cause of Road Traffic Accidents .Medicine and Philosophy ,35(12):72-75,2014

[7] 2016 white paper on sleep and occupational safety, Beijing, 2016

[8] Angie Mae Rodday, Ruth Ann Weidner, Laurel K. Leslie. Predicting Health Care Utilization for Children With Respiratory Insufficiency Using Parent-Proxy Ratings of Children's Health-Related Quality of Life. Journal of Pediatric Health Care, 31,6,654-662,2017

[9] P. Hult, T. Fjallbrant, B. Wranne, O. Engdahl, P. Ask, An improved bioacoustic method for monitoring of respiration, Technol. Health Care, 12, 323-332, 2004

[10] Tianyu Wang, Fayan Zhang, Liang Li. Awareness investigation of obstructive sleep apnea hypopnea syndrome for general population.

[11] Z. Moussavi, A. Elwali, R. Soltanzadeh, C. A. MacGregor, and B. Lithgow, Breathing Sounds Characteristics Correlate with Structural hanges of Upper Airway due to Obstructive Sleep Apnea. Engineering in Medicine and Biology Society (EMBC),5956-5959,2015.

[12] Banos, O., Villalonga, C., Damas, M., Gloesekoetter, P., Pomares, H., Rojas, I. Physiodroid: Combining wearable health sensors and mobile devices for a ubiquitous,continuous, and personal monitoring. Sci. World J, 2014

[13] Serhani, M.A., El Menshawy, M., Benharref, A., SME2EM: Smart mobile end-to-end monitoring architecture for life-long diseases. Comput. Biol. Med. 68,137-154,2016.

[14] Qi Jiang, Jianfeng Ma, Chao Yang, Xindi Ma, Jian Shen, Shehzad, A.C. Efficient end-to-end authentication protocol for wearablehealth monitoring systems. Computers and Electrical Engineering, 000,1-14, 2017

[15] Gay, V., Leijdekkers, P. A health monitoring system using smart phones and wearable sensors. Int. J. ARM,8 (2), 29-35,2007

[16] Marques, F.A.F., Ribeiro, D., Colunas, M.F., Cunha, J.P.S. A real time, wearable ECG and blood pressure monitoring system. In: 2011 6th Iberian Conference on Information Systems and Technologies (CISTI), 1-4,2011

[17] Massimo Esposito, Aniello Minutolo, Rosario Megna, Manolo Forastiere, Mario Magliulo, Giuseppe De Pietro. A smart mobile, self-configuring, context-aware architecture for personal health monitoring. Engineering Applications of Artificial Intelligence, 67,136-156,2018

[18] Ahmed Harbouche, Noureddine Djedi, Mohammed Erradi, Jalel Ben-Othman, Abdellatif Kobbane.Model driven flexible design of a wireless body sensor network for health monitoring.Computer Networks, 129,548-571,2017

[19] Haider Mshali, Tayeb Lemlouma, Damien Magoni. Adaptive monitoring system for e-health smart homes. Pervasive and Mobile Computing,43,1-19,2018

[20] Clara M. Ionescu, D. Copot. Monitoring respiratory impedance by wearable sensor device: Protocol and methodology. Biomedical Signal Processing and Control, 36,57-62,2017

[21] Dempsey, J.A., Veasey, S.C., Morgan, B.J., Donnell, C.P.Pathophysiology of sleep apnea. Physiol. Rev. 90, 47-112, 2010

[22] G. Sierra, V. Telfort, B. Popov, L.G. Durand, R. Agarwal, V. Lanzo. Monitoring Respiratory Rate Based on Tracheal Sounds. First Experiences. Proceedings of the 26th Annual International Conference of the IEEE EMBS, San Francisco, CA, USA, September 1-5, 2004

[23] F. Jin, F. Sattar , DYT Goh , and I.M. Louis. An Enhanced Respiratory Rate Monitoring Method for Real Tracheal Sound Recordings. 17th European Signal Processing Conference (EUSIPCO 2009), 642-645, 2009

[24] Jianmin Zhang, Wee Serand Daniel Yam Thiam Goh. A Novel Respiratory Rate Estimation Method for Sound-Based Wearable Monitoring Systems. 33rd Annual International Conference of the IEEE EMBS, Boston, Massachusetts USA, August 30 - September 3,3213-3216,2011

[25] Hisham Alshaer , Geoff R. Fernie, Ellen Maki, T. Douglas Bradley. Validation of an automated algorithm for detecting apneas and hypopneas by acoustic analysis of breath sounds. Sleep Medicine,14 ,562-571,2013

[26] A.I. Luik, J. Noteboom, L.A. Zuurbier, H. Whitmore, A. Hofman, H. Tiemeier. Sleep apnea severity and depressive symptoms in a population-based study, Sleep Health.1,128-132,2015

[27] Yunyoung Nam, Bersain A. Reyes and Ki H. Chon. Estimation of Respiratory Rates Using the Built-in Microphone of a Smartphone or Headset. IEEE JOURNAL OF BIOMEDICAL AND HEALTH INFORMATICS, 20(6): 1493-1501, 2016

[28] T. Emoto, U.R. Abeyratne, M. Akutagawa, S. Konaka, Y. Kinouchi, High frequency region of the snore spectra carry important information on the disease of sleep apnoea, J. Med. Eng. Technol,35,425-431,2011

[29] A.S. Karunajeewa, U.R. Abeyratne, C. Hukins, Multi-feature snore sound analysis in obstructive sleep apnea-hypopnea syndrome, Physiol. Meas.32 ,83,2010

[30] U.R. Abeyratne, S. De Silva, C. Hukins, B. Duce, Obstructive sleep apnea screening by integrating snore feature classes, Physiol. Meas. 34, 99, 2013

[31] Hirotaka Hara,Naoko Murakami, Hiroshi Yamashita. Acoustic analysis of snoring sound. Stomato-pharyngology,15(2), 245 252,2003

[32] Rajkumar Palaniappan, Kenneth Sundaraj, Sebastian Sundaraj. Adaptive neuro-fuzzy inference system for breath phase detection and breath cycle segmentation. Computer Methods and Programs in Biomedicine,145,67-72,2017

[33] Laiali Almazaydeh, Khaled Elleithy*, Miad Faezipour and Ahmad Abushakra. Apnea Detection Based on Respiratory Signal Classification. Procedia Computer Science,21,310-316,2013

[34] Baiying Lei a,b,n, Shah Atiqur Rahman b, Insu Song. Content-based classification of breath sound with enhanced features. Neurocomputing,141,139-147,2014

[35] D. Kumar, P. Carvalho, M. Antunes, J. Henriques, A.S. e. Melo, J. Habetha, Heart Murmur Recognition and Segmentation by Complexity Signatures, In 2008 30th Annual International Conference of the IEEE Engineering in Medicine and Biology Society,2128-2132,2008.

[36] M. Ruffo, M. Cesarelli, M. Romano,et al. An algorithm for FHR estimation from foetal phonocardiographic signals. Biomedical Signal Processing and Control. 5,131-141,2010

[37] H. Kieler, S. Cnattingiust, B. Haglund, J. Palmgren, O. Axelsson, Ultrasound and adverse effects, Ultrasound Obstet. Gynecol. 20(1),102-103,2002

[38] I. Hanna, M. Silverman. A history of cardiac auscultation and some of its contributors, Am. J. Cardiol. 90,259-267,2002

[39] Z. Jiang, S. Choi, A cardiac sound characteristic waveform method for in-home heart disorder monitoring with electric stethoscope, Expert Syst. Appl. 31,286-298,2006

[40] Dawid Gradolewski, Grzegorz Redlarski. Wavelet-based denoising method for real phonocardiography signal recorded by mobile devices in noisy environment. Computers in Biology and Medicine,52 ,119-129,2014.

[41] Samjin Choi, Youngkyun Shin, Hun-Kuk Park, Selection of wavelet packet measures for insufficiency murmur identification, Expert Systems with Applications, 38(4),4264-4271,2011.

[42] Yuerong Chen, Shengyong Wang, Chia-Hsuan Shen, Fred K. Choy, Matrix decomposition based feature extraction for murmur classification, Medical Engineering & Physics, 34(6),756-761,2012.

[43] Shuping Sun, Haibin Wang, Zhongwei Jiang, Yu Fang, Ting Tao, Segmentation-based heart sound feature extraction combined with classifier models for a VSD diagnosis system, Expert Systems with Applications, 41(4),1769-1780, 2014

[44] S. Jabbari, H. Ghassemian, Modeling of heart systolic murmurs based on multivariate matching pursuit for diagnosis of valvular disorders, Comput.Biol. Med. 41,802-811,2011

[45] I. Maglogiannis, E. Loukis, E. Zafiropoulos, A. Stasis, Support Vectors Machinebased identification of heart valve diseases using heart sounds, Comput. Methods Programs Biomed. 95,47-61,2009

[46] A. Kulkas, E.Huupponen, J.Virkkala, M.Tenhunen, A.Saastamoinen, E.Rauhala, S.-L.Himanen. Intelligent methods for identifying respiratory cycle phases from tracheal sound signal during sleep. Computers in Biology and Medicine, 39,1000-1005,2009

[47] Samjin Choi, Zhongwei Jiang. Comparison of envelope extraction algorithms for cardiac sound signal segmentation.Expert Systems with Applications,34(2),1056-1069, 2008

[48] Jinqun Liu, Haibin Wang, Wuchang Liu, Jinbao Zhan. Autonomous Detection and Classification of Congenital Heart Disease Using an Auscultation Vest. Journal of Computational Information Systems, 8(2),485-492,2012

[49] Zhonghong Yan, Zhongwei Jiang, Ayaho Miyamoto, Yunlong Wei. The moment segmentation analysis of heart sound pattern. Computer methods and programs in biomedicine, 98,140-150,2010

[50] Respiratory Cycle: Definition and Explanation. http://physiciandiary.com/respiratory-cycle-definition-and-explanation/

[51] Peter Hult, Bengt Wranne, Per Ask. A bioacoustic method for timing of the different phases of the breathing cycle and monitoring of breathing frequency. Medical Engineering & Physics. 22, 425-433, 2000

[52] Alqassim S, Ganesh M, Khoja S, Zaidi M, Aloul F, Sagahyroon A. Sleep apnea monitoring using mobile phones. In: Proceedings of e-health networking, applications and services (Healtcom) 2012 conference. IEEE Press, 443-6,2012

[53] R. Palaniappan, K. Sundaraj, S. Sundaraj, N. Huliraj, S.S. Revadi, A novel approach to detect respiratory phases from pulmonary acoustic signals using normalised power spectral density and fuzzy inference system, Clin. Respir. J.10, 486-494, 2016.

[54] Rajkumar Palaniappan, Kenneth Sundaraj, Sebastian Sundaraj. Adaptive neuro-fuzzy inference system for breath phase detection and breath cycle segmentation. Computer Methods and Programs in Biomedicine, 145, 67-72, 2017

[55] Abnormal Breathing, Guideline 2005/3006,Japanese Society of Laboratory Medicine,chapter 1, 24-28

[56] Laiali Almazaydeh, Khaled Elleithy*, Miad Faezipour and Ahmad Abushakra. Apnea Detection Based on Respiratory Signal Classification. Procedia Computer Science, 21, 310-316, 2013

[57] Godino-Llorente, J. I. and P. Gomez-Vilda. Automatic detection of voice impairments by means of short-term cepstral parameters and neural network based detectors. IEEE Trans. Biomed. Eng,51, 380-384, 2004

[58] T. Ganchev, N. Fakotakis, and G. Kokkinakis, Comparative evaluation of various MFCC implementations on the speaker verification task. In Proceedings of the SPECOM-2005, 1, 191-194, 2005

[59] Ping Wang, Chu Sing Lim, Sunita Chauhan.etl. Phonocardiographic Signal Analysis Method Using a Modified Hidden Markov Model, Annals of Biomedical Engineering, 35(3),367-374, 2007

[60] Mohammed Bahoura. Pattern recognition methods applied to respiratory sounds classification into normal and wheeze classes. Computers in Biology and Medicine, 39, 824-843, 2009

[61] Igor Mazic, Mirjana Bonkovic, Barbara Dzaja. Two-level coarse-to-fine classification algorithm for asthma wheezing recognition in children's respiratory sounds. Biomedical Signal Processing and Control, 21, 105-118, 2015

[62] Wenjie Fu, Xinghai Yang, Yutai Wang. Heart Sound Diagnosis Based on DTW and MFCC. 2010 3rd International Congress on Image and Signal Processing, 2920-2923, 2010

[63] Sandipan Chakrobortyt, Anindya Royt, and Goutam Saha. Fusion of a Complementary Feature Set with MFCC for Improved Closed Set Text-Independent Speaker Identification. 2006 IEEE,2006.

[64] A. F. Quiceno-manrique, Godino-llorente, M. Blanco-velasco.et al. Selection of Dynamic Features Based on Time frequency Representations for Heart Murmur Detection from Phonocardiographic Signals, Annals of Biomedical Engineering. 38(1), 118-137, 2010

[65] Yan Wang, Haibin Wang, Lihan Liu, et al. A New Diagnosis Method for Heart Valve Disease by Using Antibody Memory Clone Clustering Algorithm Based on Supervised Gath-Geva Algorithm. IEEE ICCSIT 2010, 6, 150-154,2010

[66] Report on cardiovascular disease in china (2016). China heart conference,2017

[67] Chenglang Dong, Shouqi Tao, Haozhu Chen. Practical Cardiology. Shanghai science and Technology Press.1993

[68] Chengbin Xu.Phonocardiogram.Beijing: Sciences Press.1982.

[69] Zhonghong Yan, Ayaho Miyamoto, Zhongwei Jiang,et al. An overall theoretical description of frequency slice wavelet transform. Mechanical Systems and Signal Processing, 24, 491-507, 2010

[70] Sepehri.AA,Hancq.J, Dutoit.T, Gharehbaghi.A, Kocharian.A,kiani.A. Computerized screening of children congenital heart diseases.Computer methods and programs in biomedical, 92(2), 186-192, 2008

[71] Sanjay R. Bhatikar, Curt DeGroff, Roop L. Mahajan.A classifier based on the artificial neural network approach for cardiologic auscultation in pediatrics. Artificial Intelligence in Medicine, 33, 251-260, 2005

[72] Sepehri.AA, Gharehbaghi.A, Dutoit.T, Kocharian.A, kiani.A. A novel method for pediatric heart sound segmentation without using the ECG. computer methods and programs in biomedical, 99(1), 43-48, 2010

[73] Adam T.Balogh, Ferenc Kovacs. Application of phonocardiography on preterm infants with patent ductus arteriosus. Biomedical Signal Processing and Control, 6, 337- 345, 2011

[74] Qiongmin Zhang, Haibin Wang, Yu Fang, et al. An daptive Heart Murmur Detection Method Based on SVD. Journal of Computational Information Systems, 8(21), 9085-9092,2012

[75] Saeid Sanei, Mansoureh Ghodsi, Hossein Hassani. An adaptive singular spectrum analysis approach to murmur detection from heart sounds, Medical Engineering & Physics, 33, 362-367, 2011

[76] Wang Xinpei,Liu Changchun, Li Yuanyang, et al. Heart sound segmentation algorithm based on high-order Shannon entropy, Journal of Jilin University (Engineering and Technology Edition), 40 (5), 1433-1437, 2010

[77] Samjin Choi, Zhongwei Jiang. Comparion of envelope extraction algorithms for cardiac sound signal segmentation. Expert Systems with Application, 34, 1056-1069, 2008

[78] Jinqun Liu, Haibin Wang,Wuchang Liu.et al. Autonomous Detection and Classification of Congenital Heart Disease Using an Auscultation Vest. Journal of Computational Information Systems, 8 (2), 485-492, 2012

[79] Samjin Choi, Zhongwei Jiang. Cardiac sound murmurs classification with autoregressive spectral analysis and multi-support vector machine technique. Computers in Biology and Medicine, 40(1), 8-20, 2010

[80] Zhongwei Jiang, Ting Tao, Haibin Wang. New Approach on Analysis of Pathologic Cardiac Murmurs Based on WPD Energy Distribution, Journal of Healthcare Engineering, 5(4), 375-392, 2014

Acknowledge

I would like to express my deepest gratitude to my supervisor, Prof. Zhongwei Jiang, for his great suggestions, constant encouragement and guidance on my research. Prof. Jiang show me his enthusiasm for scientific research. He always inspire me new ideas and challenge me to think in new ways. I am deeply grateful of his help during my PHD study.

I would like to extend my sincere appreciation to my associate supervisor, Prof. Haibin Wang, in School of Electrical Engineering and Electrolic Information, Xihua University, for her instructive advice and useful suggestions on my research and this thesis. I do appreciate her patience, encouragement and trust during my PHD study.

I also would like to express my heartfelt gratitude to all members of the committees, Prof. Shingo Yamaguchi, Prof. Xian Chen, associate Prof. Minoru Morita and Shota Nakashima. According to the useful and kind reviews, comments and advices from them, the thesis become better and better with great improvement.

And I would like to appreciate Prof. Zhonghong Yan and all other teachers who have guided and help me, for their patient instructions and encouragement. And I also would like to thank my seniors and the student members in our laboratory for their kind support.

I also owe my sincere gratitude to all my friends who gave me a lot of help. I should finally thank to my family for the kind and great consideration to me all through the period, who give me lots of support.